ควอนตัมดอตและสารประกอบฟลูออเรสเซนซ์สำหรับการรับรู้ไบโอเจนิกแอมีน

นางสาวมนัญญา เทพกิจอารีกุล

วิทยานิพนธ์นี้เป็นส่วนหนึ่งของการศึกษาตามหลักสูตรปริญญาวิทยาศาสตรมหาบัณฑิต
สาขาวิชาเคมี ภาควิชาเคมี
คณะวิทยาศาสตร์ จุฬาลงกรณ์มหาวิทยาลัย
ปีการศึกษา 2559

QUANTUM DOTS AND FLUORESCENCE COMPOUNDS FOR BIOGENIC AMINE SENSING

Miss Manunya Tepakidareekul

A Thesis Submitted in Partial Fulfillment of the Requirements

for the Degree of Master of Science Program in Chemistry

Department of Chemistry

Faculty of Science

Chulalongkorn University

Academic Year 2016

Thesis Title	QUANTUM DOTS AND FLUORESCENCE COMPOUNDS FOR BIOGENIC AMINE SENSING
By	Miss Manunya Tepakidareekul
Field of Study	Chemistry
Thesis Advisor	Assistant Professor Boosayarat Tomapatanaget, Ph.D.

Accepted by the Faculty of Science, Chulalongkorn University in Partial Fulfillment of the Requirements for the Master's Degree

.....Dean of the Faculty of Science
(Associate Professor Polkit Sangvanich, Ph.D.)

THESIS COMMITTEE

.....Chairman
(Associate Professor Vudhichai Parasuk, Ph.D.)

.....Thesis Advisor
(Assistant Professor Boosayarat Tomapatanaget, Ph.D.)

.....Examiner
(Numpon Insin, Ph.D.)

.....External Examiner
(Gamolwan Tumcharern, Ph.D.)

มนัญญา เทพกิจอารีกุล : ควอนตัมดอตและสารประกอบฟลูออเรสเซนซ์สำหรับการรับรู้ไบโอเจนิกแอมีน (QUANTUM DOTS AND FLUORESCENCE COMPOUNDS FOR BIOGENIC AMINE SENSING) อ.ที่ปรึกษาวิทยานิพนธ์หลัก: ผศ. ดร.บุษยรัตน์ ธรรมพัฒนกิจ, 104 หน้า.

การตรวจวัดสารประกอบไบโอเจนิกแอมีนอย่างง่าย ซึ่งอาศัยกระบวนการอิเล็กตรอนทรานซเฟอร์ (Electron transfer, ET) และการแลกเปลี่ยนลิแกนด์ (Ligand exchange mechanism) ถูกสร้างขึ้นโดยใช้ตัวตรวจวัดฟลูออโรฟอร์-ไมเซลล์ ในงานวิจัยนี้ได้สังเคราะห์ อนุพันธ์ของคูมาริน (CouS1) และ คาร์บอน ดอท ที่ถูกดัดแปรพื้นผิวด้วยพอลิเอธิลีนอิมีนแบบกิ่ง (N-CDs) เพื่อใช้เป็นฟลูออโรฟอร์ในการสร้างตัวตรวจวัดขึ้น โดยการเติมโซเดียมโดเดคซิลซัลเฟต (SDS) จะส่งผลให้สัญญาณฟลูออเรสเซนซ์ของฟลูออโรฟอร์ทั้งสองมีค่าสูงขึ้น จึงเพิ่มความไวในการตรวจวัด จากการทดลองพบว่าสัญญาณฟลูออเรสเซนซ์ของฟลูออโรฟอร์ทั้งสองชนิด ในกรณีที่มีโซเดียมโดเดซิลซัลเฟตอยู่ด้วยนั้น จะลดลงสูงสุดเมื่อมีการเติมโคบอลต์ (II) ไอออน เนื่องจากกระบวนการ ET ดังนั้นไอออนชนิดนี้จึงถูกเลือกในการสร้างตัวตรวจวัด CouS1/SDS/Co^{2+} และ N-CDs/SDS/Co^{2+} เพื่อใช้ตรวจวัดไบโอเจนิกแอมีน ในกรณีของตัวตรวจวัด CouS1/SDS/Co^{2+} สัญญาณฟลูออเรสเซนซ์จะเพิ่มขึ้นเมื่อมีการเติมฮิสทิดีน เนื่องจากโคบอลต์ (II) ไอออนถูกดึงออกจากตัวตรวจวัดโดยฮิสทิดีน ในทางกลับกันการเติมฮิสตามีนจะทำให้สัญญาณฟลูออเรสเซนซ์ลดต่ำลง เนื่องจากฮิสตามีนจะร่วมสร้างพันธะกันโคบอลต์ (II) ไอออนภายในตัวตรวจวัด นอกจากนี้ ข้อดีของตัวตรวจวัด CouS1/SDS/Co^{2+} สามารถใช้จำแนกสารประกอบไบโอเจนิกแอมีนที่มีอิมิดาโซลเป็นส่วนประกอบด้วยตาเปล่า ในกรณีของตัวตรวจวัด N-CDs/SDS/Co^{2+} สัญญาณฟลูออเรสเซนซ์จะเพิ่มขึ้นเมื่อมีการเติมฮิสทิดีนเท่านั้น โดยค่าขีดจำกัดการตรวจวัดฮิสทิดีนของตัวตรวจวัด CouS1/SDS/Co^{2+} และ N-CDs/SDS/Co^{2+} มีค่าเท่ากับ 45 และ 74 ไมโครโมลาร์ตามลำดับ ซึ่งค่าดังกล่าวสามารถนำตัวตรวจวัดทั้งสองมาประยุกต์ใช้ในการตรวจหาปริมาณฮิสทิดีนทั้งในคนปกติและผู้ป่วยโรคฮิสทิดินีเมีย (histidenemia) นอกจากนี้ molecular logic gate ได้ถูกพัฒนาขึ้นจากการตรวจวัดนี้ ภายใต้การเปลี่ยนแปลงคุณสมบัติทางแสงที่แตกต่างกัน เมื่อมีตัวกระตุ้นที่แตกต่างกันของ โคบอลต์ (II) ไอออน ฮิสทิดีน และฮิสตามีน

ภาควิชา เคมี ลายมือชื่อนิสิต .....

สาขาวิชา เคมี ลายมือชื่อ อ.ที่ปรึกษาหลัก .....

ปีการศึกษา 2559

5672837823 : MAJOR CHEMISTRY
KEYWORDS: CARBON DOTS / COUMARIN / MICELLE

MANUNYA TEPAKIDAREEKUL: QUANTUM DOTS AND FLUORESCENCE COMPOUNDS FOR BIOGENIC AMINE SENSING. ADVISOR: ASST. PROF. BOOSAYARAT TOMAPATANAGET, Ph.D., 104 pp.

The simple approach for biogenic amine sensing electron transfer (ET) process and ligand exchange mechanism has been constructed by using fluorophore-micellar probe. In this work, coumarin derivative (CouS1) and carbon nanoparticles namely branch-polyethyleneimine modified carbon dots (N-CDs) were synthesized and used as fluorophore for constructing the probe. In the presence of SDS, the fluorescence intensity of these fluorophores was enhanced leading to a high sensitivity in sensing application. Upon the addition of various metal ions into the both solutions of CouS1 and N-CDs in the presence of SDS, Co^{2+} ion exhibited the highest fluorescence quenching in the both solution due to ET process. As a result, the CouS1/SDS/Co^{2+} and N-CDs/SDS/Co^{2+} probe were constructed for discrimination of biogenic amine. In the case of CouS1/SDS/Co^{2+} probe, the fluorescence recovery of CouS1/SDS was observed upon the addition of histidine because of removal of Co^{2+} ion from the probe by histidine. On the contrary, a high fluorescence quenching of CouS1/SDS/Co^{2+} was observed due to co-bonding of histamine with Co^{2+} ion. Moreover, CouS1/SDS/Co^{2+} enables to give a benefit discrimination of imidazole based biogenic amine by naked-eye approach. In the case of N-CDs/SDS/Co^{2+} probe, the fluorescence recovery of N-CDs/SDS was observed in particular of presented histidine. The detection limits of CouS1/SDS/Co^{2+} and N-CDs/SDS/Co^{2+} over histidine were 45 μM and 74 μM, respectively. This suggests that these probes can be applied for analytical detection of histidenemia both normal and histidenemia patients. Additionally, molecular logic gate was developed form these different sensing spectrum upon the different stimuli of Co^{2+} ion, histidine and histamine.

Department: Chemistry Student's Signature .....
Field of Study: Chemistry Advisor's Signature .....
Academic Year: 2016

ACKNOWLEDGEMENTS

I would like to thank my research advisor, Assistant Professor Dr. Boosayarat Tomapatanaget, for her valuable guidance, helpful suggestion and constant encouragement throughout this research. In addition, I would like to thank and pay my respect to Associate Professor Dr. Vudhichai Parasuk, Dr. Numpon Insin and Dr. Gamolwan Tumcharern for their valuable advices, useful suggestion and valuable comments as thesis committee.

This accomplishment could not occur without the support from Chulalongkorn University. Special thanks are due to Professor Dr. Thawatchai Tuntulani for financial support, beneficial suggestion and all members of Supramolecular Chemistry Research Unit at the department of Chemistry, Chulalongkorn University for their support and giving consultant throughout my research. Furthermore, I would like to thank the Development and Promotion of Science and Technology Talents Project (DPST), and Thailand Research Fund (TRF) for financial support.

Finally, I would like to thank all member of my family for their love, care, kindness, encouragement and financial support throughout my life.

CONTENTS

Page

Page

Page

Page

Page

LIST OF FIGURES

Page

Page

Page

Page

Page

Page

Page

Page

LIST OF SCHEMES

Page

LIST OF TABLES

Page

Page

LIST OF ABBREVIATIONS

Anal. Calcd.	Analysis calculated
δ	Chemical shift
^{13}C-NMR	Carbon-13 nuclear magnetic resonance
°C	Degree Celsius (centrigrade)
CH_2Cl_2	Dichloromethane
DMSO	Dimethyl sulfoxide
EtOAc	Ethyl acetate
g	Gram
gmol^{-1}	Gram per mole
^{1}H-NMR	Proton nuclear magnetic resonance
h	Hour
HD	Histidine
HEPES	4-(2-hydroxyethyl)-1-piperazineethanesulfonic acid
HM	Histamine
Hz	Hertz
J	Coupling constant
m/z	Mazz per charge ratio
µL	Microliter
µM	Micromolar
MeOH	Methanol
mg	Milligram
min	Minute
mL	Milliliter
mmol	Millimole
%	Percentage
s, d, t, m	Splitting patterns of 1H-NMR (singlet, doublet, triplet, multiplet) .

CHAPTER I
INTRODUCTION

Among various naturally occurring biogenic amines, histidine and histamine have been paid attention in recent years due to many roles in biological processes. For example, histidine is necessary for human metabolism including a part of catalytic enzymes, neurotransmitter and histamine producing precursor [1]. The overabundant of histidine results from a deficiency of histidase enzyme or "histidinemia" leading to the developmental delay in newborn, and it has been considered as the most prevalent inborn error of metabolism. On the contrary, recent studies have shown that a lack of histidine can cause impaired nutritional state in patients with chronic kidney disease [2]. Histamine is also essential for nervous system as neurotransmitter and hormones as well as inflammatory response. Because the enzymatic process of microorganism, histamine can be found in food containing protein due to decarboxylation of histidine that can cause food allergic in human. Therefore, histamine can be used as an indicator for microbial spoilage [3]. Based on their similar chemical structures of histidinie and histamine, discrimination of histidine and histamine has become a challenge task. Fluorescence spectroscopy is one of the most useful technique which has demonstrated excellent characteristics in the detection of different biogenic amines, such as high selectivity, high sensitivity, real-time detection and simple operation. Coumarin derivatives are organic dyes containing benzopyrole that is used in many fields. Owing to their properties including photostability, high fluorescence quantum yield and easy functionalization, coumarin derivatives are of great interest in chemosensors. For metal ion sensing coumarin is a good candidate for constructing fluorescent probe due to phoinduced electron transfer (PET) between coumarin and metal ion resulting in fluorescence quenching of coumarin. Subsequent complexation of metal ions by effective analyte that pulls out metal ion from the probe leading fluorescence recovery [4, 5]. According to this approach, histdine and histamine can be detected. Furthermore, carbon dots (CDs), which are fluorescence carbon nanomaterials, are attractive materials for fluorescence probe with metal ions

in sensing applications. Due to their advantages such as emission tunabiliy, photo stability, high fluorescence quantum yield as well as biocompatibility, several researches employed this platform to detect biogenic amines such as dopamine, melamine, glutathione and cysteine [6-9].

Herein, we would like to develop fluorescent sensors for biogenic amine detection in aqueous solution. To enhance water solubility and sensitivity of biogenic amine sensing, anionic surfactant was applied to construct fluorescence probes. The interaction between dye and surfactant can improve fluorescence performance since the encapsulated fluorophore in micellar core leads a high florescence intensity and increased binding efficiency of active species. Therefore, the designs of florescent sensor by constructing fluorescence probe with surfactant have been of a great interest in developing sensors [10-12].

1.1 Fluorescence spectroscopy

Fluorescence spectroscopy is one of electromagnetic spectroscopy that can used to analyze fluorescence from a sample via exciting electron with specific absorption wavelength followed by measuring emission light from the molecule

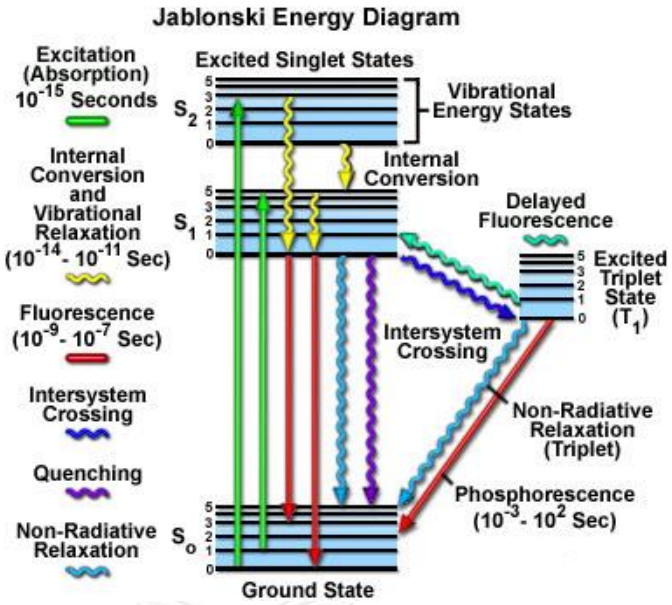

Figure 1.1 Jablonski energy diagram [13]

According to Fig 1.1 which illustrates the electronic state and transition of a molecule, electron in ground state absorb the specific light of the energy level and is stimulated to excited state ($S_0 \longrightarrow S_1$ or $S_0 \longrightarrow S_2$). Irradiation with a wide range of wavelength will originate an entire spectrum of allowed transition which populate the various vibrational energy level of excited states. Some of these transitions will have higher probability than others and when these transitions combine, it will represent as absorption spectrum of a molecule. As following this process immediately, electron in excited state will transit to several states with various probability depending on properties of molecule. In case of fluorescence, electron in excited state transits back to ground state by releasing the energy in the form of light by unchanging of spin multiplicity ($S_1 \longrightarrow S_0$) that is different from phosphorescence ($T_1 \longrightarrow S_0$). Moreover, internal conversion which is non-radiative decay process will generally occur to complete vibrational relaxation during their excited lifetime before fluorescence emission [13-15].

1.2 Electron transfer (ET) process and fluorescent sensors based on ligand exchange mechanism

Electron transfer (ET) is one of the most powerful process that is usually used in chemosensors. Based on concept of ET sensor, the sensor is generally constructed from three units including fluorophore, spacer and receptor units. Fluorophore is a fluorescence chemical compound which can emit fluorescence upon excitation with specific wavelength and receptor is a binding unit that can capture analyte. These two units connected by a spacer which must be short enough to permit reasonably ET process [16, 17]. The sensing mechanism of ET-based metal sensor has been generally designed by using electron transfer of metal-fluorophore complex. In the presence of metal ion, especially 3d-metal, electron in excited state of the metal transfers to ground state of fluorophore leading to fluorescence quenching. On contrary, fluorophore would exhibit strong fluorescence because electron transfer cannot take place in the absence of metal ions [18, 19] as shown in Fig 1.2.

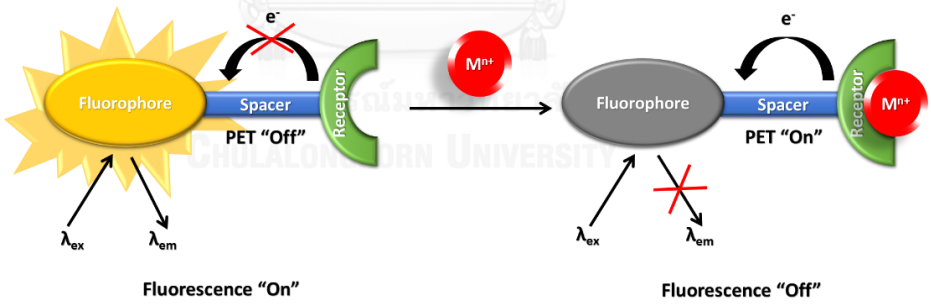

Figure 1.2 The electron transfer process in metal-fluorophore complex based sensor [19]

According to the approach, complexation between analyte and metal ion leading ligand exchange or displacement process can be applied to construct "On-Off-On" fluorescence sensor as shown in Fig 1.3. The analyte can be determined by variation of metal ions based on the binding constant for the receptor and analyte

interaction that provide a high selectivity towards the analyte and against expected levels of interferences.

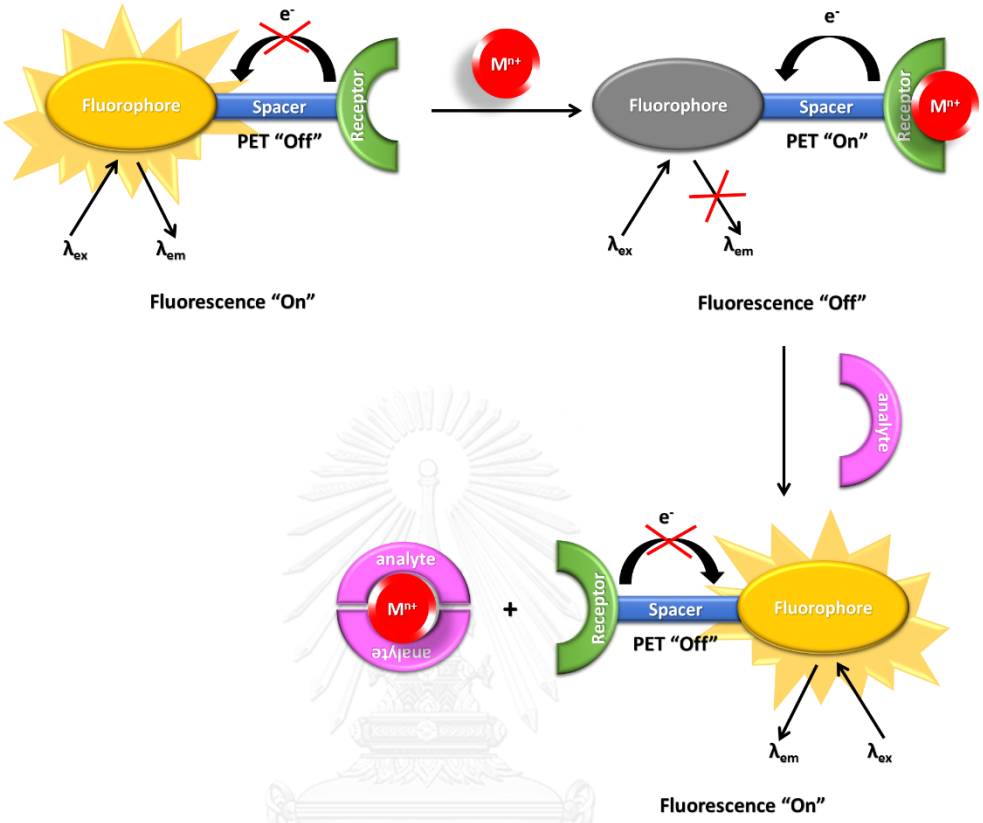

Figure 1.3 The sensing mechanism based on "On-Off-On" states of fluorescence.

For the first example, Seto and coworkers [20] synthesized calcein-Ni^{2+} complex for detection of histamine due to ligand exchange mechanism in 0.1 M PBS buffer at pH 7.4 as shown in Fig. 1.4. The fluorescent titration studies on the complex and histamine showed the fluorescence enhancement upon the increment of histamine. These results can be explained that histamine can remove nickel out from calcein to form histamine-Ni^{2+} complex leading to ET-off phenomenon.

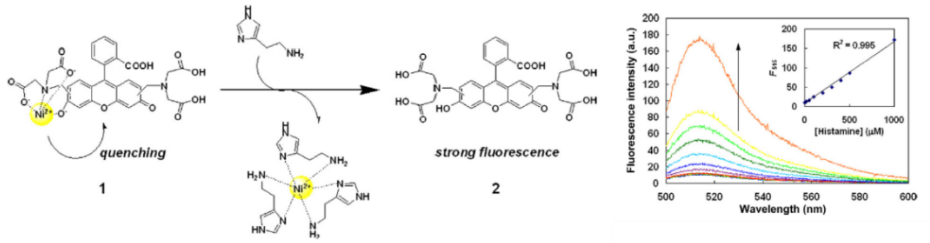

Figure 1.4 The sensing mechanism of histamine using calcein-Ni^{2+} complex

Moreover, the selectivity of this complex was examined by addition of various biogenic amines including dopamine, GABA, glycine, glutamic acid, histamine and serotonin. The fluorescence of calcein-Ni^{2+} complex at 515 nm enhanced only the addition of histamine whereas the fluorescence intensity of the others remained unchanged as shown in Fig. 1.5. This can be explained that histamine contains both an amino moiety and imidazole moiety that performs induced-fit formation with Ni^{2+} ion.

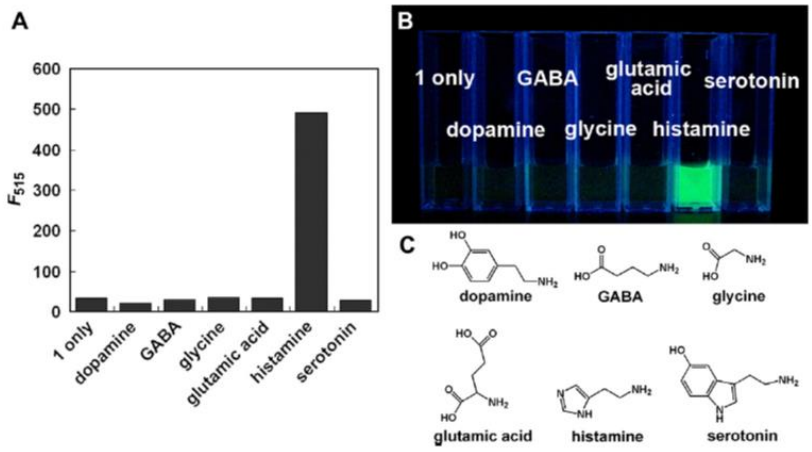

Figure 1.5 Selectivity of calcein-Ni^{2+} complex for histamine. a) Fluorescence response of the complex (1 μM) to various biogenic amines (2 mM). b) Photographs of 0.1 M PBS buffer solutions of the complex (2.5 μM) with and without dopamine, GABA, glycine, glutamic acid, histamine, serotonin (4 mM) at R.T. Each solution was excited by UV irradiation (excitation wavelength = 365 nm). c) Chemical structure of the biogenic amines used in the study

In 2013, Hou and coworkers [4] reported coumarin-Cu^{2+} complex for detection of histidine in 0.02 M HEPES buffer at pH 7.4. The sensor molecule was synthesized by appended 7-diethylamino coumarin with DPA (di(2-picolyl)amine) as receptor unit for

binding copper ion. Based on ligand exchange mechanism, The increase of fluorescence intensity at 500 nm with the increment of histidine can be explained that imidazole group and amino group based on histidine preferentially form with Cu^{2+} ion resulting in removal of Cu^{2+} from coumarin as a result of ET-off process as shown in Fig 1.6.

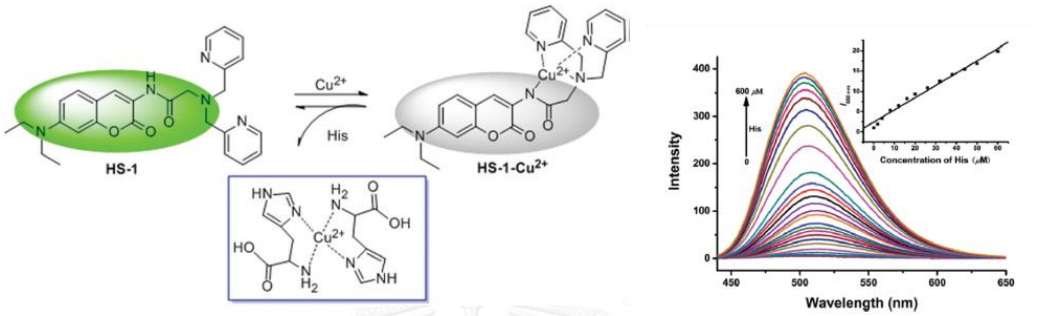

Figure 1.6 The sensing mechanism of histidine using coumarin-DPA-Cu^{2+} complex

To confirm selectivity of the complex, the fluorescence of coumarin-DPA-Cu^{2+} complex enhanced upon the addition of histidine whereas the fluorescence intensity of the others did not cause obvious fluorescence changing as shown in Fig. 1.7.

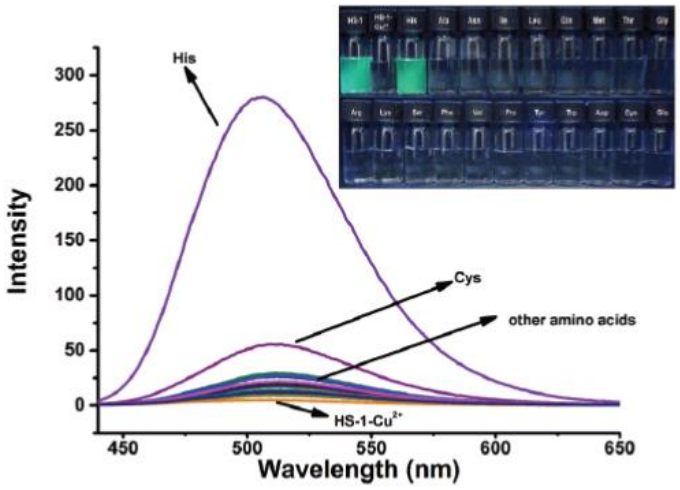

Figure 1.7 Selectivity of coumarin-DPA-Cu^{2+} complex for histidine. Inset: Fluorescence color changes of this complex upon addition of various amino acids under a UV lamp (excitation wavelength = 365 nm)

On the other hand, You and coworkers [5] reported coumarin-Ni^{2+} complex for detection of histidine in 20% CH_3CN/HEPES 0.02 M HEPES buffer at pH 7.4. The sensor molecule was synthesized by appended 7-diethylamino coumarin with 2-amino-N-(quinolin-8-yl)acetamide via EDC coupling. Based on ligand exchange mechanism, The increasing of fluorescence intensity at 480 nm with increasing of histidine concentration can be explained that imidazole group and carboxylic group based on histidine preferentially form with Ni^{2+} resulting removal of Ni^{2+} from coumarin leads to ET-off process as shown in Fig 1.8.

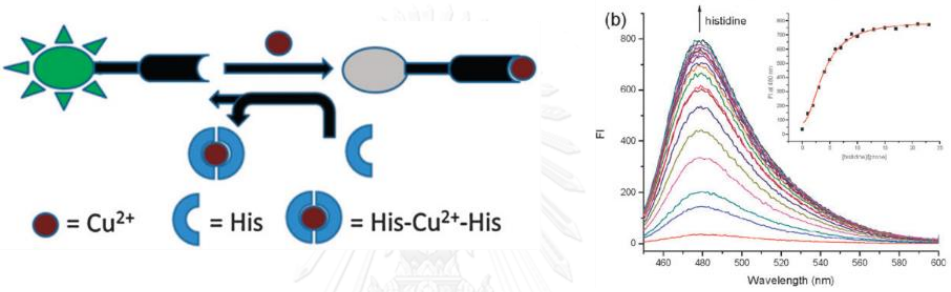

Figure 1.8 The sensing mechanism of histidine using coumarin-Ni^{2+} complex

Although, many researchers reported molecule sensors that can be used to detect histidine or histamine. However, their similar chemical structure of both biogenic amines can caused the problem to discriminate them in displacement process. Therefore, we introduce a novel nanomaterial which is the candidate for determination histidine and histamine.

1.3 Carbon dots (CDs)

Carbon dots (CDs), as novel and promising fluorescent carbon nanomaterial which can exhibit fluorescence owning to their exceptional properties including size, edge and surface chemistry. Carbon dots have been paid attention due to their advantages such as low toxicity, biocompatibility and easy to functionalize. In general, Carbon dots always possess at least one dimension with a size of less than 10 nm and

their structure compose of sp^2-sp^3 carbon and oxygen/nitrogen-based group or polymeric aggregations. Based on structure and morphology of carbon dots, it can be categorized in 3 types [21] as shown in Fig.1.9.

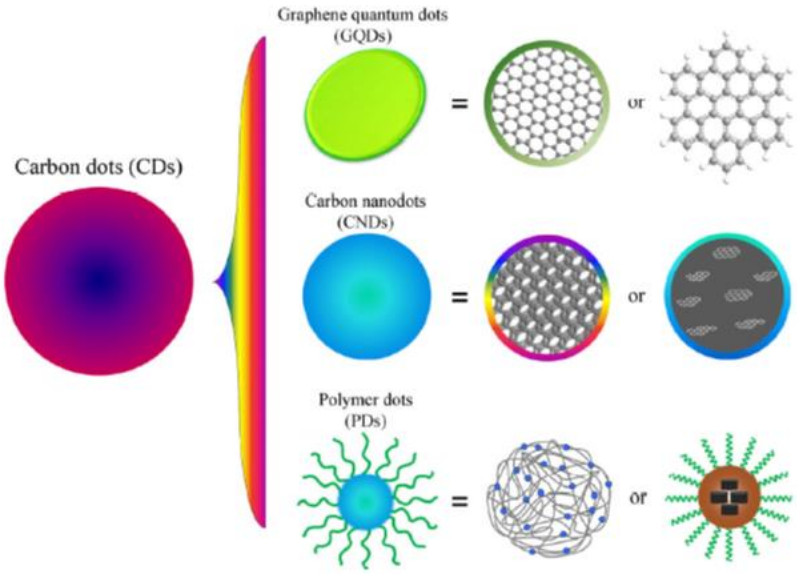

Figure 1.9 Three types of fluorescent Carbon dots: graphene quantum dots (GQDs), carbon nanodots (CNDs), and polymer dots (PDs) [21]

- Graphene quantum dots (GQDs) is one or a few layers of graphene which are anisotropic with lateral dimension larger than their height. The carbon core of GQDs connected chemical group on the surface or edge that effects the properties of GQDs. The edge type of the particles including zigzag-edge or armchair edge plays crucial role in determining the electronic, magnetic and optical properties of GQDs. Moreover, quantum confinement effect which generally found in inorganic quantum dots can also effect optical properties of GQDs because of conjugated π-domains in GQDs. Therefore, the fluorescence emission can be tuned by adjusting the size of GQDs [21, 22].

- Carbon nanodots (CNDs) can be divided into two groups including carbon nanoparticle which is always spherical and do not have a crystal lattice while carbon quantum dots (CQDs) have an obvious crystal lattice resulting in different optical properties. Various functional group can effect optical properties of CNDs because different functional group leads to different energy levels. When the light of specific excitation wavelength irradiates the CNDs, a surface state trap will dominate the fluorescence. Moreover, the modification of CNDs by organic fluorophore can also effect emission properties of CNDs [21].
- Polymer dots (PDs) are formed by aggregation of linear polymer or self-assembly between carbon core and polymer chain. Owning to more rigidity of PDs structure, non-radiative decay has been decreased resulting in increase of fluorescence signal and high stability of the particles [21].

1.3.1 Synthesis of carbon dots

To synthesize CDs, various methods have been investigated to provide a high quality of CDs including high quantum yield, high stability, emission tunability and biocompatibility. Based on how to synthesized CDs, these methods can be categorized into 2 methods as shown in Fig 1.10

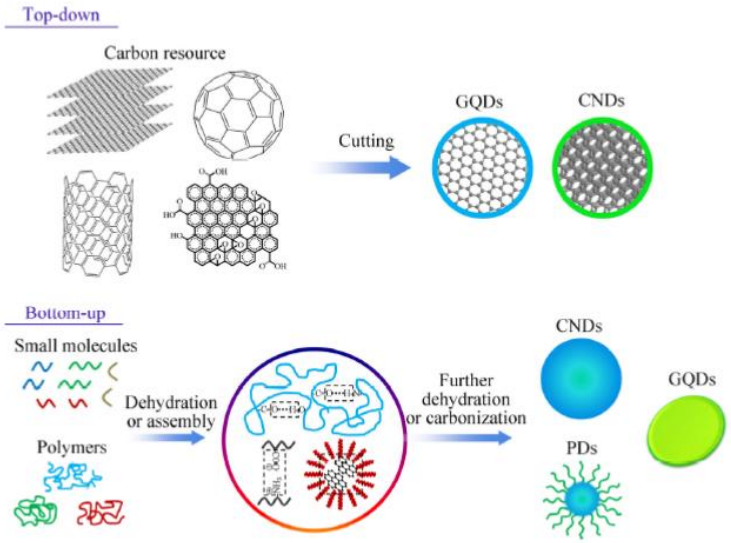

Figure 1.10 The main processes to synthesize CDs: "Top-down" cutting from various sp^2-carbon materials and "bottom-up" synthesis from small molecules [21]

- "Top-down" method is the process which cuts of sp^2-rich carbon materials such as carbon nanotube, graphene sheet or carbon black to small pieces of carbon dots. Edge or surface of these materials are modified to oxygen-based group by oxidizing agents such as concentrated H_2SO_4 or HNO_3 and subsequent by cutting them to carbon dots via hydrothermal, electrochemistry or nanolithography [23-25].
- "Bottom-up" method is the process which constructs carbon dots from small organic molecules or polymers. These molecules contain –OH, -NH_2, -COOH moieties which can undergo dehydration and further carbonization to form CDs. There are many processes to carry out dehydration and carbonization including pyrolysis, hydrothermal or microwave assisted method [26-29].

1.3.2 Carbon dots for sensing application based on ligand exchange mechanism

As same as the organic molecules, carbon dots can be used to construct "On-Off-On" sensor for biological substances due to ligand exchange process. Based on functionalization of CDs by specific ligands such as amino group, carboxylic group or thiol group. Various of analytes can be determined by variation of metal ions based on the binding constant for the functionalized CDs or analyte interaction that provide a high selectivity towards the analyte and against expected levels of interferences.

For the first example, Zhou and coworkers [30] reported unmodified carbon nanodots (C-dots) for detection of Hg^{2+} ion and biothiol in 10 mM Tris–HCl buffer at pH 8.5. The C-dots were synthesized by pyrolysis of ethylenediaminetetraacetic acid (EDTA) salts providing hydroxyl groups and carboxylic groups as functional groups of these particles after carbonization process.

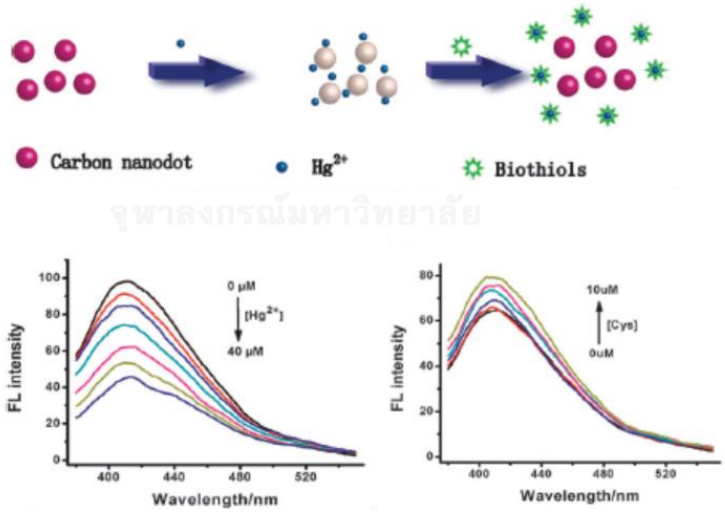

Figure 1.11 The sensing mechanism of Hg^{2+} ion and cysteine using C-dots

According to Fig.1.11, The solution of free C-dots exhibited strong fluorescence at 410 nm but in the presence of Hg^{2+} ion, the fluorescence signal was quenched due to surface state changing of C-dots. To demonstrate this platform for biothiol sensing, three biothiols including cysteine (Cys), homocystene (Hcy) and glutathione (GSH) were

added into the system. It was found that only cysteine exhibited fluorescence recovery due to binding between sulfur and Hg^{2+} ion.

In 2014, Gu and coworkers [6] synthesized carbon dots (CDs) from honey that provide amino group and carboxylic moiety which are efficient binding with Au^{3+} ion. The synthesized carbon dots can detect Au^{3+} ion and glutathione in HCl solution at pH 3.0. The sensing mechanism can be explained in Fig 1.12. The synthesized carbon dots exhibited strong blue fluorescence in the absence of Au^{3+} ion. In the presence of Au^{3+} ion, the fluorescence response of CDs was quenched. It can be explained that a strong interaction between thiol groups on carbon dots and Au^{3+} ion causes the formation of carbon dot-Au^{3+} cluster (CDC) that can be confirmed by TEM images as show in Fig 1.13.

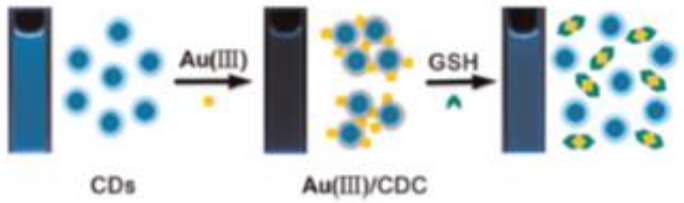

Figure 1.12 The sensing mechanism of Au^{3+} ion and glutathione using CDs

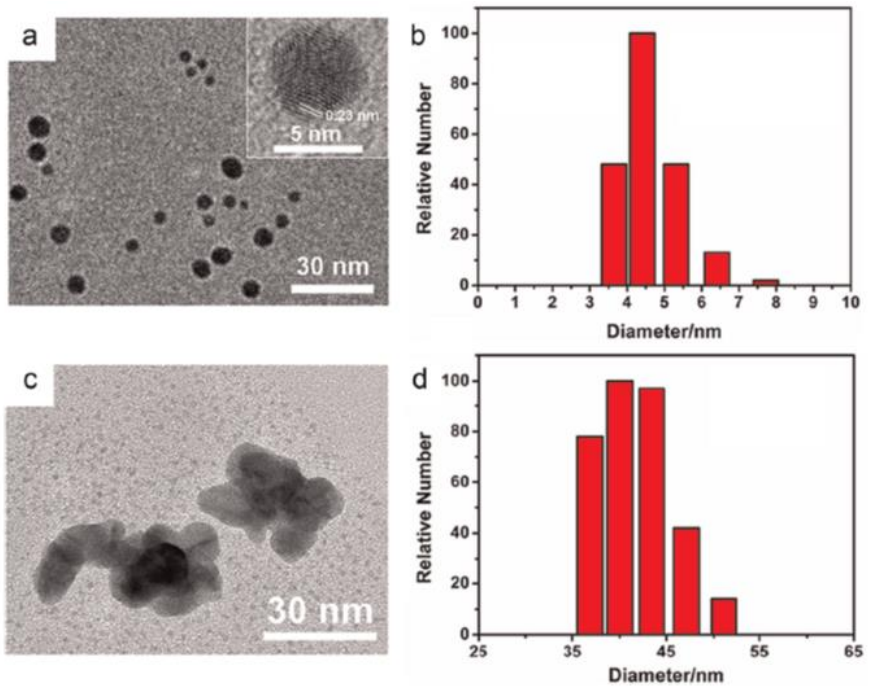

Figure 1.13 TEM images (a, c) and the size distribution histograms (b, d) of CDs and Au(III)/CDC. Inset: the HRTEM image of individual CDs. (a, b) CDs and (c, d) Au(III)/CDC.

Upon the addition of glutathione, thiol group of glutathione can bind Au^{3+} ion stronger than amino group and carboxylic group on carbon dots. As a result, Au^{3+} ion was removed from the cluster leading to fluorescence recovery as shown in Fig 1.14 a. However, the detection of glutathione can be interfered by cysteine due to the thiol group of cysteine which can also form complex with Au^{3+} ion as shown in Fig 1.14 b.

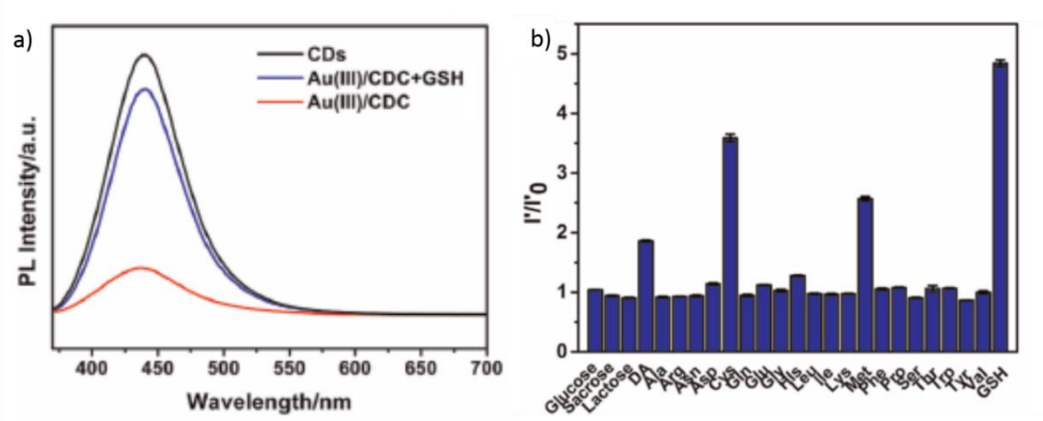

Figure 1.14 a) Fluorescence spectra of CDs, Au(III)/CDC and Au(III)/CDC+GSH. b) Relative fluorescence responses of Au(III)/CDC system to 300 μM different biological molecules (excitation wavelength = 360 nm, emission wavelength = 440 nm)

In 2013, Qu and coworkers [9] reported luminescent carbon nanoparticles (CNPs) prepared from hydrothermal of dopamine for Fe^{3+} and dopamine determination in 10 mM HEPES buffer at pH 7.0. The as-prepared carbon dots possess hydroquinone moiety and catechol group due to the self-polymerization of dopamine under high temperature and pressure. In the presence of Fe^{3+} ion, a fluorescence of CNPs was quenched. They explained that hydroquinone groups on the surface of CNPs were oxidized to form quinone leading to electron transfer process. Upon the addition of dopamine, hydroquinone group of dopamine can partly reduce the influence of Fe^{3+} to the CNPs fluorescence. Then, the CNPs showed the fluorescence recovery as shown in Fig 1.15

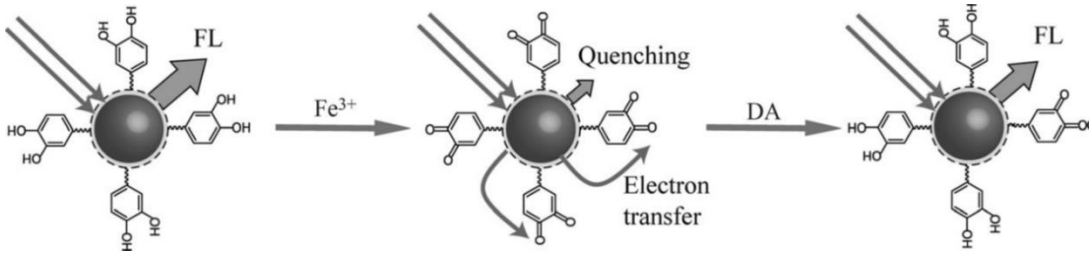

Figure 1.15 The sensing mechanism of Fe^{3+} ion and dopamine using CNPs

Moreover, the selectivity of CNPs-Fe^{3+} platform towards possible interferential molecules including ascorbic acid (AA), uric acid (UA), glucose, lactose and amino acids.

It was found that this platform provides high selectivity towards dopamine as shown in Fig 1.16.

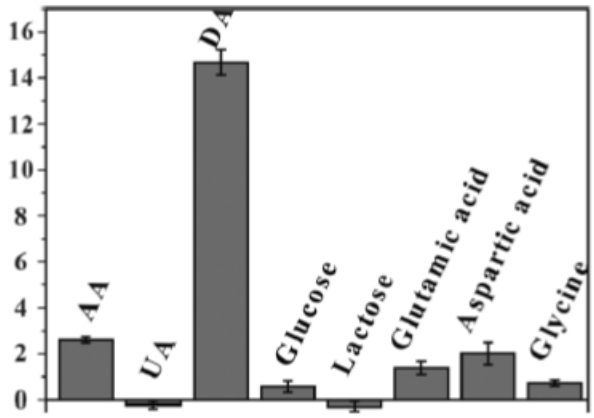

Figure 1.16 Fluorescence responses of the CNPs/Fe^{3+} system to DA (50 mm) and other interferential biological molecules

1.4 Sensing activity improving by using anionic surfactant

Based on the expected sensing mechanism, a low amount of metal for construction of the biogenic amine probe is necessary. To enhance sensitivity of fluorophore toward metal ion, anionic surfactant such as sodium dodecyl sulfate (SDS) has been introduced to the metal sensing application as shown in Fig 1.17.

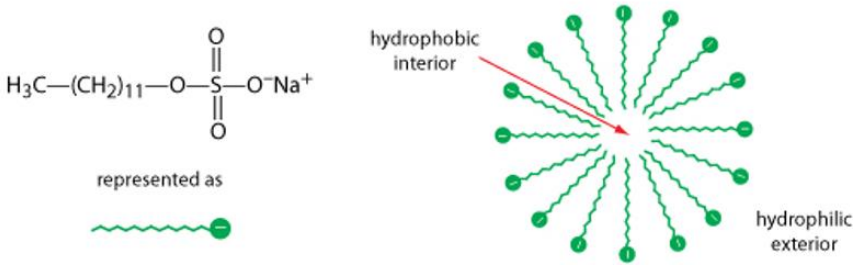

Figure 1.17 Chemical structure and micelle structure of SDS

Zhao and coworker [12] synthesized a hybrid foldamer from six cholate units and two methionines with a dansyl group for Hg^{2+} ion determination in micellar media.

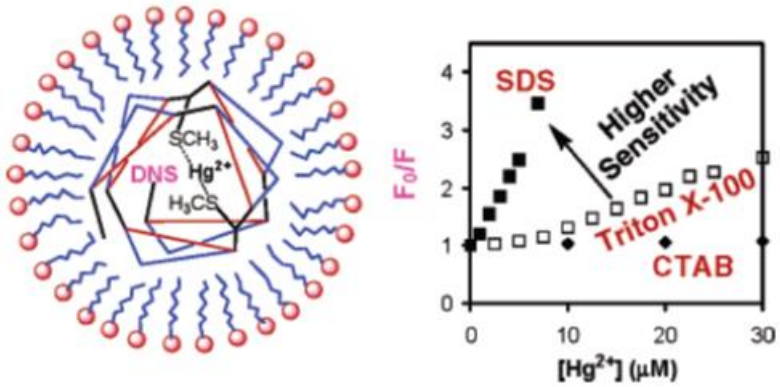

Figure 1.18 Structure of foldamer-SDS micelle and relative fluorescence intensity of foldmer towards Hg^{2+} ion in different micellar solutions.

Based on the non-polar structure of this sensor which is insoluble in water, three surfactants including SDS, CTAB and Triton X-100 were added into the solution at their CMC. According to Fig 1.18, it was found that SDS exhibited the strong emission quenching toward Hg^{2+} ion. Alternatively, the fluorescence of the dansyl group in the presence of Hg^{2+} ion was not be quenched in CTAB solutions but easily quenched in Triton X-100 because of the electrostatic repulsion between the positive charge of Hg^{2+} ion and CTAB. Nonionic micelles give an intermediate affinity because neither favorable nor unfavorable electrostatic interactions are involved.

In 2014, Ding and coworkers [10] reported bis-pyrene based fluorescent sensor (Py-diIM-Py) for chemical explosive determination in micellar media including SDS, DTAB and Triton X-100. According to Fig 1.19, the fluorescence of this sensor was enhanced upon the addition of SDS, DTAB and Triton X-100, respectively. It was expected that the different fluorophore locations in the micellar solutions significantly effected on fluorescence enhancement and selectivity toward explosive substance as shown in Fig 1.19.

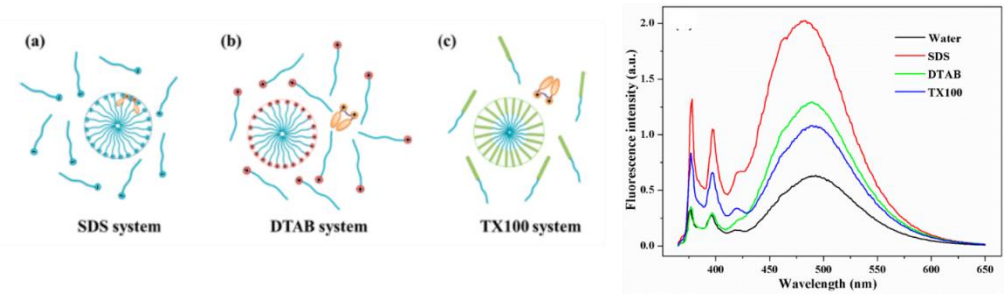

Figure 1.19 Proposed location and fluorescence spectra of fluorophore in different micellar solutions

In the case of SDS, a certain amount of fluorophore was encapsulated by SDS micelle. It could protected the excited fluorophore from quenching/deactivation process by dissolved O_2 and promoted de-excitation by the radiative process. To detect nitro-aromatic explosives, concentration of SDS was used at its CMC. It was found that the largest fluorescence response was observed in case of picric acid (PA) over other guests as shown in Fig 1.19 a). Moreover, PA may possess electrostatic attraction with the micelle surface located in fluorophore resulting in larger quenching efficiency. The fluorescence responses of this fluorophore/SDS system to PA is shown in Fig 1.20. It can be seen that the emission of this sensor was quenched significantly in the presence of PA.

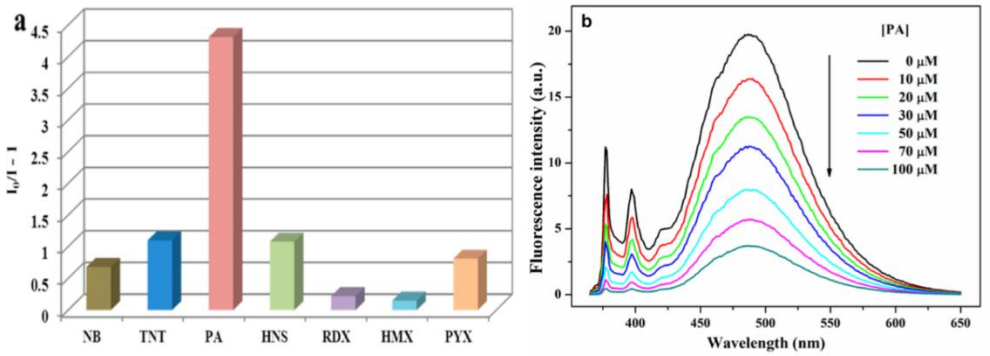

Figure 1.20 Fluorescence quenching efficiency of explosives to Py-diIM-Py/SDS sensor system and Fluorescence spectra of Py-diIM-Py/SDS upon titration of PA from 0 to 100 μM ([Py-diIM-Py] = 1.0 μM, [SDS] = 8 mM, excitation wavelength = 345 nm)

1.5 Molecular logic gate

According to ET process and ligand exchange mechanism, two chemicals including metal ions and biogenic amines can be defined as inputs for molecular logic gate. Two or more inputs in form of chemical or physical stimuli exhibit one output of chemical or properties of the system such as fluorescence, UV absorption or electrochemical signals. The absence of inputs and outputs are assigned as "0" or "Off" whereas in the presence of inputs and outputs are assigned as "1" or "On". Based on Boolean algebra, the 8-basic gates depend on the number of inputs including NOT, AND, OR, NOR, NAND, EXOR and EXNOR. Their gates and truth tables are shown in Fig 1.21-1.27.

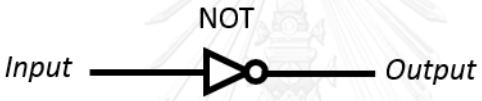

Input	Output
0	1
1	0

Figure 1.21 NOT gate and its truth table

The NOT gate generates an inverted output of the input at its output. It is also known as an inverter. If the input is A, the inverted output is known as NOT A.

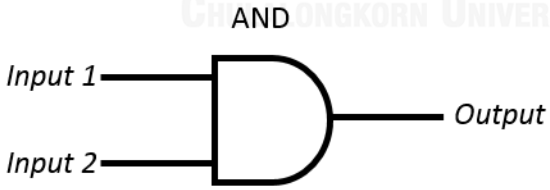

Input 1	Input 2	Output
0	0	0
1	0	0
0	1	0
1	1	1

Figure 1.22 AND gate and its truth table

The AND gate will generate a "1" or "On" output only if all inputs are "1" or "On".

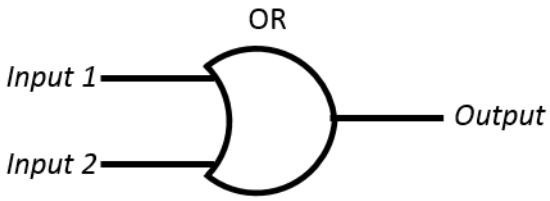

Input 1	Input 2	Output
0	0	0
1	0	1
0	1	1
1	1	1

Figure 1.23 OR gate and its truth table

The OR gate will generate a “1” or “On” output if one or more of its inputs are “1” or “On”.

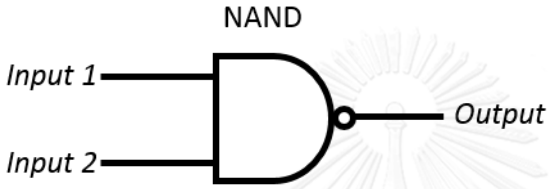

Input 1	Input 2	Output
0	0	1
1	0	1
0	1	1
1	1	0

Figure 1.24 NAND gate and its truth table.

The NOT-AND or NAND gate which is equal to an AND gate followed by a NOT gate. The outputs of all NAND gates are “1” or “On” if any of the inputs are “0” or “Off”.

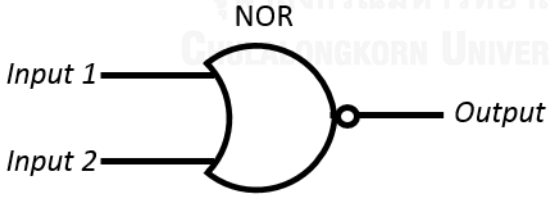

Input 1	Input 2	Output
0	0	1
1	0	0
0	1	0
1	1	0

Figure 1.25 NOR gate and its truth table

The NOT-OR or NOR gate which is equal to an OR gate followed by a NOT gate. The outputs of all NOR gates are “0” or “Off” if any of the inputs are “1” or “On”.

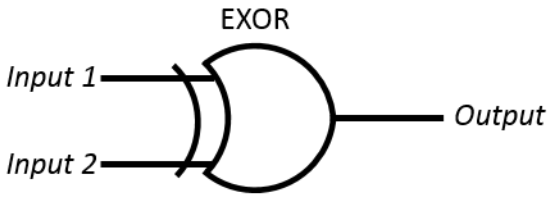

Input 1	Input 2	Output
0	0	0
1	0	1
0	1	1
1	1	0

Figure 1.26 EXOR gate and its truth table

The Exclusive-OR or EXOR gate will generate a “1” or “On” output if either, but not both, of its two inputs are “1” or “On”.

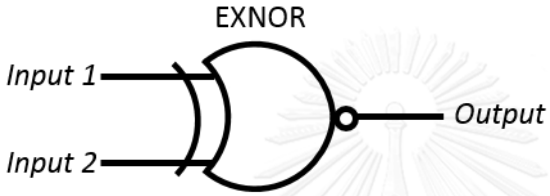

Input 1	Input 2	Output
0	0	1
1	0	0
0	1	0
1	1	1

Figure 1.27 EXNOR gate and its truth table

The Exclusive-NOR or EXNOR gate circuit performs the opposite to the EXOR gate. It will generate a “0” or “Off” output if either, but not both, of its two inputs are “1” or “On”.

This approaches have been applied for sensing applications due to its advantages of no sample modification. The detection of analyte can be specified at the expected level of signal to reduce interference effects.

1.6 Concept of this study

Design and synthesis of fluorescent probes for discrimination of biogenic amine have been research challenge. Recently, many researchers have been paid attention on the sensors that function in aqueous solution due to the benefit applications in biological system such as urine and blood. Fluorescent-based ET probe constructed from fluorophore-metal complex is widely used to detect several analytes by using

ligand exchange mechanism. This approach is one of the most interesting methods because of its advantages namely high selectivity, high sensitivity and simple. Therefore, in this research we have designed fluorescent-based ET probes by using rhodamine B derivative (**Rho2**), coumarin derivative (**CouS1**) and branch-polyethyleneimine modified carbon dots (**N-CDs**) as a fluorophore to construct fluorophore-metal complex for biogenic aminies determination. Moreover, anionic surfactant namely SDS was introduced to the system for improving sensing activity in aqueous solution. Moreover, molecular logic gate was applied to the system for sensing application

The proposed sensing mechanism is illustrated in Fig 1.28. Ideally, these fluorophores exhibit low fluorescence due to hydrophobicity and low rigidity. Upon the addition of anionic surfactant of SDS, the micelle would be formed resulting in fluorescence enhancement of the fluorophore. Then, the emission band would be quenched with increasing the specific metal ion due to electron transfer (ET) process. Finally, the addition of various biogenic amines would exhibit different fluorescence recovery signal due to their different binding affinity.

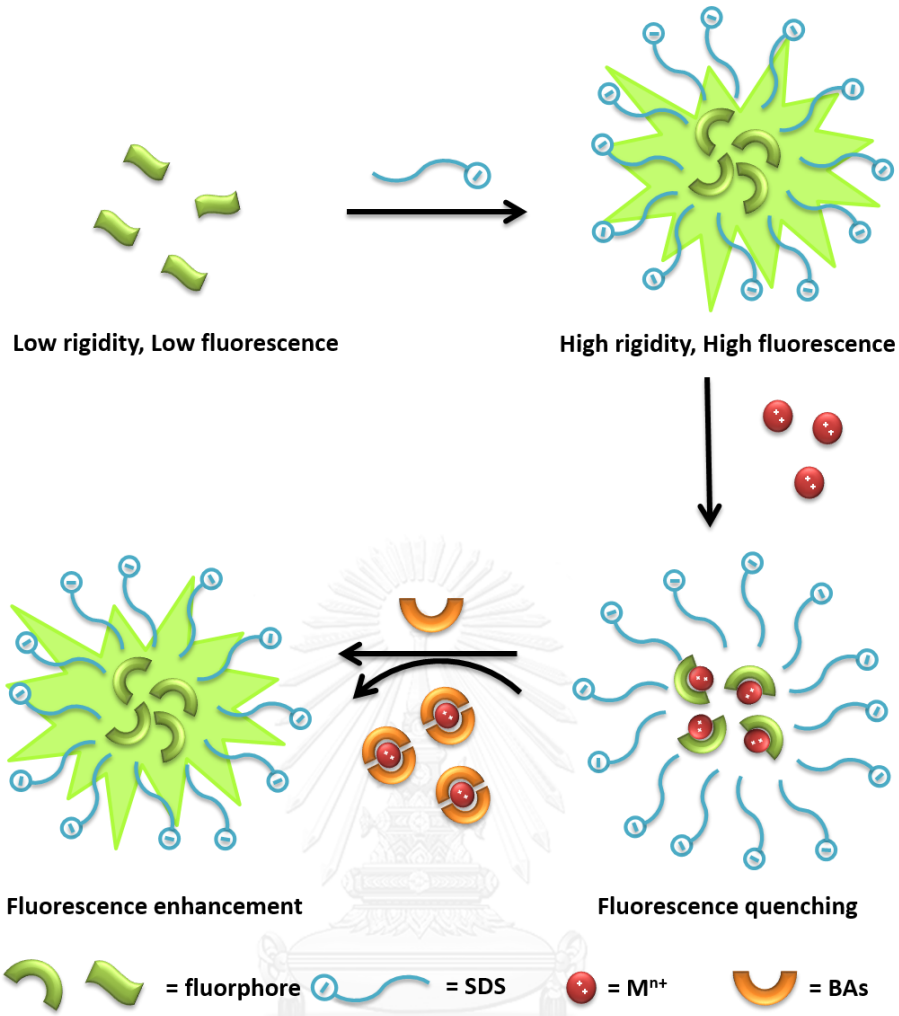

Scheme 1.1 the conceptual design of fluorophore-micellar probe for biogenic amine sensing.

1.7 Objective and scope of the research

To synthesize

- Rhodamine B derivative (**Rho2**)
- Coumarin derivative (**CouS1**)
- Branch-polyethyleneimine modified carbon dots (**N-CDs**)

To study the sensing abilities via photophysical properties under fluorescence spectroscopy

To apply the photophysical changes for construction of molecular logic gate upon the stimuli of analytes

CHAPTER II

EXPERIMENTAL

2.1 General Procedure

2.1.1 Analytical measurements

^{1}H NMR spectra and ^{13}C NMR spectra were collected by Varian Mercury 400 NMR spectrometer and Bruker DRX 400 MHz nuclear magnetic resonance spectrometer. All chemical shifts were reported in part per million (ppm) using the residual proton or carbon signal in deuterated solvent namely $CDCl_3$. MALDI-TOF mass spectra were recorded on Biflex Bruker Mass spectrometer using 2-cyano-4-hydroxycinnamic acid (CCA) as a matrix. All UV-Visible spectra were measured by Varian Cary 50 Probe UV-Visible spectrometer. All fluorescence spectra were measured by Varian Cary Eclipse Probe fluorescence spectrometer with personal computer data processing unit. The light source is Cary Eclipse pulsed xenon lamp and a detector is photomultiplier tube. All IR spectra were collected by using dried sample and performed on Thermo, Nicolet 6700 FT-IR. TEM images were recorded on a transmission electron microscopy (JEOL, JEM-2100 electron microscope). XPS Spectra were recorded on Kratos AXIS Ultra DLD X-ray photoelectron spectrometer.

2.1.2 Materials

Chemicals and solvents being standard analytical grade were purchased from Fluka, Sigma-Aldrich, Carlo erba, Merck, OmniPur, TCI or Labs scan and used without further purification. Dichloromethane was distilled using calcium hydride as drying agent under nitrogen atmosphere prior to use. Column chromatography was carried out using silica gel (Kieselgel 60, 0.063 0.200 mM, Merck). Thin layer chromatography (TLC) was performed on silica gel plates (Kieselgel 60, F_{254}, 1mM). Dimethyl sulfoxide

and acetonitrile as spectrochemical grade used in spectrophotometric measurement were used without drying. In this work, the rhodamine derivative (**Rho2**), coumarin derivative (**CouS1**) and bPEI-modified carbon dots (**N-CDs)** were synthesized for metals and biogenic amines detection in aqueous solution.

2.2 Synthesis

2.2.1 Synthesis of Rhodamine B derivatives

*2.2.1.1 Synthesis of 2-(2-aminoethyl)-3',6'-bis(diethylamino)spiro[isoindoline-1,9'-xanthen]-3-one (**Rho1**)*

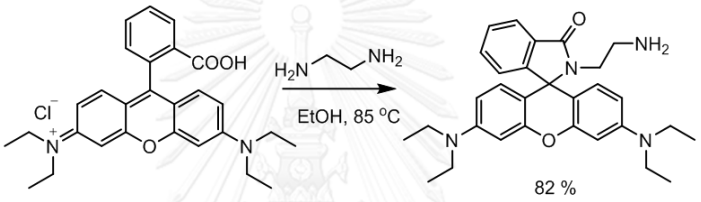

Scheme 2.1 Synthesis of **Rho1**

Rho1 was synthesized as literature [31]: A solution of rhodamine B (200 mg, 0.418 mmol) in anhydrous EtOH (5 mL) was added with ethylenediammine (502 mg, 8.35 mmol). The reaction mixture was stirred and refluxed at 85°C for 16 h. After that, the reaction mixture was cooled to room temperature and the solvent was removed by using rotary evaporator. Then, water (50 mL) was added and the mixture was extracted with CH_2Cl_2 (3×50 mL). The organic phase was washed with water and brine solution. Then, the solution was dried over Na_2SO_4. After filtration of drying agent, the solvent was evaporated followed by recrystallization in CH_2Cl_2/MeOH to give orange powder (166 mg, 82%)

Characterization data for **Rho1**

^{1}H-NMR (400 MHz, $CDCl_3$): δ (in ppm) = δ 7.74 (m, 1H), δ 7.47 (m, 2H), δ 6.98 (m, 1H), δ 6.42 (d, *J* = 8.8 Hz, 2H), δ 6.36 (s, 2H), δ 6.25 (d, *J* = 2.4 Hz, 2H), δ 3.34 (q, *J* = 4.8 Hz, 12H), δ 2.94 (t, *J* = 6.8 Hz, 2H), δ 2.16 (t, *J* = 7.6 Hz, 2H) δ 1.06 (t, *J* =6.8 Hz, 12H)

*2.2.1.2 Synthesis of N-(2-(3',6'-bis(diethylamino)-3-oxospiro[isoindoline-1,9'-xanthen]-2-yl)ethyl)octanamide (**Rho2)***

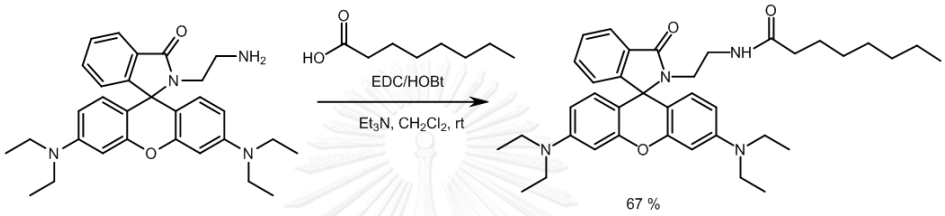

Scheme 2.2 Synthesis of **Rho2**

A solution of octanoic acid (100 mg, 0.206 mmol) in anhydrous CH_2Cl_2 (5 mL) was added with EDC (47.5 mg, 0.248 mmol), HOBt (38.0 mg, 0.248 mmol) and triethylamine (25.1 mg, 0.248 mmol). The reaction mixture was stirred at 0°C for 30 min. Then, a solution of **Rho1** in anhydrous CH_2Cl_2 (49 mg, 0.100 mmol) was added into the reaction mixture which was kept stirring at room temperature for 4 h. After that, the solvent was removed by using rotary evaporator. Then, water (50 mL) was added and the mixture was extracted with EtOAc (3×50 mL). The organic phase was washed with water and brine solution. Then, the solution was dried over Na_2SO_4. After filtration of drying agent, the solvent was evaporated and the crude product was purified by column chromatography eluting with 10% MeOH/CH_2Cl_2 to give pale solid (41 mg, 67%).

Characterization data for **Rho2**

^{1}H-NMR (400 MHz, $CDCl_3$): δ (in ppm) = 7.74 (m, 1H), δ 7.47 (m, 2H), δ 6.98 (m, 1H), δ 6.42 (d, *J* = 8.8 Hz, 2H), δ 6.36 (s, 2H), δ 6.25 (d, *J* = 2.4 Hz, 2H), δ 3.34 (q, *J* = 4.8 Hz, 12H), δ 3.05 (t, *J* = 4.8 Hz, 2H), δ 2.08 (t, *J* = 7.6 Hz, 2H) δ 0.86 (t, *J* = 6.0 Hz, 12H).

^{13}C-NMR (400 MHz, $CDCl_3$): δ (in ppm) = δ 205.73, 172.07, 168.81, 152.77, 152.22, 147.89, 131.64, 129.43, 127.32, 127.04, 122.82, 121.70, 107.20, 103.80, 96.77, 64.57, 43.26, 39.50, 39.19, 35.68, 30.65, 29.79, 28.60, 28.16, 27.96, 24.66, 21.52, 12.96, 11.52

MALDI-TOF (*m/z*) *calcd* for $C_{38}H_{50}N_4O_3$: 610.39; found 610.40 (M^+).

2.2.2 Synthesis of Coumarin derivative

*2.2.2.1 Synthesis of 7-(diethylamino)-3-(thiophen-2-yl)-2H-chromen-2-one (**CouS1)***

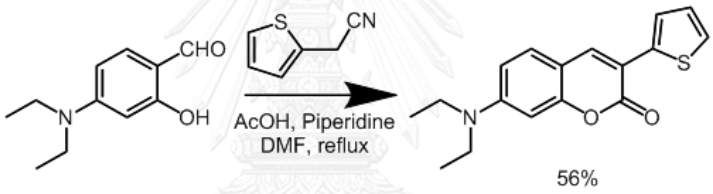

Scheme 2.3 Synthesis of **CouS1**

CouS1 was synthesized as literature [32]: A solution of 4-(Diethylamino)salicylaldehyde (2.5 g, 1294 mmol) and 2-(thiophen-2-yl)acetonitrile (1.8 g, 14.23 mmol) in DMF (20 mL) was added with AcOH (10 mL) and piperidine (5.16 mL, 51.74 mmol). The solution was stirred and refluxed under nitrogen atmosphere overnight. After that, the solution was cooled to room temperature and the solvent was evaporated. The crude product was extracted by using CH_2Cl_2/H_2O system followed by drying over Na_2SO_4. After filtration, the crude product was purified by column chromatography eluting with 30% CH_2Cl_2/hexane and recrystallized with a mixture of CH_2Cl_2 and MeOH to obtain brown solid (2.08 g, 56%).

Characterization data for **CouS1**

^{1}H-NMR (400 MHz, $CDCl_3$): δ (in ppm) = δ 7.9 (s, 1H), δ 7.7 (d, J = 7.9 Hz, 1H), δ 7.35 (d, J = 8.78 Hz, 1H), δ 7.2 (d, J = 3.8 Hz, 2H), δ 6.75 (d, J = 7.6 Hz, 1H), δ 6.55 (s, 1H), δ 3.45 (q, 4H), δ 1.2 (t, J = 7.0 Hz,6H) MALDI-TOF (*m/z*) calcd for $C_{17}H_{17}NO_2S$: 299.098; found 299.1472 (M^+).

2.2.3 Synthesis of N-CDs

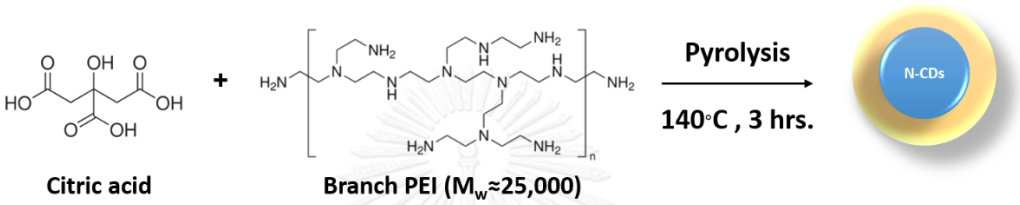

Scheme 2.4 Synthesis of **N-CDs**

N-CDs were synthesized as literature [27]: Citric acid (1.00 g) and 25 kDa bPEI (0.50 g) were mixed in 10 mL hot water and the solution was heated to 140°C. After 30 minutes, most water was evaporated, pale-yellow gel was observed. 1 mL of water would be added before the gel was burnt and kept heating. The same process was repeated until the color of gel turned to orange. Finally, the synthesized **N-CDs** were adjusted to 10 mL and purified by 12000 MW-cut off dialysis bag overnight. In the case of **CDs,** the same procedure was used to synthesize except the addition of bPEI. The solution of **CDs** and **N-CDs** were kept in 4°C for spectrophotometric measurements and the products were dried by freeze dryer for characterization.

Characterization of **N-CDs**

*Size and morphology of **N-CDs***

The morphologies and size of bPEI-modified carbon dots (**N-CDs**) have been measured and compared with **CDs** by transmission electron microscope (TEM). TEM samples of these particles were prepared by dispersion particles in 10 mM HEPES buffer

pH 7.4 by ultrasonication for 30 minutes. A drop of the solution was placed on carbon-coated copper grid. After 5 minutes, the droplet was removed by adsorbing to a piece of filter paper. The samples were dried and monitored by TEM.

Compositions and functional groups of **N-CDs**

The composition of **N-CDs** was investigated by X-ray photoelectron spectroscopy (XPS) and infrared spectroscopy. The dries samples were mounted on sample holder using TorrSeal epoxy and silver epoxy. After that, the samples were dried in ultrahigh vacuum chamber until the pressure reached to 10^{-7} torr and data were collected by XPS. The functional groups of **N-CDs** were characterized by using dried samples. For IR measurements, all samples were prepared by KBr plate method to observe functional groups of these particles compared with precursors.

2.3 Optical property studies

2.3.1 Chemicals

All chemicals were standard analytical grade. The solvents were spectrochemical grade. Metals used to complex in this study are $AgNO_3$, $AlCl_3$, $Cd(NO_3)_2 \cdot 4H_2O$, $Co(ClO_4)_2 \cdot 6H_2O$, $Cr(NO_3)_3 \cdot 9H_2O$, $Cu(ClO_4)_2 \cdot 6H_2O$, $HgCl_2$, $Mn(ClO_4)_2 \cdot 6H_2O$, $Ni(ClO_4)_2 \cdot 6H_2O$, and $Zn(ClO_4)_2 \cdot 6H_2O$. Biogenic amines used as guest molecules in this work are histidine (HD), histamine (HM), alanine (Ala), glycine (Gly), leucine (Leu), lysine (Lys), methionine (Met), phenylalanine (Phe) and threonine (Thr).

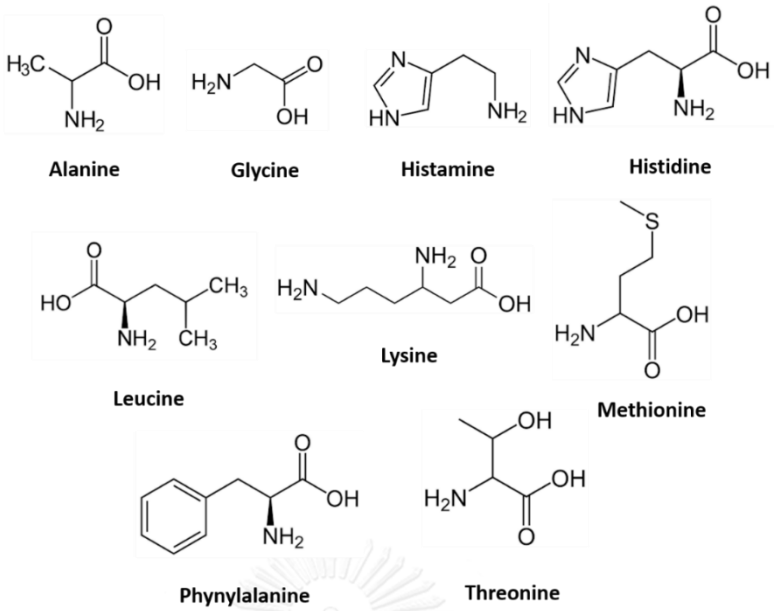

Figure 2.1 Biogenic amines that used in the experiment

2.3.2 Studies of rhodamine-QDs probe for biogenic amines sensing

The conditions set in each fluorescence experiment are illustrated below:

Excitation wavelength: 530 nm

Range of emission spectrum: 550-700 nm

Width of excitation and emission slit: 5 nm

Smoothing factor: 19

Scan rate: medium

PMT voltage: 600

*2.3.2.1 Selectivity of **Rho2** towards different metal ions in acetonitrile and 10%acetonitrile/HEPES buffer (0.01 M, pH 7.4)*

The fluorescence response of **Rho2** upon the addition of 10 μM of different metal ions in acetonitrile and 10% acetonitrile/HEPES buffer (0.01 M, pH 7.4) was studied. The stock solutions of 0.01 M of various metal ions were prepared in acetonitrile as shown in Table 2.1.

Table 2.1 Preparation of metal ion stock solutions (0.01 M)

Metal ion	Molecular weight ($gmol^{-1}$)	Weight (mg)	Volume (mL)
$AgNO_3$	169.87	3.40	2
$AlCl_3$	133.34	2.67	2
$Cd(NO_3)_2•4H_2O$	308.48	6.17	2
$Co(ClO_4)_2•6H_2O$	365.93	7.32	2
$Cr(NO_3)_3•9H_2O$	400.15	8.00	2
$Cu(ClO_4)_2•6H_2O$	370.54	7.41	2
$HgCl_2$	271.50	5.43	2
$Mn(ClO_4)_2•6H_2O$	361.93	7.23	2
$Ni(ClO_4)_2•6H_2O$	365.69	7.31	2
$Zn(ClO_4)_2•6H_2O$	372.38	7.45	2

Firstly, 2 µL of each metal stock solution was mixed with 20 µL of 1 mM **Rho2** in a 1.5 mL Eppendorf tube. The mixture was diluted to 100 µL with acetonitrile and stored at room temperature for 1 h. Then, each solution was transferred to a 1cm path length quartz cuvette and the final volume was adjusted to 2 mL with acetonitrile or 10% acetonitrile/HEPES buffer before fluorescence measurement.

*2.3.2.2 Sensitivity of **Rho2** toward different metal ions in acetonitrile*

To a 1.5 mL Eppendorf tube, the different amount of 1 mM Cu^{2+} stock soltion and 30 µL of 1 mM **Rho2** stock solution were added. The mixture was diluted to 100 µL with acetonitrile and stored at room temperature for 1 h. Then, 20 uL of each solution was transferred to a 1 cm cuvette and the final volume was adjusted to 2 mL with acetonitrile. The fluorescence spectrum was recorded.

2.3.3 Studies of coumarin-micellar probe for biogenic amines sensing

The conditions set in each fluorescence experiment are illustrated below:

Excitation wavelength: 443 nm

Range of emission spectrum: 453-700 nm

Width of excitation and emission slit: 5 nm

Smoothing factor: 19

Scan rate: medium

PMT voltage: 500

2.3.3.1 Fluorescence stability of CouS1 in 10% DMSO/HEPES buffer (0.01 M, pH 7.4) in the presence of 0.01 M Sodium dodecyl sulfate (SDS)

The fluorescence stability of **CouS1** with and without 0.01 M SDS in 10% DMSO/HEPES buffer was investigated. The stock solution of 0.1 M SDS was prepared 10 mL HEPES buffer and the stock solution of 1 mM **CouS1** was prepared in 5 mL DMSO. To a 1 cm-path length quartz cuvette, the volume of stock solutions in each condition was added as shown in Table 2.2. Before fluorescence measurement, the solution was stirred for 1 minute and fluorescence intensity was recorded with the excitation wavelength at 443 nm every 1 min for 30 min

Table 2.2 The amount of **CouS1** and SDS used for investigating of the effect of SDS on fluorescence stability of **CouS1**

Condition	1 mM **CouS1**		0.1 M SDS		V_{HEPES} (μL)	V_{total} (μL)
	[**CouS1**] (μM)	Volume (μL)	[SDS] (mM)	Volume (μL)		
No SDS	1	2	0	0	1998	2000
10 mM SDS	1	2	10	200	1798	2000

2.3.3.2 Critical micelle concentration of SDS in 10% DMSO/HEPES buffer (0.01 M, pH 7.4)

The critical micelle concentration of SDS was verified by measurement of fluorescence intensity at 518 nm with various concentration of SDS. To a 1 cm-path length quartz cuvette, the volume of stock solutions in each condition was added as shown in Table 2.3. Then, the solution was stirred for 30 minutes and fluorescence response was measured.

Table 2.3 The amount of **CouS1** and SDS used for critical micelle concentration of SDS

0.1 M SDS		1 mM **CouS1**		V_{HEPES} (µL)	V_{Total} (µL)
[SDS] (mM)	Volume (µL)	[**CouS1**] (µM)	Volume (µL)		
0.00	0	1	2	1998	2000
1.00	20	1	2	1978	2000
2.00	40	1	2	1958	2000
3.00	60	1	2	1938	2000
4.00	80	1	2	1918	2000
5.00	100	1	2	1898	2000
6.00	120	1	2	1878	2000
7.00	140	1	2	1858	2000
8.00	160	1	2	1838	2000
10.00	200	1	2	1798	2000

2.3.3.3 Selectivity of CouS1/SDS towards different metal ions in 10% DMSO/HEPES buffer (0.01 M, pH 7.4)

The fluorescence response of **CouS1** upon the addition of different metal ions in the presence of 10 mM SDS was investigated. The stock solutions of 0.01 M of various metal ions were prepared in Milli-Q water as shown in Table 2.1. To a 1 cm-path length quartz cuvette, 20 µL of 1 mM **CouS1** and 200 µL of 0.1 M SDS were mixed. The volume of solution was adjusted to 2 mL by using 10% DMSO/HEPES buffer solution and the mixture solution was stirred for 30 minutes. Then, 100 µL of various metal ion solution was added into the mixture solution which was stirred for 5 minutes. After that, the fluorescence intensity was measured.

2.3.3.4 Sensitivity of CouS1/SDS towards Co^{2+} ion in 10% DMSO/HEPES buffer (0.01 M, pH 7.4)

The fluorescence response of **CouS1** towards Co^{2+} ion in this system was investigated. The stock solution of 5 mM Co^{2+} ion was prepared by diluting 1 mL of 10 mM Co^{2+} ion stock solution in 1 mL HEPES buffer. The titration was carried out via classical titration method. Various amounts of Co^{2+} ion were directly added to the solution consisting of 10 µM of **CouS1** and 0.01 M of SDS in a 1 cm-path length quartz cuvette. The volume of Co^{2+} ion stock solutions in each condition was added as shown in Table 2.4.

Table 2.4 The concentration of Co^{2+} used for complexation study of **CouS1/SDS** by fluorescence titration technique

Entry	$V_{\textbf{1mM CouS1}}$ (µL)	$V_{0.1\ M\ SDS}$ (µL)	$V_{10\%\ DMSO/\textbf{HEPES}}$ (µL)	$V_{5mM\ Co^{2+}}$ (µL)	V_{total} (mL)	$[Co^{2+}]$ (mM)
1	2	200	1798	0	2000	0.00
2	2	200	1798	20	2020	0.05
3	2	200	1798	40	2040	0.10

4	2	200	1798	60	2060	0.15
5	2	200	1798	80	2080	0.19
6	2	200	1798	100	2100	0.24
7	2	200	1798	120	2120	0.28
8	2	200	1798	140	2140	0.33
9	2	200	1798	160	2160	0.37
10	2	200	1798	180	2180	0.41
11	2	200	1798	200	2200	0.45
12	2	200	1798	240	2240	0.54
13	2	200	1798	280	2280	0.61
14	2	200	1798	320	2320	0.69
15	2	200	1798	360	2360	0.76
16	2	200	1798	400	2400	0.83
17	2	200	1798	500	2500	1.00
18	2	200	1798	600	2600	1.15

*2.3.3.5 Selectivity of **CouS1/SDS/Co^{2+}** towards different biogenic amines in 10% DMSO/HEPES buffer (0.01 M, pH 7.4)*

The fluorescence response of **CouS1_SDS_Co^{2+}** upon the addition of different biogenic amines in this system was investigated. The stock solutions of 0.1 M various biogenic amines were prepared in Milli-Q water as shown in Table 2.5. To a 1 cm-path length quartz cuvette, 20 µL of 1 mM **CouS1**, 200 µL of 0.1 M SDS were added. The volume was adjusted to 2 mL by using 10% DMSO/HEPES buffer solution and then, the mixture solution was stirred for 10 min. After that, 100 µL of 0.01 M Co^{2+} ion was added into the solution and stirred for 10 min. Then, 50 µL of various biogenic amines

solution was added into the mixture which was stirred for 5 min. Finally, the fluorescence spectrum was measured.

Table 2.5 Preparation of biogenic amine stock solutions (0.1 M)

Biogenic amines	Molecular weight ($gmol^{-1}$)	Weight (mg)	Volume (mL)
alanine (Ala)	89.09	4.45	0.5
glycine (Gly)	75.07	3.75	0.5
histidine (HD)	155.16	7.76	0.5
histamine (HM)	111.15	5.56	0.5
leucine (Leu)	131.17	6.56	0.5
lysine (Lys)	146.19	7.31	0.5
methionine (Met)	149.21	7.46	0.5
phenylalanine (Phe)	165.19	8.26	0.5
threonine (Thr)	119.12	5.96	0.5

2.3.3.6 Sensitivity of ***CouS1/SDS/Co^{2+}*** *towards histidine in 10% DMSO/HEPES buffer (0.01 M, pH 7.4)*

The fluorescence response of **CouS1/SDS/Co^{2+}** towards histidine in this system was investigated. The stock solution of 0.01 M histidine was prepared by diluting 400 µL of 0.1 M histidine stock solution in 3.6 mL HEPES buffer. The titration was carried out via classical titration method. Various amounts of histidine were directly added to the solution consisting of 10 µM of **CouS1** and 0.01 M of SDS in a 1 cm-path length quartz cuvette. The volume of histidine stock solutions in each condition was added as listed in Table 2.6.

Table 2.6 The concentration of histidine used for complexation study of **CouS1/SDS/Co^{2+}** probe by fluorescence titration technique

Entry	$V_{1\ mM\ CouS1}$ (μL)	$V_{0.1\ M\ SDS}$ (μL)	$V_{10\mu M\ Co^{2+}}$ (μL)	$V_{10\%\ DMSO/HEPES}$ (μL)	V_{HD} (μL)	V_{total} (μL)	[HD] (mM)
1	2	200	100	1698	0	2000	0.00
2	2	200	100	1698	20	2020	0.10
3	2	200	100	1698	40	2040	0.20
4	2	200	100	1698	60	2060	0.29
5	2	200	100	1698	80	2080	0.38
6	2	200	100	1698	100	2100	0.48
7	2	200	100	1698	120	2120	0.57
8	2	200	100	1698	140	2140	0.65
9	2	200	100	1698	160	2160	0.74
10	2	200	100	1698	200	2200	0.91
11	2	200	100	1698	240	2240	1.07
12	2	200	100	1698	280	2280	1.23
13	2	200	100	1698	320	2320	1.38
14	2	200	100	1698	400	2400	1.67

*2.3.3.7 Sensitivity of **CouS1/SDS/Co^{2+}** towards histamine in 10% DMSO/HEPES buffer (0.01 M, pH 7.4)*

The fluorescence response of **CouS1/SDS/Co^{2+}** towards histamine in this system was investigated. The stock solution of 0.01 M histamine was prepared by diluting 400 μL of 0.1 M histamine stock solution in 3.6 mL HEPES buffer. The titration was carried out via classical titration method. Various amounts of histamine were directly added to the solution consisting of 10 μM of **CouS1** and 0.01 M of SDS in a 1

cm-path length quartz cuvette, the volume of histamine stock solutions in each condition was added as listed in Table 2.7.

Table 2.7 The concentration of histamine used for complexation study of **CouS1/SDS/Co^{2+}** probe by fluorescence titration technique

Entry	$V_{1\ mM\ CouS1}$ (μL)	$V_{0.1\ M\ SDS}$ (μL)	$V_{10\mu M\ Co^{2+}}$ (μL)	$V_{10\%\ DMSO/HEPES}$ (μL)	V_{HM} (μL)	V_{total} (μL)	[HM] (mM)
1	2	200	100	1698	0	2000	0.00
2	2	200	100	1698	20	2020	0.10
3	2	200	100	1698	40	2040	0.20
4	2	200	100	1698	60	2060	0.29
5	2	200	100	1698	80	2080	0.38
6	2	200	100	1698	100	2100	0.48
7	2	200	100	1698	120	2120	0.57
8	2	200	100	1698	140	2140	0.65
9	2	200	100	1698	160	2160	0.74
10	2	200	100	1698	200	2200	0.91
11	2	200	100	1698	240	2240	1.07
12	2	200	100	1698	280	2280	1.23
13	2	200	100	1698	320	2320	1.38
14	2	200	100	1698	400	2400	1.67

*2.3.3.8 Naked-eye studies of **CouS1/SDS/Co^{2+}** with various biogenic amines*

To study naked-eye fluorescence responses under ambient light and UV light of **CouS1/SDS/Co^{2+}** probe, each solution consisting of 10 μM of **CouS1**, 0.01 M of SDS and 5 mM Co^{2+} was added by 50 μL of 0.1 M various biogenic amines and the mixture

solution was stirred for 5 min before investigation under ambient light and 365nm-UV light.

*2.3.3.9 Molecular logic gate of **CouS1/SDS/Co^{2+}** for histidine and histamine detection*

To construct molecular logic gate by using **CouS1/SDS** platform for histidine sensing, the solutions were prepared as shown in Table 2.8.

Table 2.8 The amount of Co^{2+} ion and histidine used for study of molecular logic behavior of **CouS1/SDS** platform

Input	$V_{1\ mM}$ **CouS1** (μL)	$V_{0.1\ M\ SDS}$ (μL)	$V_{10mM\ Co^{2+}}$ (μL)	$V_{0.1\ M\ HD}$ (μL)	$V_{10\%}$ DMSO/**HEPES** (μL)	V_{total} (μL)
(0,0)	2	200	0	0	1798	2000
(1,0)	2	200	100	0	1698	2020
(0,1)	2	200	0	50	1748	2000
(1,1)	2	200	100	50	1648	2000

Firstly, the stock solution of **CouS1** and SDS was mixed in 10% DMSO/HEPES buffer solution to construct the **CouS1/SDS** platform. Then, the Co^{2+} ion and histidine stock solution relating to each condition were added and stirred for 5 min followed by absorbance measurement and fluorescence measurement. In the case of histamine sensing, preparation of each condition was shown in Table 2.9.

Table 2.9 The amount of Co^{2+} ion and histamine used for study of molecular logic behavior of **CouS1/SDS** platform

Input	V_{1mM} **CouS1** (μL)	$V_{0.1\ M\ SDS}$ (μL)	$V_{10mM\ Co^{2+}}$ (μL)	$V_{0.1\ M\ HM}$ (μL)	$V_{10\%}$ DMSO/**HEPES** (μL)	V_{total} (μL)
(0,0)	2	200	0	0	1798	2000
(1,0)	2	200	100	0	1698	2020

(0,1)	2	200	0	50	1748	2000
(1,1)	2	200	100	50	1648	2000

2.3.4 Studies of N-CDs-micellar probe for biogenic amine sensing

The conditions set in each fluorescence experiment are illustrated below:

Excitation wavelength: 354 nm

Range of emission spectrum: 364-700 nm

Width of excitation and emission slit: 5 nm

Smoothing factor: 29

Scan rate: medium

PMT voltage: 700

*2.3.4.1 Dependent excitation study **N-CDs** in HEPES buffer (0.01 M, pH 7.4)*

The dependtdent-excitation study of **N-CDs** in this system was investigated. Firstly, 20 µL **N-CDs** stock solution was added into a 1 cm-path length quartz cuvette and the total volume was adjusted to 2 mL by using HEPES buffer solution. The solution was stirred for 1 min and fluorescence response was recorded by varying excitation wavelength from 300-380 nm.

*2.3.4.2 Fluorescence stability of **N-CDs** in HEPES buffer (0.01 M, pH 7.4)*

The fluorescence stability of **N-CDs** in this system was investigated. 10 µL **N-CDs** stock solution was added into a 1 cm-path length quartz cuvette and the total volume was adjusted to 2 mL. Before fluorescence measurement, the solution was stirred for 1 min and fluorescence spectrum was recorded every 2 min for 60 min.

*2.3.4.3 Critical micelle concentration verification of SDS for **N-CDs** in HEPES buffer (0.01 M, pH 7.4)*

The critical micelle concentration of SDS for this system was verified by fluorescence intensity at 443 nm with various concentration of SDS. To a 1 cm-path length quartz cuvette, the volume of stock solutions in each condition was prepared as shown in Table 2.10. The solutions were stirred for 30 min and fluorescence spectrum was measured.

Table 2.10 The amount of **N-CDs** and SDS used for critical micelle concentration of SDS

Volume of **N-CDs** (μL)	0.1 M SDS		V_{HEPES} (μL)	V_{total} (μL)
	[SDS] (mM)	Volume (μL)		
10	0.00	0	1990	2000
10	0.25	5	1985	2000
10	0.50	10	1980	2000
10	0.75	15	1975	2000
10	1.00	20	1970	2000
10	1.25	25	1965	2000
10	1.50	30	1960	2000
10	1.75	35	1955	2000
10	2.00	40	1950	2000
10	2.50	50	1940	2000
10	3.00	60	1930	2000
10	3.50	70	1920	2000
10	4.00	80	1910	2000

*2.3.4.4 Selectivity of **N-CDs/SDS** upon the addition of different metal ions in HEPES buffer (0.01 M, pH 7.4)*

The fluorescence responses of **N-CDs** and **CDs** toward various metal ions with and without SDS were investigated. The stock solutions of metal ions were prepared as shown in Table 2.1. To a 1 cm-path length quartz cuvette, each condition was prepared as shown in Table 2.11 and 2.12, respectively. Before adding metal ion, each stock solution was mixed and stirred for 10 min. Then, each metal ion was added into each cuvette and stirred for 5 min before fluorescence measurement.

Table 2.11 The amount of **CDs** and SDS used for selectivity study toward different metal ions.

Condition	V_{CDs} (μL)	0.1 M SDS		V_{HEPES} (μL)	0.1 M Metal		V_{total} (μL)
		[SDS] (mM)	Volume (μL)		[metal] (mM)	Volume (μL)	
No SDS	10	0	0	1970	1	20	2000

Table 2.12 The amount of **N-CDs** and SDS used for selectivity study toward different metal ions.

Condition	$V_{N\text{-}CDs}$ (μL)	0.1 M SDS		V_{HEPES} (μL)	0.01 M Metal		V_{total} (μL)
		[SDS] (mM)	Volume (μL)		[metal] (mM)	Volume (μL)	
No SDS	10	0	0	1970	0.05	10	2000
2 mM SDS	10	2	40	1930	0.05	10	2000

*2.3.4.5 Sensitivity of **N-CDs/SDS** towards Co^{2+} ion in HEPES buffer (0.01 M, pH 7.4)*

The fluorescence response of **N-CDs/SDS** upon the addition of Co^{2+} ion was investigated. The stock solution of 2 mM Co^{2+} ion was prepared by diluting 200 µL of 10 mM Co^{2+} ion stock solution in 800 µL HEPES buffer solution. The titration was carried out via classical titration method. Various amounts of Co^{2+} ion were directly added into the solution consisting of 10 µL **N-CD** and 2 mM SDS (0.1 M, 40 µL) which was adjusted to 2 mL by using HEPES buffer solution. The volume of Co^{2+} ion stock solutions in each condition was added as shown in Table 2.13.

Table 2.13 The concentration of Co^{2+} ion used for complexation study of **N-CDs/SDS** probe by fluorescence titration technique

Entry	$V_{N\text{-}GQDs}$ (µL)	V_{SDS} (µL)	V_{HEPES} (µL)	$V_{cobalt(II)}$ (µL)	V_{total} (µL)	$[Co^{2+}]$ (mM)
1	10	40	1950	0	2000	0.00
2	10	40	1950	2	2002	0.01
3	10	40	1950	4	2004	0.02
4	10	40	1950	6	2006	0.03
5	10	40	1950	8	2008	0.04
6	10	40	1950	10	2010	0.05
7	10	40	1950	12	2012	0.06
8	10	40	1950	14	2014	0.07
9	10	40	1950	16	2016	0.08
10	10	40	1950	20	2020	0.10

*2.3.4.6 Selectivity of **N-CDs/SDS/Co^{2+}** toward various biogenic amines in HEPES buffer (0.01 M, pH 7.4)*

The fluorescence response of **N-CDs/SDS/Co^{2+}** upon the addition of various biogenic amines was investigated. Firstly, 10 µL of **N-CDs** and 40 µL of 0.1 M SDS stock

solution were mixed and the volume was adjusted to 1990 µL by using HEPES buffer solution. After stirring for 10 minutes, 10 µL of 2 mM Co^{2+} ion stock solution was added and stirrer for 5 min. Then, various biogenic amine stock solutions (50 µL, 0.1 M) including alanine (Ala), glycine (Gly), histidine (HD), histamine (HM), leucine (Leu), lysine (Lys), methionine (Met), phenylalanine (Phe) and threonine (Thr) were added into each cuvette. Before fluorescence measurement, each solution was stirred for 5 min.

*2.3.4.7 Sensitivity of **N-CDs/SDS/Co^{2+}** towards histidine in HEPES buffer (0.01 M, pH 7.4)*

The fluorescence response of **N-CDs/SDS/Co^{2+}** upon the addition of histidine was investigated. The stock solution of 0.05 M histidine was prepared by diluting 1 mL of 0.1 M histidine stock solution in 1 mL HEPES buffer (0.01 M, pH 7.4). The titration was carried out via classical titration method. Various amounts of histidine were directly added into the solution consisting of 10 µL **N-CDs** and 2 mM SDS which was adjusted to 2 mL by using HEPES buffer solution. The volume of histidine stock solution in each condition was added as shown in Table 2.14.

Table 2.14 The concentration of histamine used for complexation study of **N-CDs/SDS/Co^{2+}** probe by fluorescence titration technique

Entry	$V_{N\text{-}GQDs}$ (µL)	V_{SDS} (µL)	V_{HEPES} (µL)	$V_{Co^{2+}}$ (µL)	V_{HD} (µL)	V_{total} (µL)	[HD] (mM)
1	10	40	1940	10	0	2000	0.00
2	10	40	1940	10	10	2010	0.25
3	10	40	1940	10	20	2020	0.50
4	10	40	1940	10	30	2030	0.74
5	10	40	1940	10	40	2040	0.98
6	10	40	1940	10	50	2050	1.22

7	10	40	1940	10	60	2060	1.46
8	10	40	1940	10	70	2070	1.69
9	10	40	1940	10	80	2080	1.92
10	10	40	1940	10	90	2090	2.15
11	10	40	1940	10	100	2100	2.38
12	10	40	1940	10	120	2120	2.83
13	10	40	1940	10	140	2140	3.27
14	10	40	1940	10	160	2160	3.70
15	10	40	1940	10	180	2180	4.13
16	10	40	1940	10	200	2200	4.55

*2.3.4.8 Proposed mechanism of **N-CDs/SDS** complex toward Co^{2+} ion in HEPES buffer (0.01 M, pH 7.4)*

The solution of **N-CDs**, **N-CDs/SDS** and **N-CDs/SDS/Co^{2+}** were prepared for TEM measurement as shown in Table 2.15. All of solutions were sonicated for 30 min before dropping on the grid.

Table 2.15 Preparation of TEM measurement

Condition	$V_{N\text{-}CDs}$ (μL)	$V_{0.1\ M\ SDS}$ (μL)	$V_{2\ mM\ Co^{2+}}$ (μL)	$V_{0.1\ M\ HD}$ (μL)	V_{HEPES} (μL)	V_{total} (μL)
N-CDs	10	0	0	0	1990	2000
N-CDs/SDS	10	40	0	0	1950	2020
N-CDs/SDS/Co^{2+}	10	40	10	0	1940	2000

*2.3.4.9 Molecular logic gate of **N-CDs**/SDS for histidine detection*

To construct molecular logic gate by using **N-CDs/SDS** platform for histidine sensing, the solutions were prepared as shown in Table 2.16.

Table 2.16 The amount of Co^{2+} ion and histamine used for study of molecular logic behavior of **N-CDs/SDS** platform

Input	$V_{N\text{-}CDs}$ (μL)	$V_{0.1\ M\ SDS}$ (μL)	$V_{2\ mM\ Co^{2+}}$ (μL)	$V_{0.1\ M\ HD}$ (μL)	$V_{\mathbf{HEPES}}$ (μL)	V_{total} (μL)
(0,0)	10	40	0	0	1950	2000
(1,0)	10	40	10	0	1940	2020
(0,1)	10	40	0	50	1900	2000
(1,1)	10	40	10	50	1890	2000

Firstly, the stock solution of **N-CDs** and SDS were mixed with 10%DMSO/HEPES to construct the **N-CDs/SDS** platform. Then, the Co^{2+} ion and histidine stock solution relating to each condition were added and stirred for 5 min followed by absorbance measurement and fluorescence measurement.

CHAPTER III

RESULTS AND DISCUSSION

3.1 Conceptual design of rhodamine-QDs probe for biogenic amine sensing

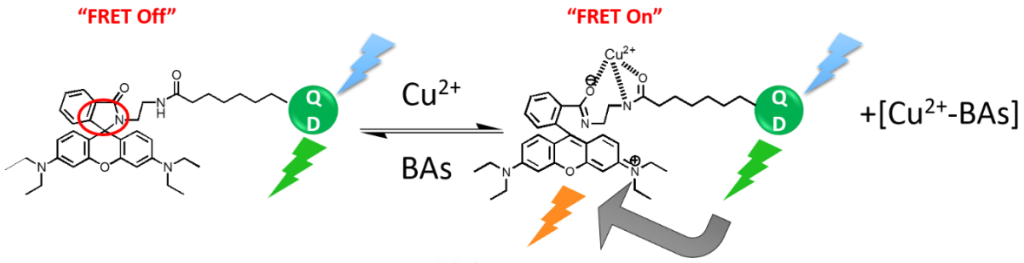

Scheme 3.1 The proposed mechanism of rhodamine-modified quantum dots probe for biogenic amine sensing

The rhodamine-modified quantum dots probe was designed and synthesized by using quantum dots (**QDs**) that appended with rhodamine derivative 2 **(Rho2)** via hydrophobic interaction between octyl chain of **Rho2** and **QDs**. In the sensing process as shown in Scheme 3.1, **QDs** and **Rho2** act as donor and acceptor, respectively. In the absence of Cu^{2+} ion, fluorescence resonance energy transfer or FRET process would not occurred or "FRET Off" when **QDs** were excited at their excitation wavelength due to spirolactam which actually the non-fluorescence performance. Upon the addition of Cu^{2+} ion, the spirolactam ring based **Rho2** would be opened leading to the fluorescence enhancement of **Rho2.** Consequently, FRET-On process would be occurred resulting in fluorescence quenching of **QDs** and fluorescence enhancement of **Rho2**. As proposed, the addition of biogenic amines, which can remove Cu^{2+} ion from the complex of **Rho2-Cu^{2+}** would decreased fluorescence signal of **Rho2** due to ring closing spirolactam resulting in the increment of fluorescence intensity of **QDs** or "FRET Off"**.** Therefore, this probe can be used for ratiometric biogenic amine determination.

Firstly, the optical properties of rhodamine derivative 2 (**Rho2**) were studied to find out the optimum condition for constructing biogenic amine probe.

3.1.1 Complexation studies of rhodamine B derivative

The complexation between **Rho2** and metal ions for biogenic amine sensing was investigated. **Rho2** containing spirolactam ring actually undergo "ring-closing" and "ring-opening" reactions upon the addition of proton or metal ions. According to Fig 3.1, no fluorescence spectrum was observed in case of free **Rho2** upon excitation wavelength of 554 nm due to its closing form of spirolactam ring.

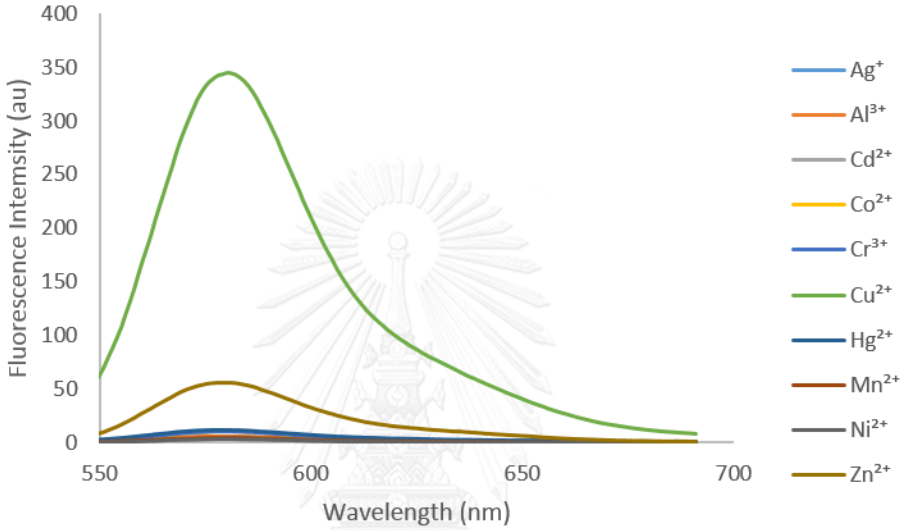

Figure 3.1 Fluorescence spectra of **Rho2** (10 μM) upon the addition of different metal ions (10 μM) in acetonitrile (excitation wavelength = 554 nm and emission wavelength = 580 nm)

Upon the addition of different metal ions, **Rho2** exhibited a strong fluorescence at 580 nm for Cu^{2+} ion and a small fluorescence response in case of Zn^{2+} ion under the excitation wavelength of 554 nm while the fluorescence spectra of other metals remained unchanged. It was expected that amide group of spirolactam ring bind to Cu^{2+} ion resulting in ring opening. This suggests a high selectivity of **Rho2** toward Cu^{2+} ion. The sensitivity of **Rho2** upon the addition of Cu^{2+} was examined. The fluorescence intensity of **Rho2** was increased with the increment of Cu^{2+} from 0 to 5 μM as shown in Figure 3.2.

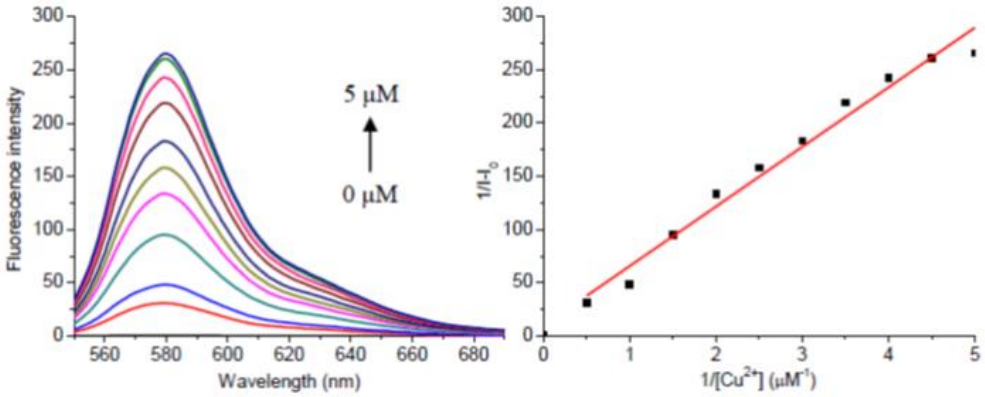

Figure 3.2 Fluorescence intensity changes and the Benesi-Hildebrand plot of **Rho2** (5 μM) upon the addition of increasing concentration of Cu^{2+} (0-5 μM) in acetonitrile.

According to Benesi-Hildebrand method, plotting of $1/(I-I_0)$ versus $1/[Cu^{2+}]$ showed a linear relationship with the correlation coefficient over 0.975 and the binding constant was calculated to be 2.20×10^5. Furthermore, the detection limit of Cu^{2+} over **Rho2** was determined by using 3σ/slope. It was found that limit of detection is approximately 5 nm. Therefore, **Rho2** enables to detect copper nanomolar level.

To use this approach for biogenic amines sensing, fluorescence measurement in aqueous solution is necessary. **Rho2** cannot be dissolved in aqueous solution due to hydrophobic octyl chain in the molecule. To improve the solubility of **Rho2** in aqueous solution, anionic surfactant sodium dodecyl sulfate (SDS) was added into the solution to form micelle inducing more dispersion of **Rho2** in solution.

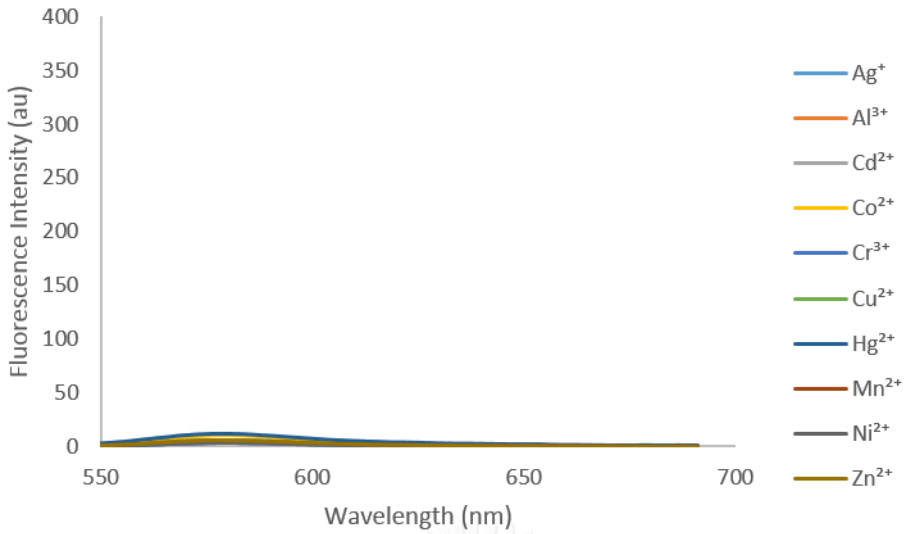

Figure 3.3 Fluorescence spectra of **Rho2** (10 μM) upon the addition of different metal ions (10 μM) in the presence of 10 mM SDS and 10% DMSO/10 mM HEPES pH 7.4 (excitation wavelength = 554 nm and emission wavelength = 580 nm)

As shown in Fig 3.3, **Rho2** cannot exhibit fluorescence spectrum at 580 nm upon the addition of various metal ions. As a result, **Rho2** cannot be used to construct the sensor for biogenic amine. Although, the rhodamine-QDs based FRET probe cannot be constructed for biogenic amine sensing. Coumarin derivative (**CouS1**) and branch-polyethyleneimine-containing carbon dots (**N-CDs**) were synthesized for constructing dye-micellar based ET probe for histidine and histamine determination as shown in Scheme 3.2

3.2 Conceptual design of fluorophore-micellar probe for biogenic amine sensing

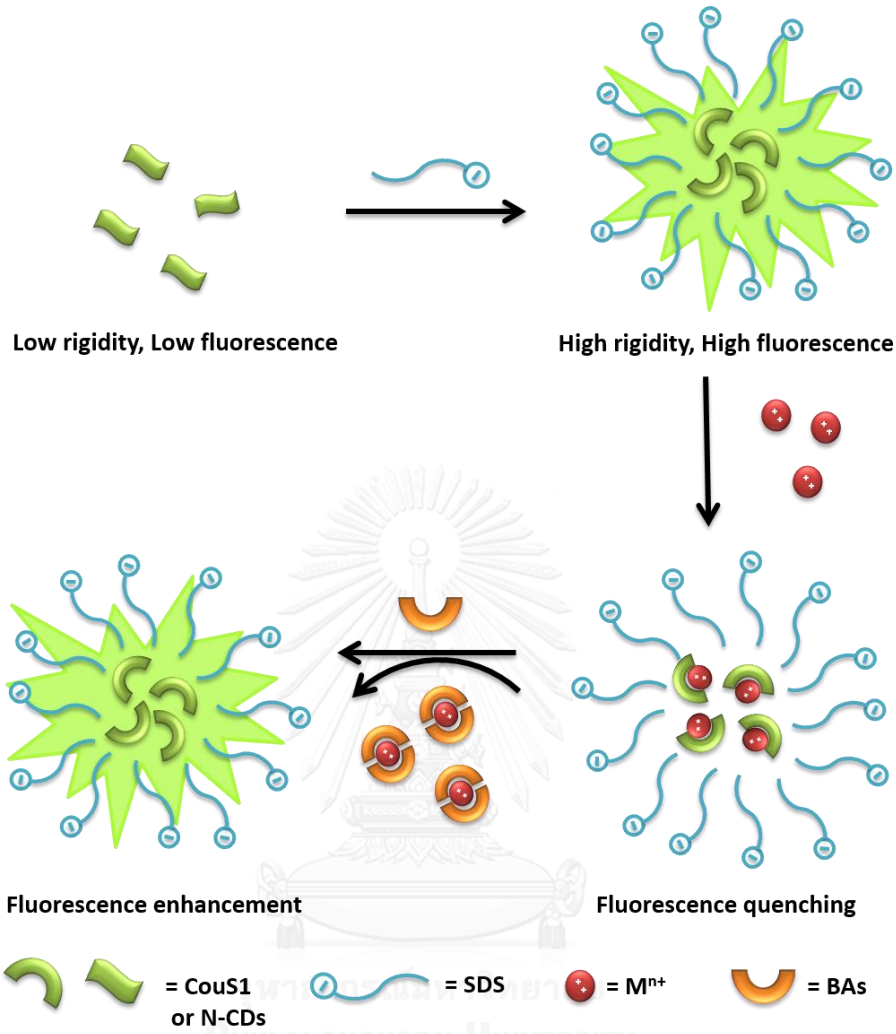

Scheme 3.2 The proposed mechanism of fluorophore-micellar probe for biogenic amine sensing.

The sensing mechanism of this probe was shown in Scheme 3.2. It was expected that dye sensors including **CouS1** or **N-CDs** exhibit low fluorescence in aqueous due to their hydrophobicity and low rigidity. Upon the addition of SDS which is anionic surfactant, the micelle would be formed and entrap the dye of **CouS1** and **N-CDs** resulting in fluorescence enhancement of the dye signal. Then, the emission band would be quenched in the presence of specific metal ion because of electron transfer (ET) process. Finally, the addition of various biogenic amines would exhibit different fluorescence recovery signal due to their different binding affinity of biogenic

amine and metal ion. Therefore, this probe was expected to be used for a specific detection of biogenic amine.

First of all, the optical properties of **CouS1/SDS** probe and **N-CDs/SDS** probe were studied to find out the optimum condition for biogenic amines sensing.

3.2.1 Complexation studies of coumarin derivative

*3.2.1.1 Fluorescence stability of **CouS1** in 10% DMSO/HEPES buffer (0.01 M, pH 7.4)*

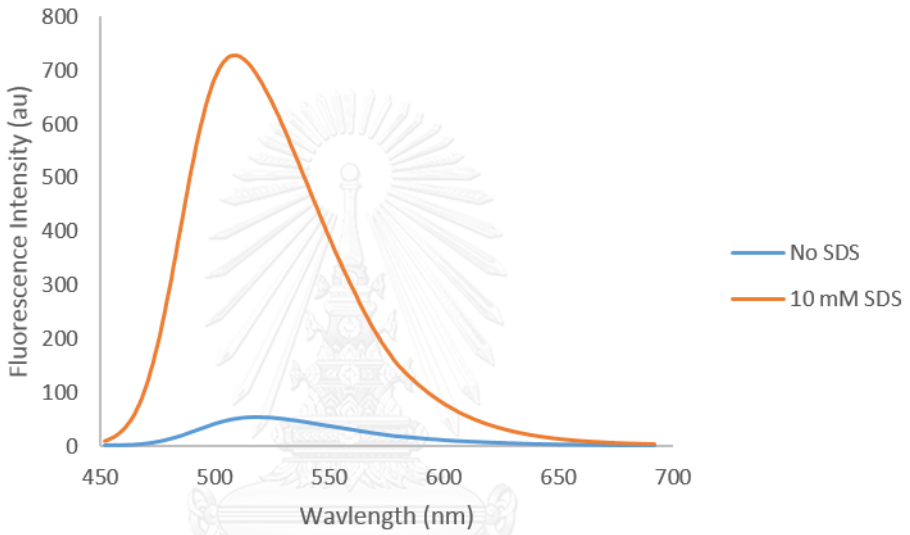

Figure 3.4 Fluorescence spectra of **CouS1** in the absence and presence of SDS at 30 min in 10% DMSO/10 mM HEPES pH 7.4 buffer (excitation wavelength = 443 nm).

The fluorescence spectra of **CouS1** were measured in mixed DMSO/HEPES buffer solutions. The solution of **CouS1** exhibits a maximum emission band at 518 nm under an excitation wavelength at 443 nm. According to the Fig 3.4, the fluorescence intensities of **CouS1** without SDS were low and decreased with the increment of time possibly caused by low rigidity of **CouS1** and interaction between **CouS1** and water. As a result, **CouS1** cannot be used to detect biogenic amine in aqueous solution. To improve the fluorescence response and stability of **CouS1** in aqueous solution, SDS was used to prepare micellar media.

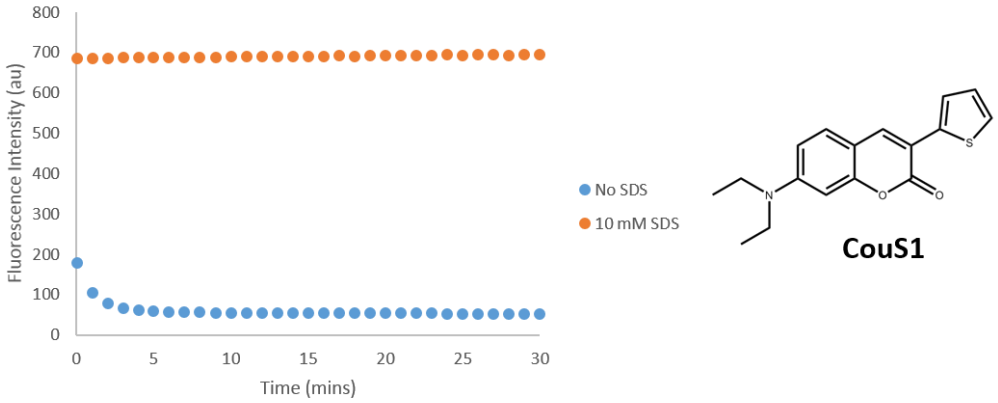

Figure 3.5 Fluorescence stability of **CouS1** at 518 nm in the absence and presence of SDS in 10% DMSO/10 mM HEPES pH 7.4 buffer (excitation wavelength = 443 nm) and chemical structure of **CouS1**.

In the presence of SDS, the fluorescence intensity remained unchanged upon increment of time because a consequent micelle enables to obstruct the interaction between **CouS1** and water. This causes the stable fluorescence intensity. Moreover, the micelle made the rigidity of **CouS1** and inhibited the interaction of dye and water causing 14-fold fluorescence enhancement in the micellar system as shown in Fig. 3.5

3.2.1.2 Critical micelle concentration (CMC) verification of SDS in 10% DMSO/HEPES buffer

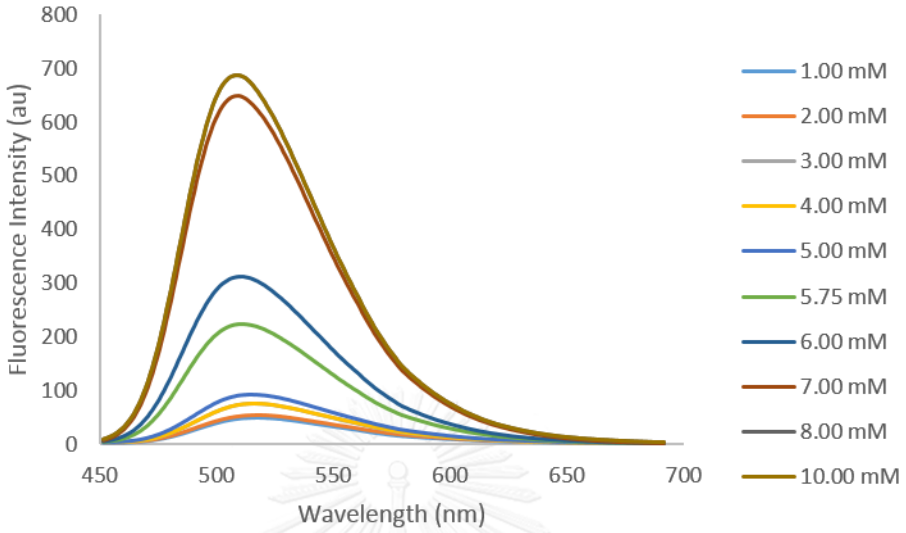

Figure 3.6 Fluorescence spectra of **CouS1** (1 μM) upon the addition of different concentration of SDS in 10% DMSO/10 mM HEPES pH 7.4 buffer (excitation wavelength = 443 nm).

To find out the appropriate concentration of SDS for the system, the critical micelle concentration of SDS was investigated. It was found that the fluorescence intensity of **CouS1** was increased upon increasing of SDS and the maximum emission wavelength was changed from 518 nm to 509 nm as shown in Fig 3.6.

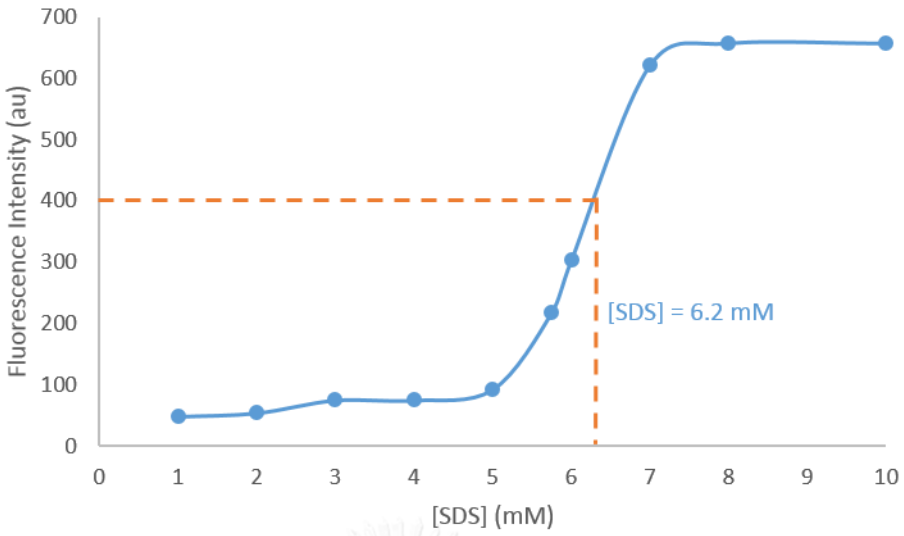

Figure 3.7 Critical micelle concentration (CMC) of SDS in 10% DMSO/10 mM HEPES pH 7.4 buffer (excitation wavelength = 443 nm and emission wavelength = 518 nm).

According to Fig 3.7, the fluorescence intensity curve of **CouS1** showed a dramatically increased from 5 mM of SDS and remained constant at 7 mM of SDS. Therefore, The critical micelle concentration (CMC) of this system was approximately 6.2 mM which is quite low compared to others finding [33, 34] possibly caused the assistant of HEPES as co-surfactant resulting in low amount of SDS to construct the micelle. However, the concentration of SDS used in all experiments was 10 mM to maintain fluorescence intensity of the system.

*3.2.1.3 Selectivity and sensitivity of **CouS1/SDS** towards different metal ions in 10% DMSO/HEPES buffer*

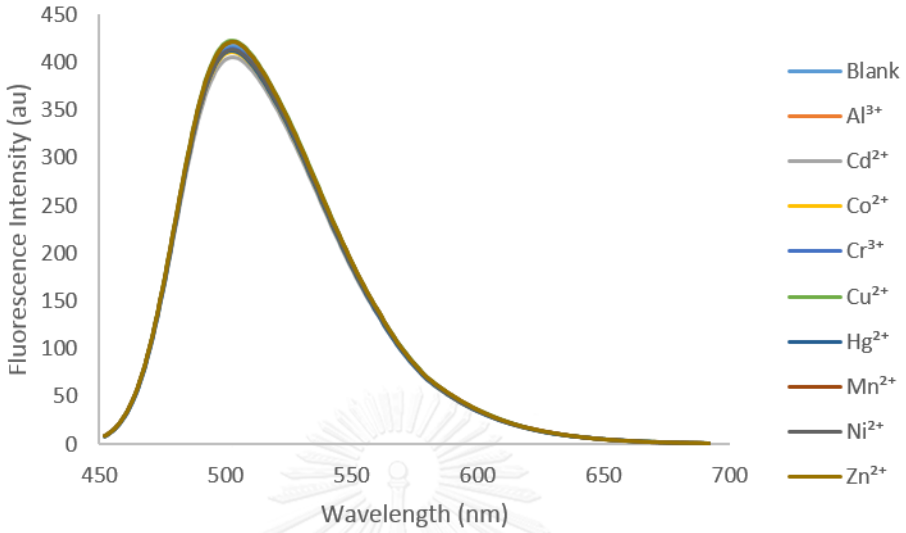

Figure 3.8 Fluorescence spectra of **CouS1** (1 μM) upon the addition of different metal ions (0.5 mM) in the absence of SDS and 10% DMSO/10 mM HEPES pH 7.4 buffer (excitation wavelength = 443 nm).

The selectivity of **CouS1** upon the addition of various metal ions in the absence and presence of 10 mM SDS was investigated. To construct the platform for biogenic amine sensing, the metal ions exhibit a large fluorescence change to **CouS1** implying high selectivity and sensitivity towards each biogenic amine. Based on electron transfer (ET) process between dye and metal, **CouS1** exhibited high fluorescence band because of ET-off state. In the absence of SDS, **CouS1** cannot interact with metals because of its low rigidity of the molecule. Even though it can bind metal cation through oxygen and sulfur in the molecule. As a result, the fluorescence spectra remained unchanged for all metal cations as shown in Fig 3.8.

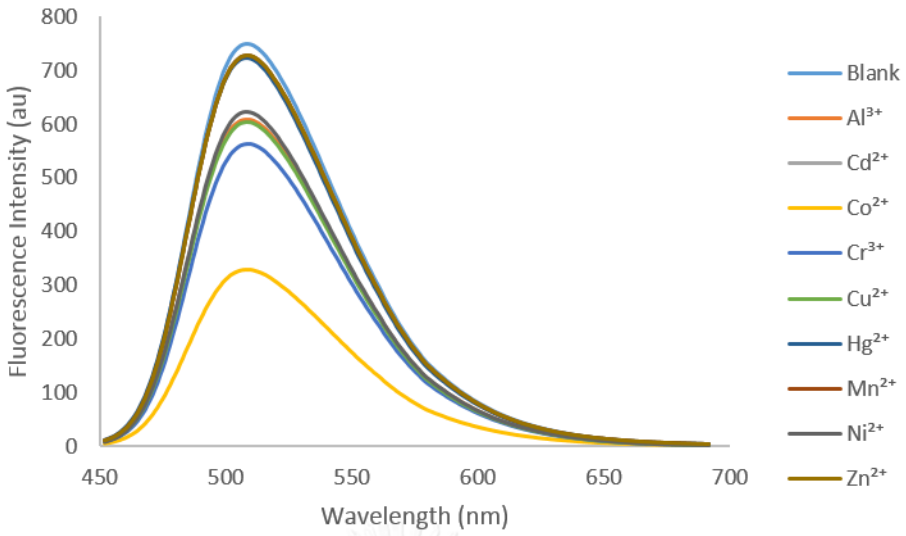

Figure 3.9 Fluorescence spectra of **CouS1** (1 μM) upon the addition of different metal ions (0.5 mM) in the presence of SDS (10 mM) and 10% DMSO/10 mM HEPES pH 7.4 buffer (excitation wavelength = 443 nm and emission wavelength = 518 nm).

In the presence of SDS, the fluorescence quenching of **CouS1** at 518 was observed. It can be explained that the hydrophobic tail of SDS can interact with **CouS1** due to hydrophobic interaction which makes it more rigid and the sulfate anions of SDS also induced metal cation into micelle by using electrostatic force. Therefore, metal cation can be captured by **CouS1** resulting in florescence changes of the dye due to PET-On process as shown in Fig 3.9. According to Fig 3.10, it was found that Co^{2+} ion exhibited the highest quenching of relative fluorescence intensity. Hence, **CouS1/SDS/Co^{2+}** is a good platform for biogenic amine detection.

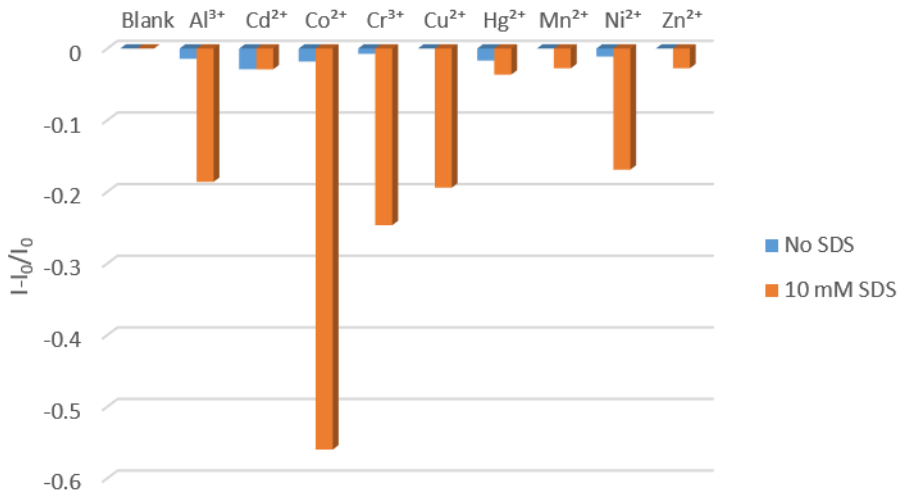

Figure 3.10 Relative fluorescence responses of **CouS1** at 518 nm toward different metal ions in the absence (blue) and presence (orange) of SDS.

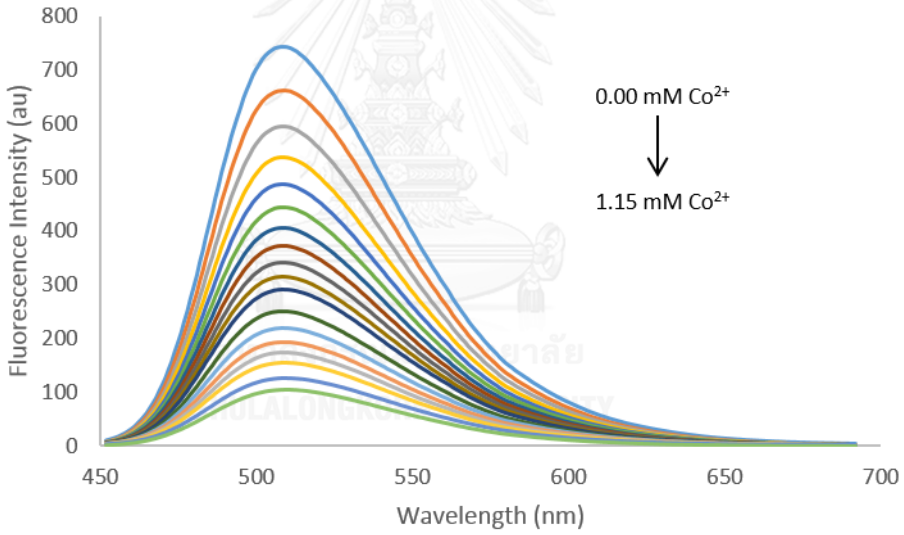

Figure 3.11 Fluorescence spectra of **CouS1/SDS** upon the addition of Co^{2+} ion in 10% DMSO/10 mM HEPES pH 7.4 buffer (excitation wavelength = 443 nm)

The proper amount of Co^{2+} ion for construction of biogenic amine probe was verified by the fluorescence quenching of **CouS1/SDS** upon the addition of Co^{2+} ion. According to Fig 3.11, the fluorescence spectra were quenched with the increasing of Co^{2+} ion concentration. The fluorescence intensity at 518 nm of **CouS1/SDS** was depreciated with the increment of Co^{2+} ion from 0-0.5 mM and it was gradually decreased until concentration of Co^{2+} ion reached to 1.15 mM as shown in Fig 3.12.

Therefore, the appropriate concentration of Co^{2+} ion in **CouS1/SDS/Co^{2+}** probe was 0.5 mM which was used to construct the probe for biogenic amine detection in all experiments. Furthermore, the binding constant (K_{sv}) and detection limit of Co^{2+} ion over **CouS1/SDS** were calculated by using Stern-Volmer plot method and 3σ/slope, respectively. It was found that the binding constant and limit of detection is approximately $2.70x10^3$ M^{-1} and 4 μM, respectively. This suggests **CouS1/SDS** enables to detect Co^{2+} ion in micromolar level.

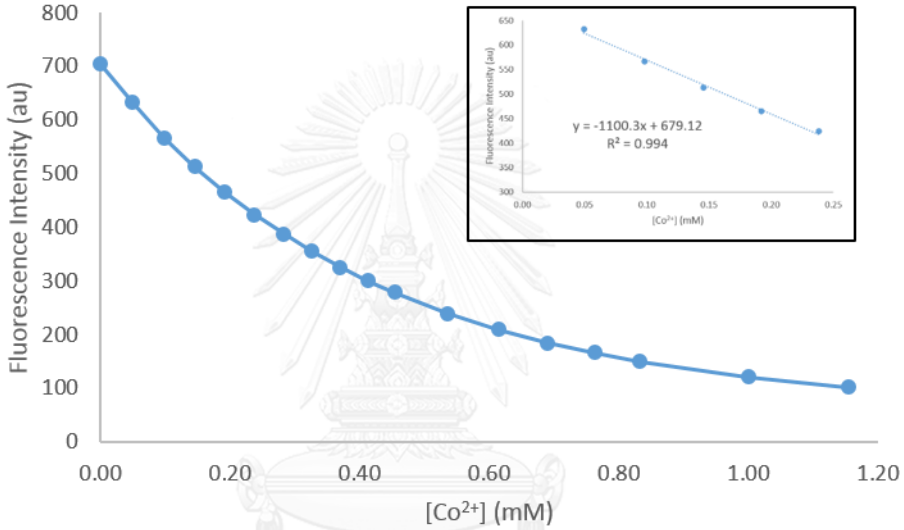

Figure 3.12 Fluorescence quenching plot between concentration of Co^{2+} ion and fluorecence intensity at 518 nm in 10% DMSO/10 mM HEPES pH 7.4 buffer (excitation wavelength = 443 nm)

3.2.1.4 Selectivity and sensitivity of ***CouS1/SDS/Co^{2+}*** *towards different biogenic amines in 10% DMSO/HEPES buffer*

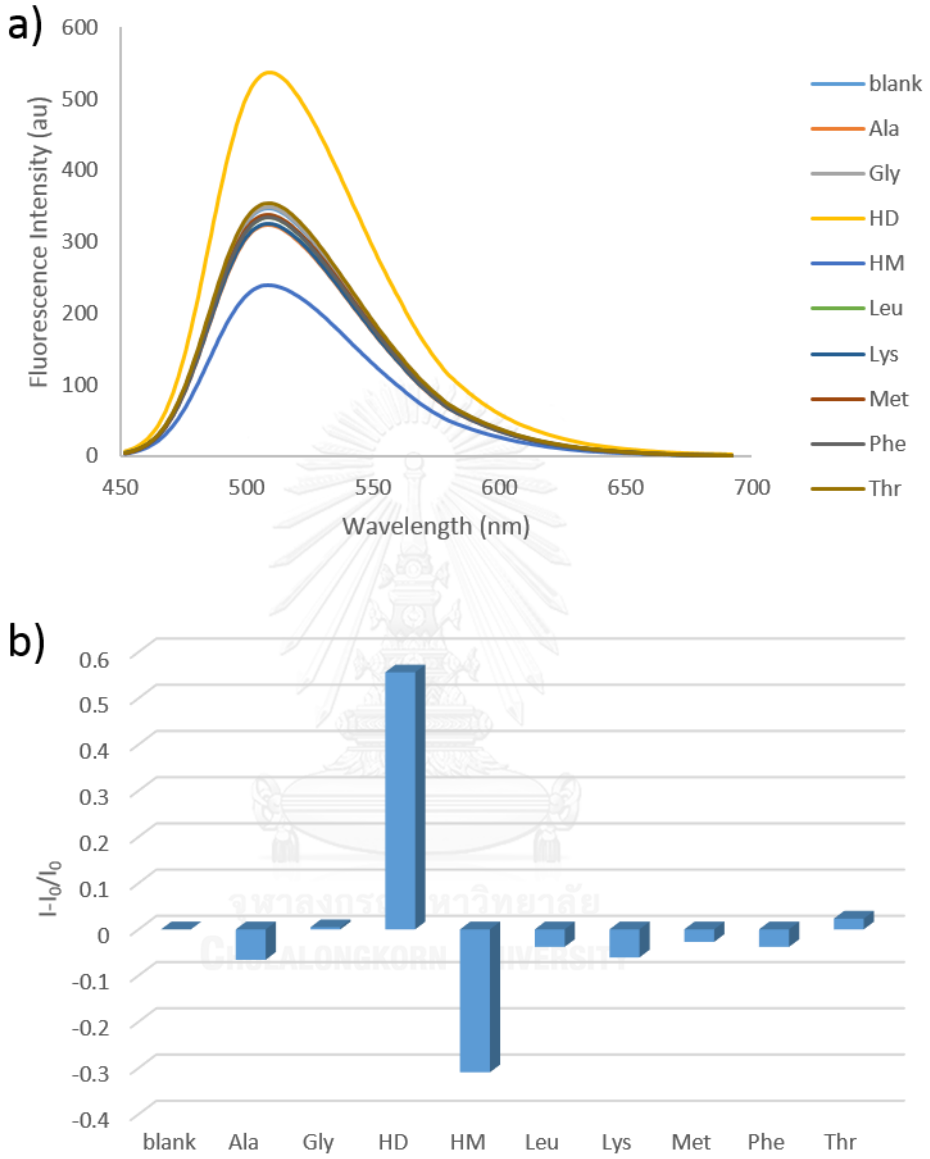

Figure 3.13 a) Fluorescence spectra and b) relative fluorescence responses at 518 nm of **CouS1/SDS/Co^{2+}** probe upon the addition of different biogenic amines (2.5 mM) in 10% DMSO/10 mM HEPES pH 7.4 buffer (excitation wavelength = 443 nm).

For biogenic amine sensing, the selectivity of **CouS1/SDS/Co^{2+}** probe was examined by the addition of various biogenic amines. From the fluorescence spectra in Fig 3.13 a), histidine showed the fluorescence enhancement of **CouS1/SDS/Co^{2+}** at 518 nm while fluorescence quenching was observed upon the addition of histamine.

For other biogenic amines, the relative fluorescence responses remained unchanged as shown in Fig 3.13 a) and b).

Based on the core structure of these biogenic amines, they consist of carboxylic and amine group which is able to complex with Co^{2+} ion**.** A recovery of fluorescence response of **CouS1/SDS/Co^{2+}** probe in the presence of histidine. It can be explained that an amino moiety and carboxylic group based on histidine preferentially form with Co^{2+} resulting in removal of Co^{2+} ion from the probe. Consequently, the performance of fluorescence enhancing of the probe was observed. Alternatively, the case of histamine induced fluorescence quenching of **CouS1/SDS/Co^{2+}** probe possibly caused by co-ordination between imidazole and amino group based histamine with the probe.

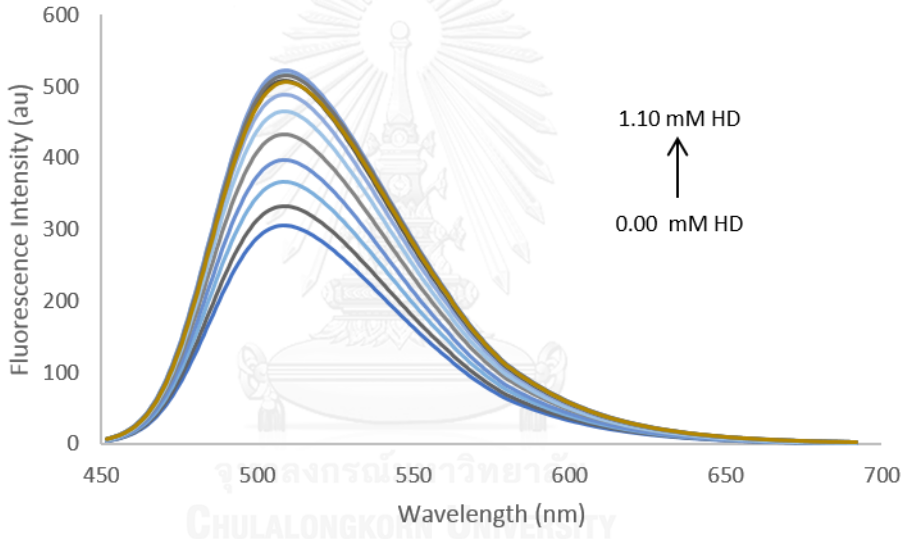

Figure 3.14 Fluorescence spectra of **CouS1/SDS/Co^{2+}** probe upon the addition of histidine in 10% DMSO/10 mM HEPES pH 7.4 buffer (excitation wavelength = 443 nm)

The fluorescence titration between the **CouS1/SDS/Co^{2+}** probe and histidine was examined. The fluorescence intensity of probe was gradually enhanced with the increasing of histidine from 0 to 0.7 mM as shown in Fig 3.14 due to ligand exchange between the probe and histidine.

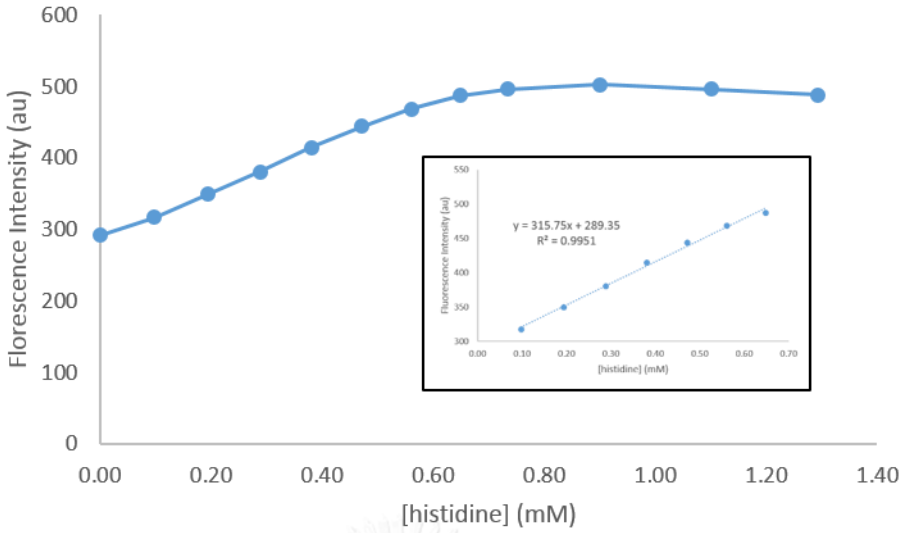

Figure 3.15 Fluorescence titration curve between concentration of histidine and fluorescence intensity at 518 nm in 10% DMSO/10 mM HEPES pH 7.4 buffer (excitation wavelength = 443 nm).

According to fluorescence titration curve, the plot of fluorescence intensity versus concentration of histidine showed a linear relationship with the correlation coefficient of 0.995 as shown in Fig 3.15. Furthermore, the detection limit of histidine over the probe was approximated 45 μM. This limit of detection of this probe suggests that **CouS1/SDS/Co^{2+}** probe enabled to apply to determine amount of histidine in both normal and histidenemia patients [2].

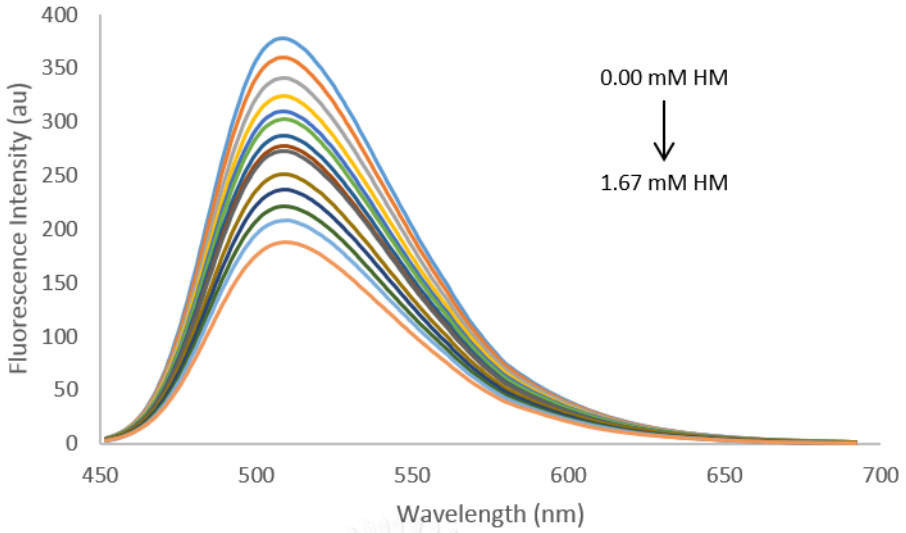

Figure 3.16 Fluorescence spectra of **CouS1/SDS/Co^{2+}** probe upon the addition of histamine in 10% DMSO/10 mM HEPES pH 7.4 buffer (excitation wavelength = 443 nm).

The fluorescence titration between the **CouS1/SDS/Co^{2+}** probe and histamine was also examined. The fluorescence intensity of probe was quenched upon the increment of histamine from 0 to 1.67 mM as shown in Fig 3.16. The plot of fluorescence intensity versus concentration of histamine showed a linear relationship with the correlation coefficient of 0.998 as shown in Fig 3.17. Furthermore, the detection limit of histamine over the probe was 85 μM which is lower than the limited level found in red wine [3].

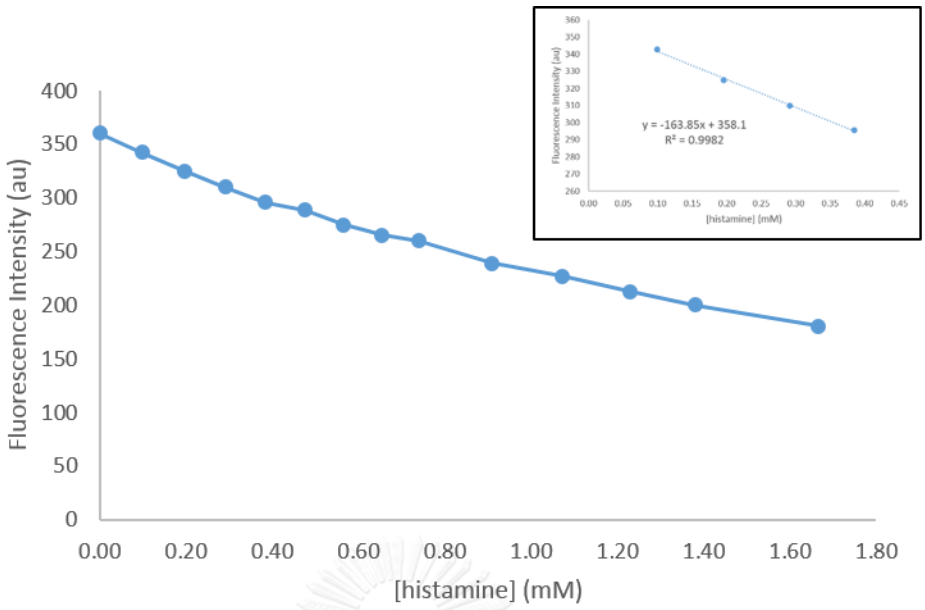

Figure 3.17 Fluorescence quenching plot between concentration of histamine and fluorescence intensity at 518 nm in 10% DMSO/10 mM HEPES pH 7.4 buffer (excitation wavelength = 443 nm).

3.2.1.5 Naked-eye studies of ***CouS1/SDS/Co^{2+}*** *probe with various biogenic amines*

It is particularly important to selectively examine the visual detection of biogenic amine. Upon the addition of different biogenic amines, the **CouS1/SDS/Co^{2+}** probe can be used to sequentially discriminate biogenic amines. By naked-eye approach, histidine and histamine exhibited the color changes from colorless to yellow because of formation of cobalt (II) complex. Among other guests including alanine, glycine, leucine, lysine, methionine, phenylalanine and threonine, the color of **CouS1/SDS/Co^{2+}** still remained unchanged. Regarding to the luminescence property of **CouS1/SDS/Co^{2+}**, the solution of **CouS1/SDS/Co^{2+}** in the presence of histidine exhibited a highly green luminescence. On the other hand, histamine induced the fluorescence darkened of **CouS1/SDS/Co^{2+}** as shown in Fig 3.18. Hence, the **CouS1/SDS/Co^{2+}** platform is the powerful tool to discriminate imidazole based biogenic amines from the other biogenic amines by visual detection. Moreover, this sensor offers the differentiate detection of histidine and histamine by luminescent behavior.

Biogenic amines	Blank	HD	HM	Ala	Gly	Leu	Lys	Met	Phe	Thr
Naked eye										
Fluorescence										

Figure 3.18 Photographs of **CouS1/SDS/Co^{2+}** upon the addition of various biogenic amines under ambient light (top) and 365nm-UV light (bottom) in 10% DMSO/10 mM HEPES pH 7.4 buffer.

*3.2.1.6 Molecular logic gate of **CouS1/SDS/Co^{2+}** for histidine and histamine detection*

Regarding to the different optical properties of CouS1/SDS with different analytes, our further attention is to apply the different fluorescence responses for creating the molecular logic gate. The combination of logic circuit was applied to molecular sensing by using **CouS1/SDS** as molecular logic gate. For histidine sensing, the two chemical inputs Co^{2+} ion and histidine are designed as *In* Co and *In* HD. The presence of these inputs is assigned as "1" while the absence of the inputs is assign as "0". The emission band at 509 nm and absorption band at 443 nm are designed as *Output* 1 and *Output* 2, respectively. The threshold values of fluorescence intensity at 509 nm and absorbance at 443 nm are 400 and 0.3 a.u. as shown in Fig 3.19 and Fig 3.21, respectively. The optical signal is higher than the threshold values assigned as "1" and the signal lower than the threshold values assigned as "0", corresponding to the "on" and "off" states of the readout signals as shown in Fig 3.20 and Fig 3.22.

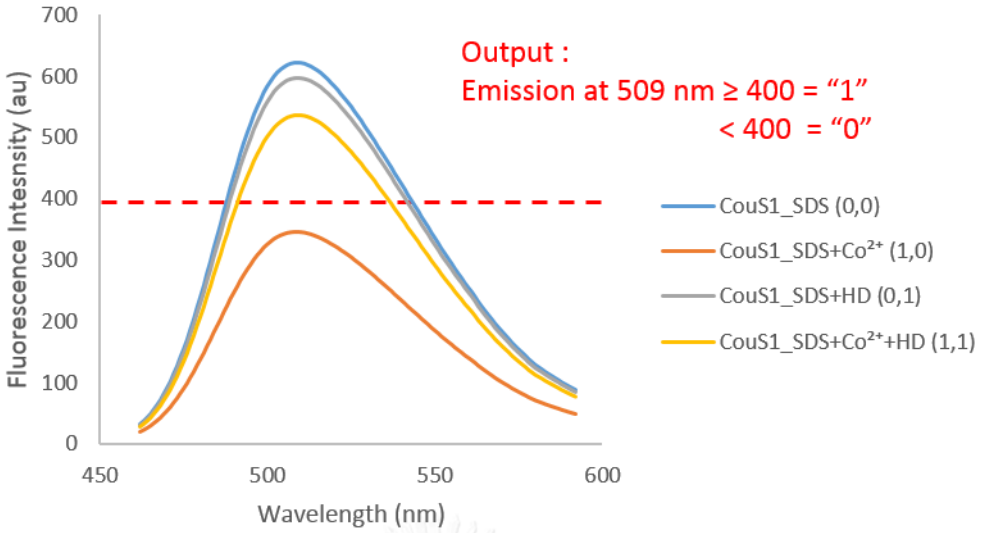

Figure 3.19 Fluorescence emission spectra of **CouS1/SDS** at different input conditions for histidine detection in 10% DMSO/10 mM HEPES pH 7.4 buffer.

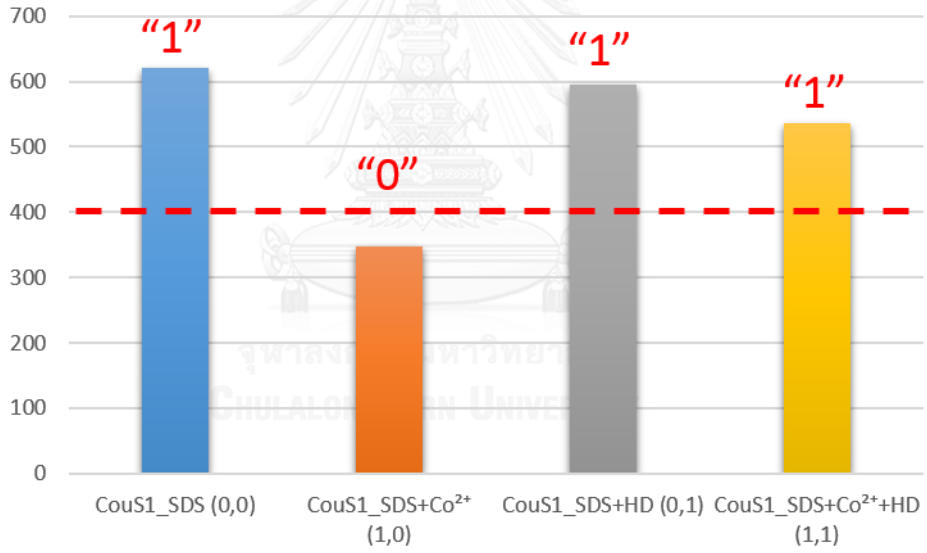

Figure 3.20 Fluorescence intensity of **CouS1/SDS** at different input conditions for histidine detection in 10% DMSO/10 mM HEPES pH 7.4 buffer.

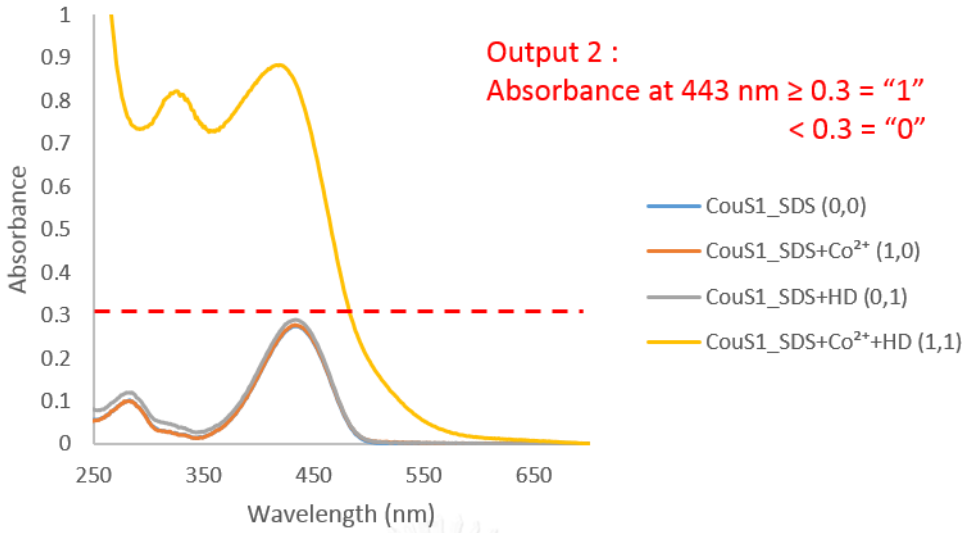

Figure 3.21 Absorption spectra of **CouS1/SDS** at different input conditions for histidine detection in 10% DMSO/10 mM HEPES pH 7.4 buffer.

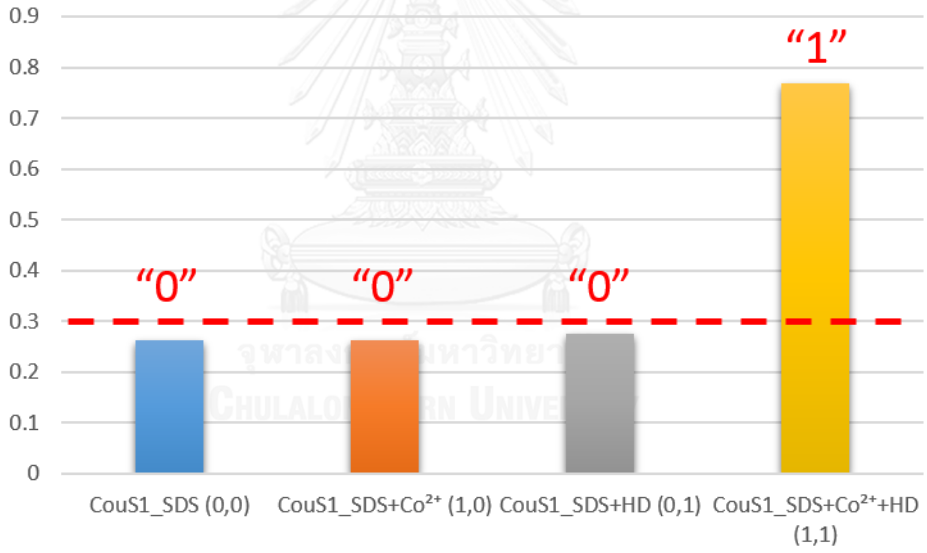

Figure 3.22 Absorbance of **CouS1/SDS** at different input conditions for histidine detection in 10% DMSO/10 mM HEPES pH 7.4 buffer.

From these information, the combinatorial logic circuit with NOT, OR, AND gates was constructed from **CouS1/SDS** platform as shown in Fig 3.23. In the absence of all inputs (0,0), this platform exhibits fluorescence intensity at 509 nm which is higher than the threshold of *output* 1 and absorbance is lower than the threshold of *output* 2. Therefore, the outputs become "1" and "0", respectively. In the presence of Co^{2+} ion with input (1,0), the fluorescence intensity quenched to 300 which is lower than the

threshold and the absorbance is also lower than 0.3 a.u. As a result, the outputs become “0” and “0”, respectively. In the case of histidine with input (0,1), the fluorescence intensity and the absorbance of the platform remained unchanged. Therefore, the outputs become “1” and “0” as same as the first condition. However, the *output* 1 and *output* 2 become “1” because the fluorescence intensity and the absorbance of the platform are higher than the thresholds upon the addition of both Co^{2+} ion and histidine (1,1). Therefore, this platform can be used as molecular logic circuit for histdine detection.

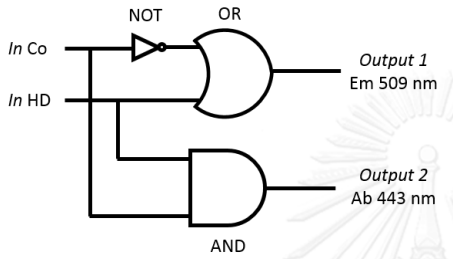

In Co	*In* Co “NOT”	*In* HD	*Output 1* “OR”	*Output 2* “AND”
0	1	0	1	0
1	0	0	0	0
0	1	1	1	0
1	0	1	1	1

Figure 3.23 The combinatorial logic circuit diagram and its truth table for histidine detection.

In case of histamine detection, the combinatorial of logic circuit with AND gates was also constructed. The two chemical inputs Co^{2+} ion and histamine were designed as *In* Co and *In* HM. The emission band at 509 nm and the absorption at 287 nm were designed as *Output* 1 and *Output* 2, respectively. The threshold values of *output* 1 at 509 nm and *output* 2 at 287 nm are 300 a.u. and 0.15 as shown in Fig 3.24 and Fig 3.26, respectively. The fluorescence intensity of *output* 1 is higher than the threshold values assigned as “1” and the intensity is lower than the threshold values assigned as “0”. Whereas the absorbance of *output* 2 is higher than the threshold assigned as “1” and it is lower than the threshold assigned as “0” as shown in Fig 3.25 and Fig 3.27.

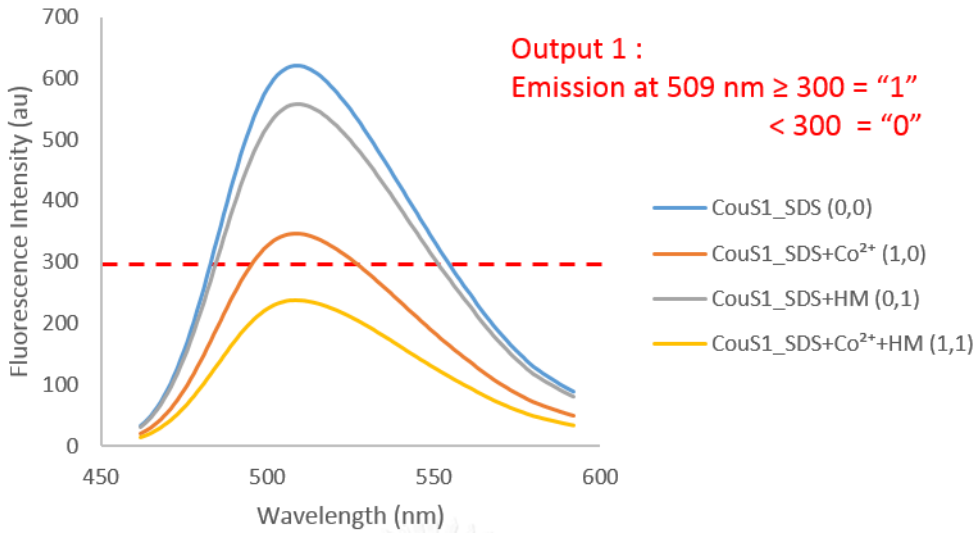

Figure 3.24 Fluorescence emission spectra and at different input conditions for histamine detection in 10% DMSO/10 mM HEPES pH 7.4 buffer.

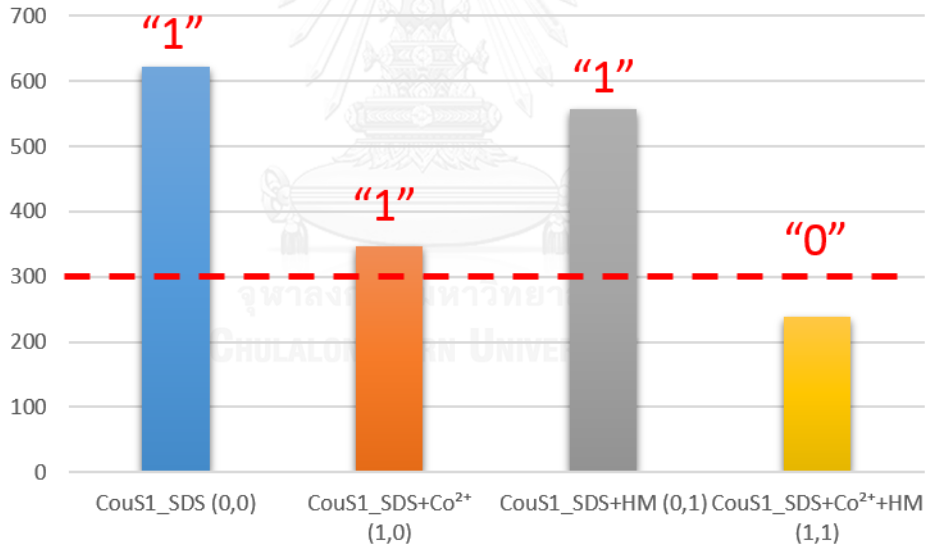

Figure 3.25 Fluorescence intensity of **CouS1/SDS** at different input conditions for histamine detection in 10% DMSO/10 mM HEPES pH 7.4 buffer.

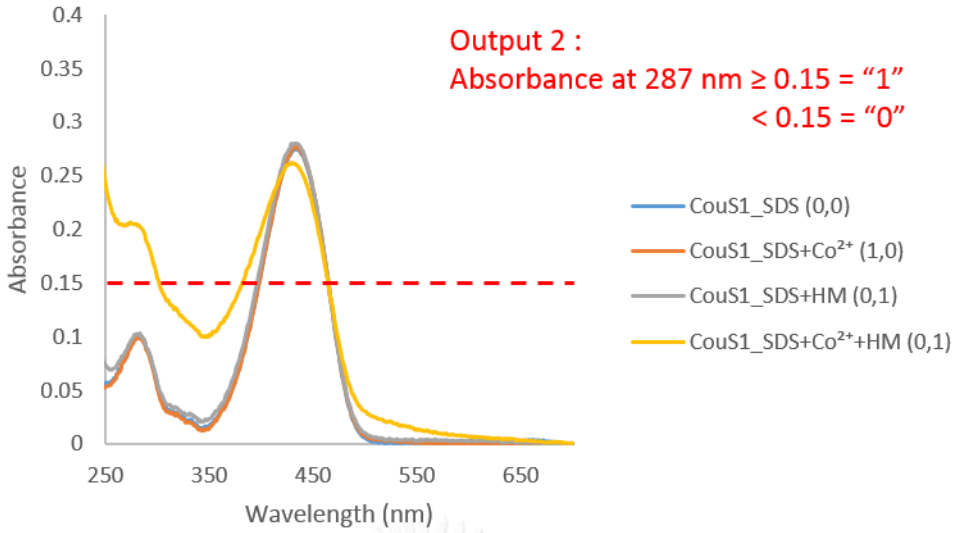

Figure 3.26 Absorption spectra of **CouS1/SDS** at different input conditions for histamine detection in 10% DMSO/10 mM HEPES pH 7.4 buffer.

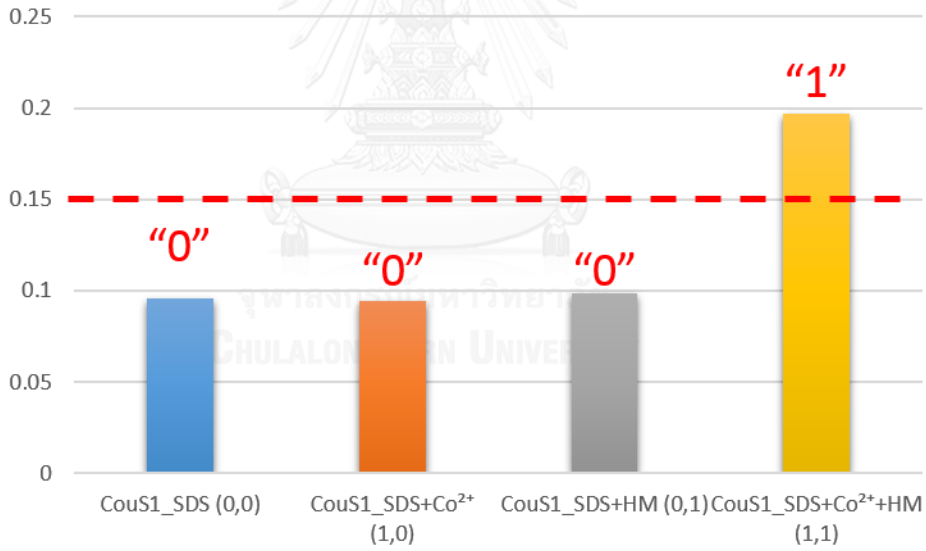

Figure 3.27 Absorbance of **CouS1/SDS** at different input conditions for histamine detection in 10% DMSO/10 mM HEPES pH 7.4 buffer.

From these information, the truth table of the circuit can be generated regarding to different conditions as shown in Fig 3.28. In the absence of all inputs (0,0), this platform exhibits fluorescence intensity at 509 nm which is higher than the threshold of *output* 1 and an absorbance is lower than the threshold of *output* 2. As a result, the outputs become "1" and "0", respectively. In the presence of Co^{2+} ion

with input (1,0), the fluorescence intensity is still higher than the threshold while the absorbance remained unchanged. Therefore, the outputs become “1” and “0” which is the same as in the case of histamine with input (0,1). However, the output 1 and output 2 become “0” and “1”, respectively, because the addition of both Co^{2+} ion and histamine in the **CouS1_SDS** solution lowered fluorescence intensity and exhibited the higher absorbance than threshold. As a result, this platform can be used as molecular logic circuit for histamine detection.

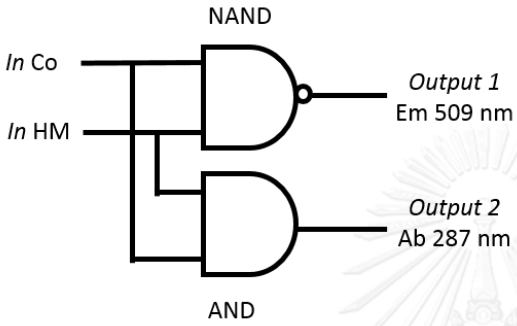

In Co	*In* HM	*Output 1* “NAND”	*Output 2* “AND”
0	0	1	0
1	0	1	0
0	1	1	0
1	1	0	1

Figure 3.28 The combinatorial logic circuit diagram and its truth table for histamine detection

3.2.2 Complexation studies of N-CDs

Besides using organic molecule as a probe for biogenic amine sensing, fluorescence nanomaterial of carbon dots (**CDs**) can also be used as a probe. Here, branch-polyethyleneimine modified carbon dots (**N-CDs**) were synthesized by pyrolysis of citric acid and polyethyleneimine at 140 °C. The structure and morphology of N-CDs were compared with bare carbon dots which were synthesized by using only citric acid. All of precursors were shown in Fig 3.29

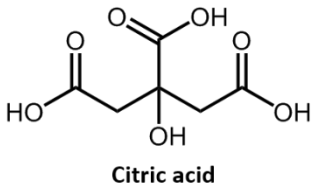

Citric acid

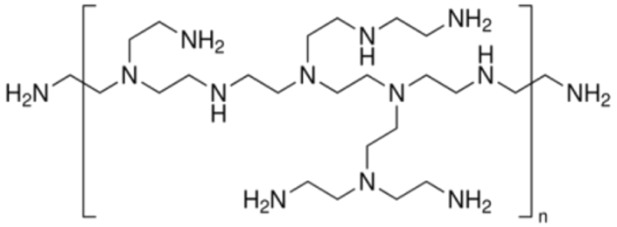

Branch-polyethyleneimine (MW ≈ 25,000)

Figure 3.29 Precursors for **CDs** and **N-CDs** synthesis

3.2.2.1 Structure and morphology of synthesized carbon dots

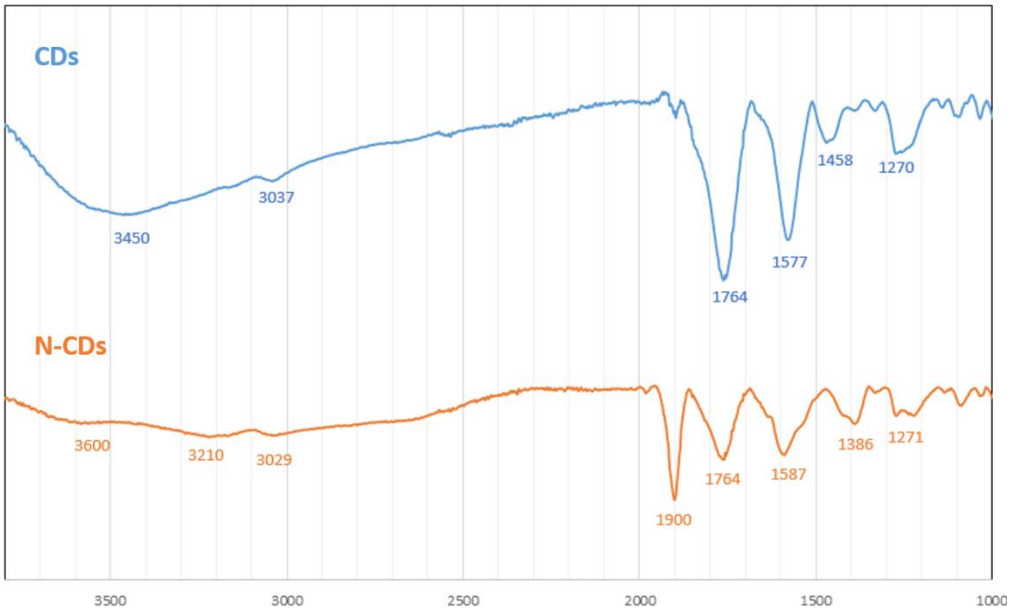

Figure 3.30 Infrared spectra of **CDs** and **N-CDs**

To find out the functional group of **N-CDs** compared with **CDs**, the dried samples of **N-CDs** and **CDs** were measured by infrared spectroscopy technique. According to Fig 3.30, it can be seen that the **CDs** have many characteristic transmittance bands including O-H stretching of alcohol and carboxylic groups (3450 cm^{-1}) , C-H stretching (3033 cm^{-1}), C=O stretching of carboxylic groups (1764 cm^{-1}), C=C stretching of aromatic groups (1578 cm^{-1}), C-H bending (1453 cm^{-1}) and C-O stretching (1282 cm^{-1}). This indicates that citric acid could undergo carbonization to form graphitic core of carbon dots and provided carboxylic groups on their edge. The case of **N-CDs** spectrum exhibited the characteristic bands including N-H stretching of amine and amide groups (3568 cm^{-1}) O-H stretching of alcohol and carboxylic groups (3220 cm^{-1}) , C-H stretching (3033 cm^{-1}), C=O stretching of amide groups (1900 cm^{-1}), C=O stretching of carboxylic groups (1764 cm^{-1}), C=C stretching of aromatic groups (1588 cm^{-1}), N-H bending of amine and amide groups (1535 cm^{-1}), C-H bending (1387 cm^{-1}) and C-O stretching (1282 cm^{-1}). This suggests that bPEI can be modified to CDs by amide formation between carboxylic groups of citric acid and amino groups of BPEI. However, the characteristic bands of carboxylic groups and amino moieties was observed. This

implied that these functional groups still remained in **N-CDs** due to an incomplete carbonization at low temperature.

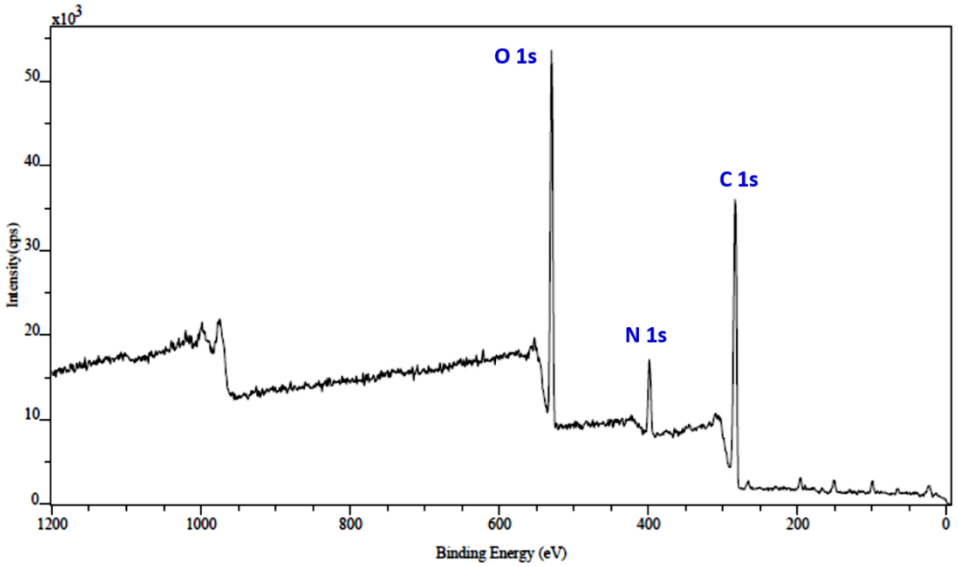

Figure 3.31 XPS survey spectrum of N-CDs

X-ray photoelectron spectroscopy measurements were measured to determine the composition of **N-CDs**. The XPS survey spectrum of **N-CDs** showed a graphitic C 1s at ca. 284 eV, N 1s at ca. 400 eV and O 1s at ca. 532 eV. This suggests that branch-polyethyleneimine which contains nitrogen atom was successfully incorporated with citric acid to form carbon dots by pyrolysis as shown in Fig 3.31.

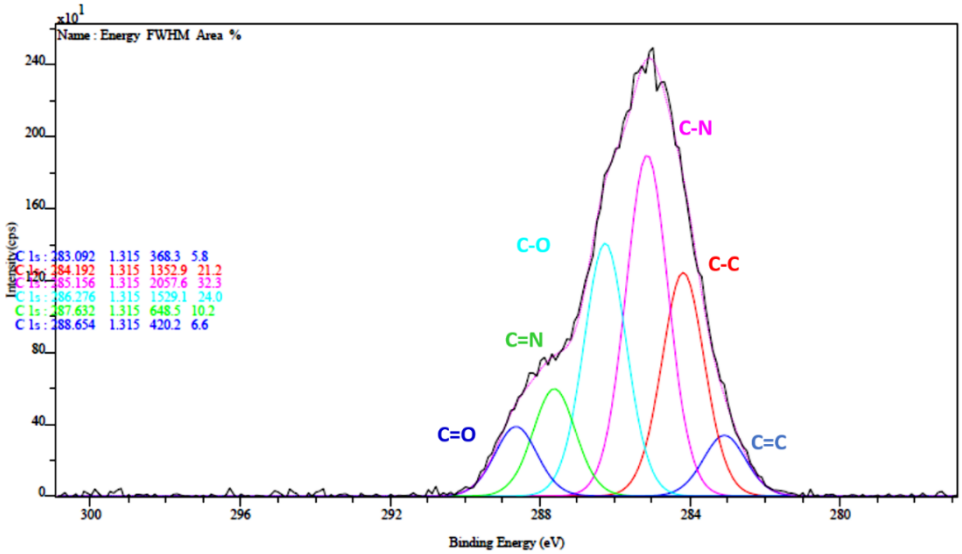

Figure 3.32 XPS C 1s spectrum of **N-CDs**

The high resolution C 1s spectrum of **N-CDs** confirmed the presence of N-rich groups including C=N (287.6 eV and C-N (285.2 eV). It can be seen that **N-CDs** also contained oxygen groups due to the occurrence of C=O (288.6 eV) and C-O (286.3 eV) as shown in Fig 3.32. Furthermore, C-C peak (284.2 eV) and C=C peak (283.1 eV) were observed due to graphitic carbon on **N-CDs**.

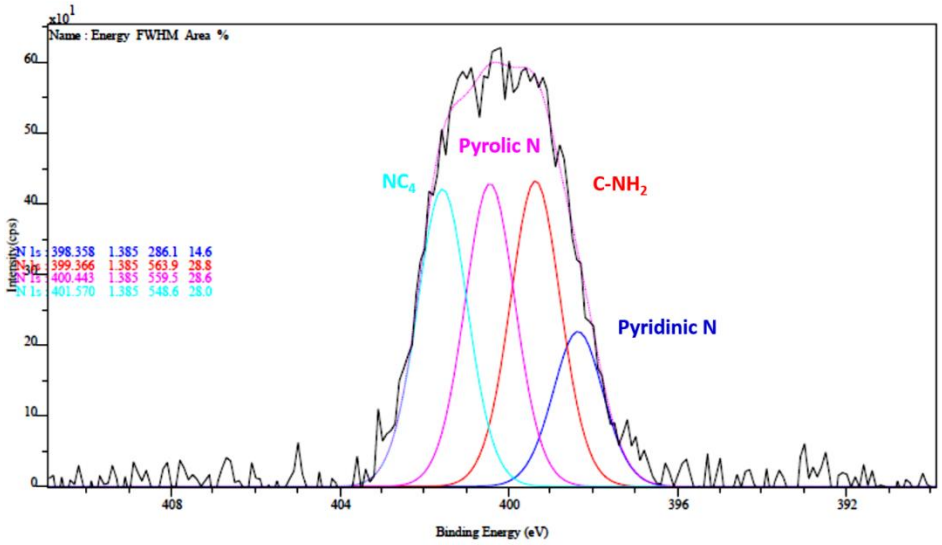

Figure 3.33 XPS N 1s spectrum of **N-CDs**

The high resolution N 1s spectrum of **N-CDs** insisted the types of nitrogen atom on **N-CDs**. The appearance of NC_4 peak (401.6 eV), pyrolic N paek (400.4 eV) and pyridinic N (398.4 eV) confirmed that nitrogen atoms of bPEI were participated in carbonization of citric acid to form carbon core of graphene. In addition, the $C\text{-}NH_2$ peak (399.4 eV) confirmed that bPEI was retained due to incomplete pyrolysis under low temperature.

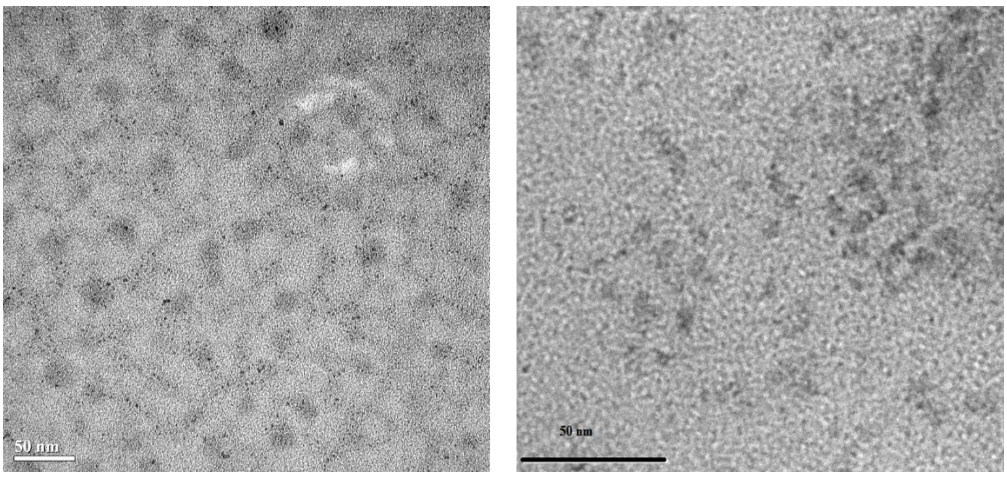

Figure 3.34 TEM images of **N-CDs** and **CDs**

According to Fig 3.34, TEM images showed morphology and size of **N-CDs** and **CDs**. It can be seen that **N-CDs** particles consisted of small particles of carbon dots that modified by bPEI. It was found that average particle size of **N-CDs** and **CDs** are 22 nm and 6 nm, respectively. The average particle size of **N-CDs** is bigger than **CDs** due to modification of bPEI .This suggests that bPEI can reduce agglomeration of the particle resulting in high fluorescence intensity of **N-CDs**. Moreover, bPEI can reduce non-radiative decay process because of more rigidity of the particle.

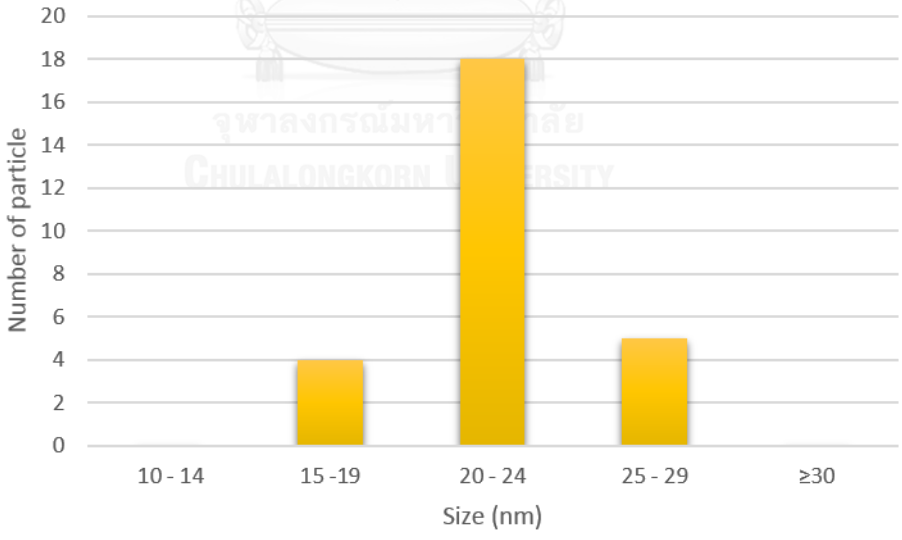

Figure 3.35 Size distribution of **N-CDs**

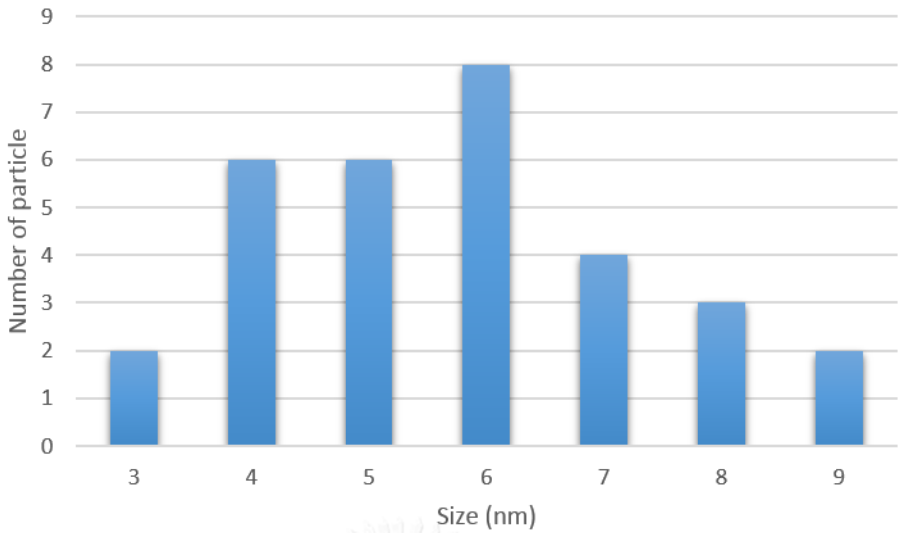

Figure 3.36 Size distribution of **CDs**

3.2.2.2 *Dependent excitation study* ***N-CDs*** *in 10%DMSO/HEPES buffer*

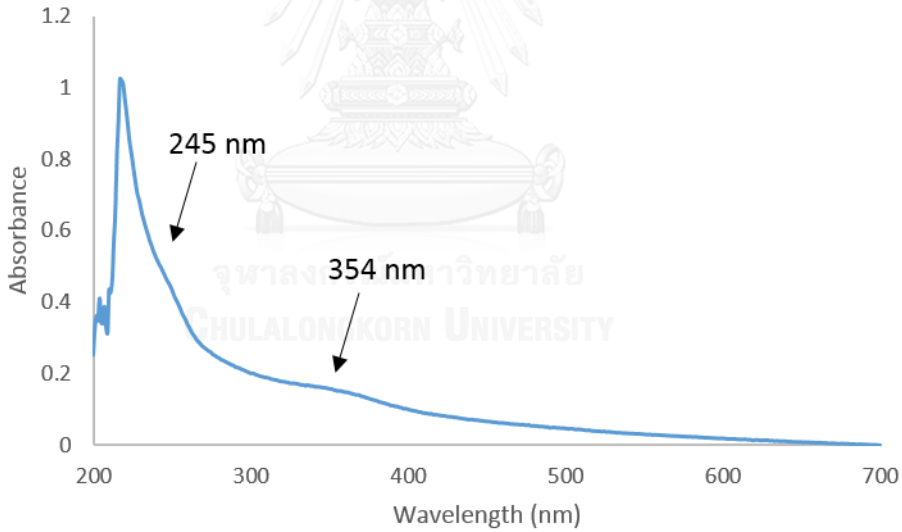

Figure 3.37 UV-Vis spectrum of N-CDs in 10 mM HEPES pH 7.4 buffer

The dependent excitation property of **N-CDs** was examined by varying excitation wavelength. To find out the appropriate excitation range for the experiment, the absorption of N-CDs solution was measured. According to Fig 3.37, the N–CDs solution has two evident absorption bands at 245 and 354 nm while citric acid and bPEI have no absorption above 240 nm [27]. Therefore, the excitation wavelengths for dependent excitation study was ranged from 300 -380 nm.

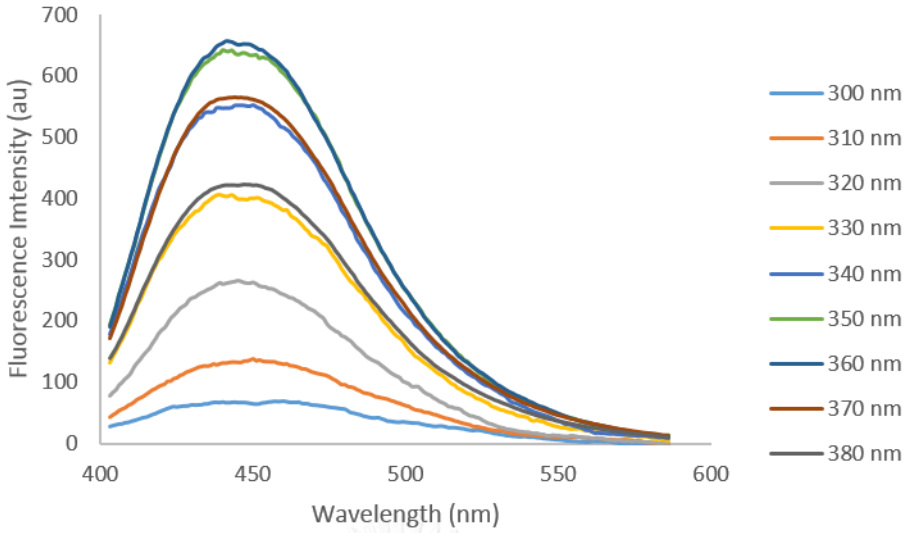

Figure 3.38 Fluorescence spectra of **N-CDs** with various excitation wavelengths in 10 mM HEPES pH 7.4 buffer.

From Fig 3.38, the fluorescence spectra of **N-CDs** solutions were measured by varying excitation wavelength. All of fluorescence spectra exhibit broad fluorescence band with the maximum emission wavelength at 443 nm. From the plot of fluorescence intensity at 443 nm and excitation wavelength in Fig 3.38, the fluorescence intensities were enhanced upon the increment of excitation wavelength from 300 to 360 nm and dramatically decreased upon the increment of excitation wavelength from 360 to 380 nm.

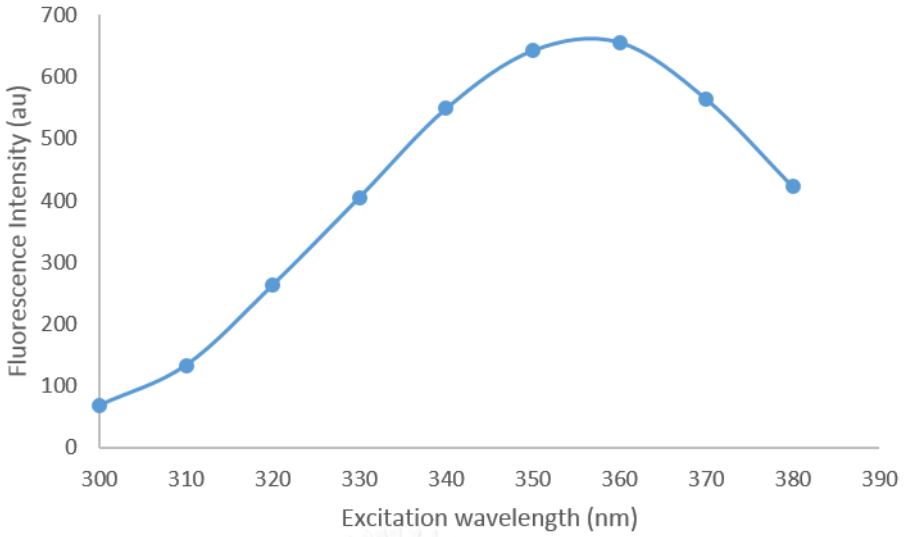

Figure 3.39 The relation between fluorescence intensity of **N-CDs** and excitation wavelengths in 10 mM HEPES pH 7.4 buffer

Interestingly, the maximum emission wavelength of the **N-CDs** remained unchanged with varying excitation wavelengths. It has been expected that the passivation of bPEI which nitrogen-containning polymer can exhibit crosslink-enhanced emission (CEE) effect. The crosslinked skeleton of the polymer will decrease the vibration and rotation relaxation which are non-radiative decay process. As a result, the independent excitation aspect of **N-CDs** has been occurred [22]. Moreover, bPEI modified on the particles can enhance the fluorescence because edge state of the particle has been change due to nitrogen atoms on **N-CDs** [21, 22, 35].

According to Fig 3.39, the highest fluorescence intensity of **N-CDs** was observed under the excitation wavelength of 354 nm. Therefore, the further fluorescence studies of **N-CDs** have been carried out under an excitation wavelength of 354 nm.

*3.2.2.3 Fluorescence stability of **N-CDs** in HEPES buffer (0.01 M, pH 7.4)*

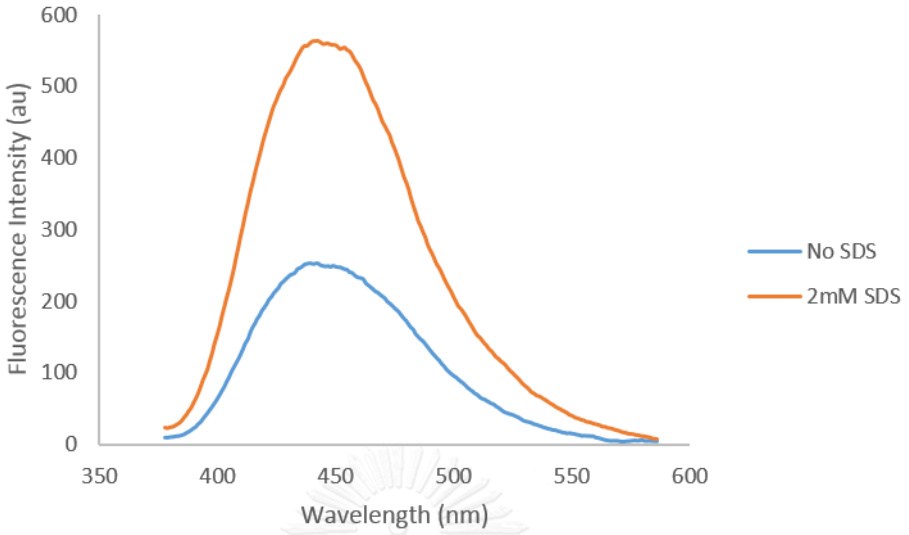

Figure 3.40 Fluorescence spectra of **N-CDs** in the absence and presence of 10 mM SDS at 60 minutes in 10 mM HEPES pH 7.4 buffer (excitation wavelength = 354 nm)

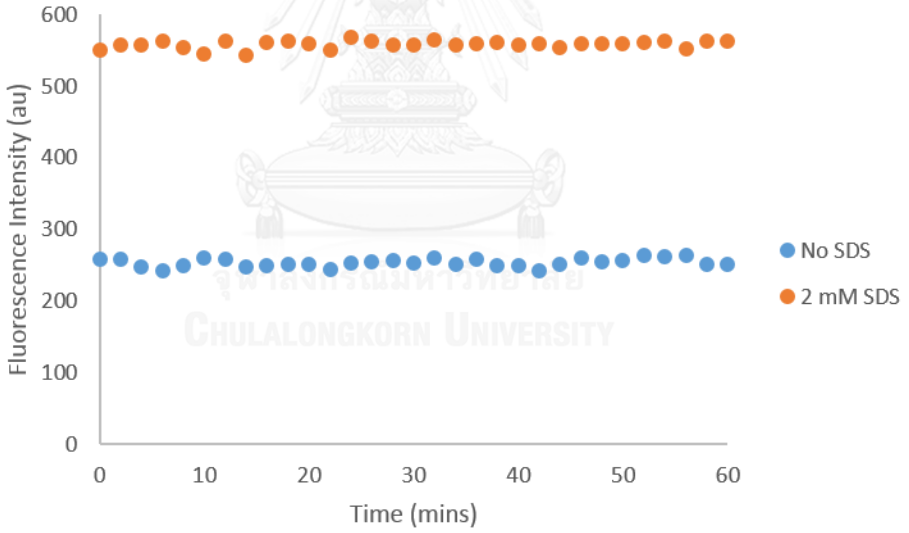

Figure 3.41 Fluorescence stability of **N-CDs** at 443 nm in the absence and presence of 10 mM SDS in 10 mM HEPES pH 7.4 buffer (excitation wavelength = 354 nm and emission wavelength = 443 nm).

The fluorescence spectra of **N-CDs** were measured at 443 nm in HEPES buffer solutions which are suitable for biogenic amines detection. Moreover, the addition of SDS has been expected to stabilize and enhance the fluorescence of N-CDs. The **N-CDs** solution in the presence of SDS exhibited a strong emission band hydrophobic

tails of SDS can cooperate with branch of PEI chain based on **N-CDs** to construct micelle that induce more rigidity of particle and more solubility in aqueous solution. The addition of SDS exhibited 2-fold increase of fluorescence intensity compared to **N-CDs** in solution without SDS as shown in Fig 3.40. Furthermore, fluorescence intensities of **N-CDs** with and without SDS showed an excellent stability upon the increment of time as illustrated in Fig 3.40. As a result, the **N-CDs/SDS** provides a benefit of a strong fluorescence response that is necessary for constructing biogenic amine probe.

*3.2.2.4 Critical micelle concentration verification of SDS for **N-CDs** in HEPES buffer*

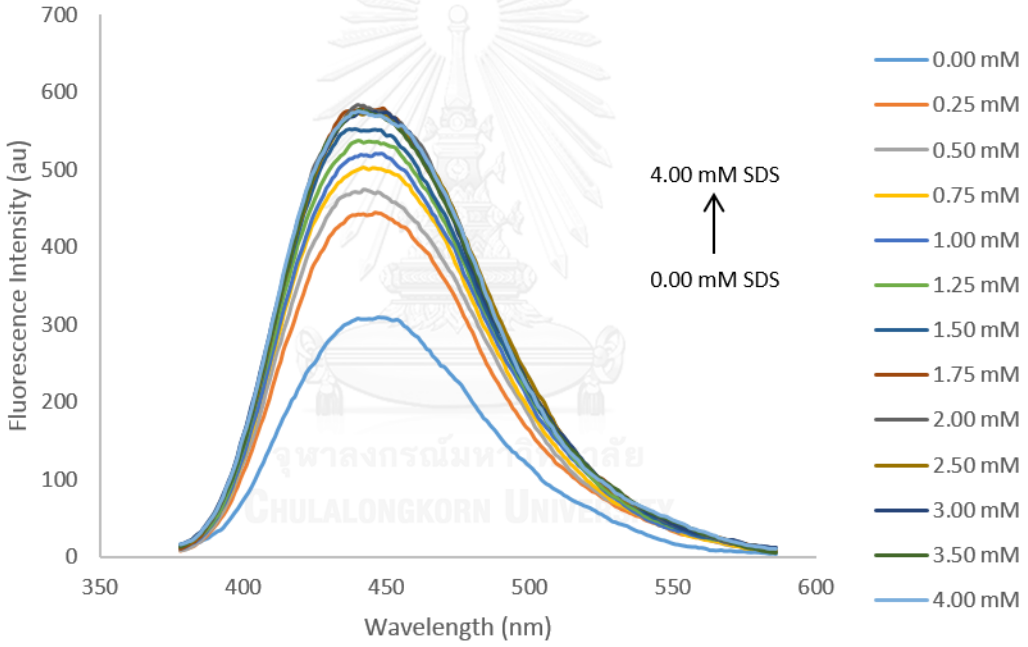

Figure 3.42 Fluorescence spectra of **N-CDs** upon the addition of different concentration of SDS in 10 mM HEPES pH 7.4 buffer (excitation wavelength = 354 nm and emission wavelength = 354 nm)

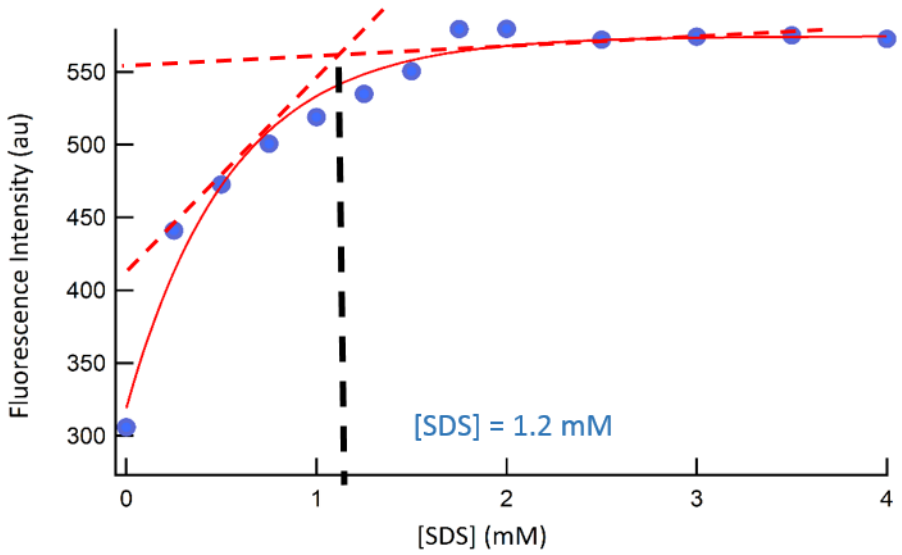

Figure 3.43 Critical micelle concentration (CMC) of SDS in 10 mM HEPES pH 7.4 buffer (excitation wavelength = 354 nm and emission wavelength = 354 nm)

To verify the appropriate concentration of SDS for the system, the critical micelle concentration of SDS was investigated. It was found that the fluorescence intensity of **N-CDs** gradually increased with increasing of SDS and the maximum emission wavelength shifted from 443 nm to 441 nm as shown in Fig 3.42. From the Fig 3.43 regarding to the critical micelle concentration, the fluorescence intensity of **N-CDs** was dramatically increased from 0 mM and remained constant at 2 mM. Therefore, The critical micelle concentration (CMC) of this system was approximatly 1.2 mM which is lower than others finding [33, 34] because branch polymer chain of **N-CDs** and HEPES molecules are the assistance of SDS to construct the micelle. However, the concentration of SDS at 2 mM was used in all experiment to ensure the micellar formation in the system.

*3.2.2.5 Selectivity and sensitivity of **N-CDs_SDS** upon the addition of different metal ions*

The effect of nitrogen based polymer which was modified on carbon dots on the selectivity and the sensitivity towards different metal ions was investigated. The fluorescence responses of **CDs** were measured upon the addition of 1.00 mM different metal ions as shown in Fig 3.44.

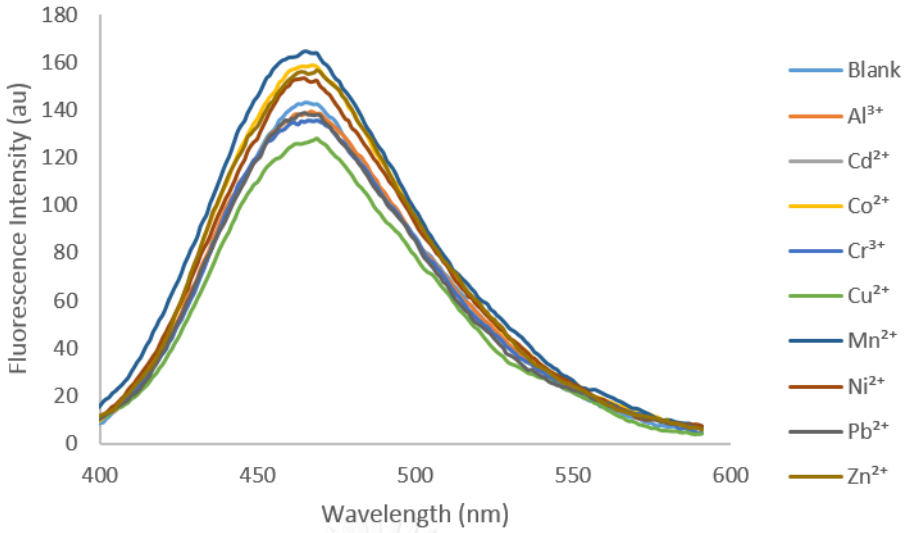

Figure 3.44 Fluorescence spectra of **CDs** upon the addition of 1.00 mM different metal ions in 10 mM HEPES pH 7.4 buffer (excitation wavelength = 360 nm)

The fluorescence spectra of **CDs** showed the slight changes in the excess of metal ions. On the contrary, the fluorescence spectra of **N-CDs** were quenched upon the addition of Co^{2+} ion, Cu^{2+} ion and Ni^{2+} ion. Based on hard-soft acid-base property of these metal ions, they preferred to bind with amino group on the **N-CDs** surface to form complex leading fluorescence quenching whereas the surface of **CDs** containing oxygen based carboxylic and hydroxyl moiety performed a weak binding with transition metal ion resulting in the observation of very small change of emission band. As a result, the synthesized **N-CDs** are capable of performing the biogenic amine probe.

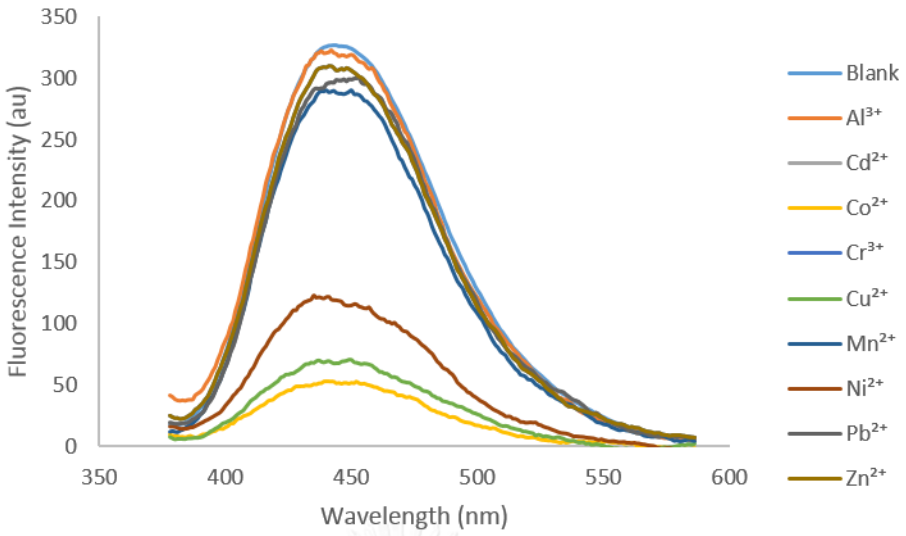

Figure 3.45 Fluorescence spectra of **N-CDs** upon the addition of 0.05 mM different metal ions in 10 mM HEPES pH 7.4 buffer (excitation wavelength = 354 nm).

As mentioned above about the benefit of SDS, we have studied the fluorescence responses of N-CDs/SDS toward various metal ions. It is known that the addition of anionic surfactant of SDS would make **N-CDs** more rigid providing and stability of the particle. The selectivity of **N-CDs** upon the addition of various metal ions in the absence and presence of 2 mM SDS was investigated. In the absence of SDS, free **N-CDs** actually exhibited an emission band at 443 nm about 325 a.u. as shown in Fig 3.45 whereas in the presence of SDS, free **N-CDs** exhibited very strong fluorescence spectrum at 443 nm about 550 a.u. as shown in Fig 3.46 because hydrophobic interaction between hydrophobic tail of the surfactant and branch polymer chains of N-CDs induced more rigidity of the particles resulting in more CEE effect [21].

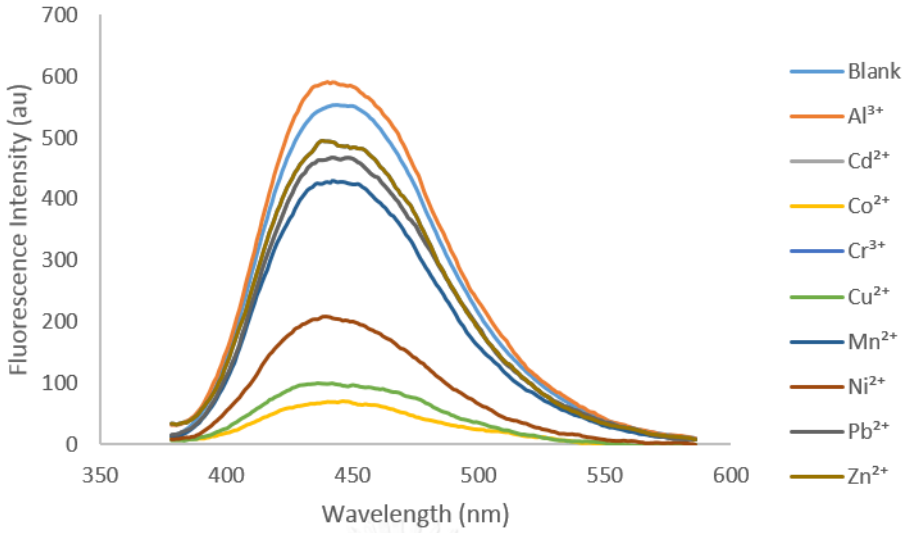

Figure 3.46 Fluorescence spectra of **N-CDs** upon the addition of 0.05 mM different metal ions in 10 mM SDS and 10 mM HEPES pH 7.4 buffer (excitation wavelength = 354 nm).

According to Fig 3.47, the trend of fluorescence changes upon the addition of various metal ions in the absence and presence of SDS is similar. However, the relative intensities between both conditions were different due to higher sensitivity of **N-CDs** in the presence of SDS. It was found that fluorescence spectra of the particles were quenched by Co^{2+} ion, Cu^{2+} ion and Ni^{2+} ion, respectively. Based on amino groups on the **N-CDs** surface, metal cations can be bound by the particles leading the florescence quenching. In the case of Co^{2+} ion, it also exhibited the significant fluorescence quenching of the **N-CDs/SDS** platform. This signified a good sensing probe of **N-CDs/SDS/Co^{2+}** for biogenic amine sensing.

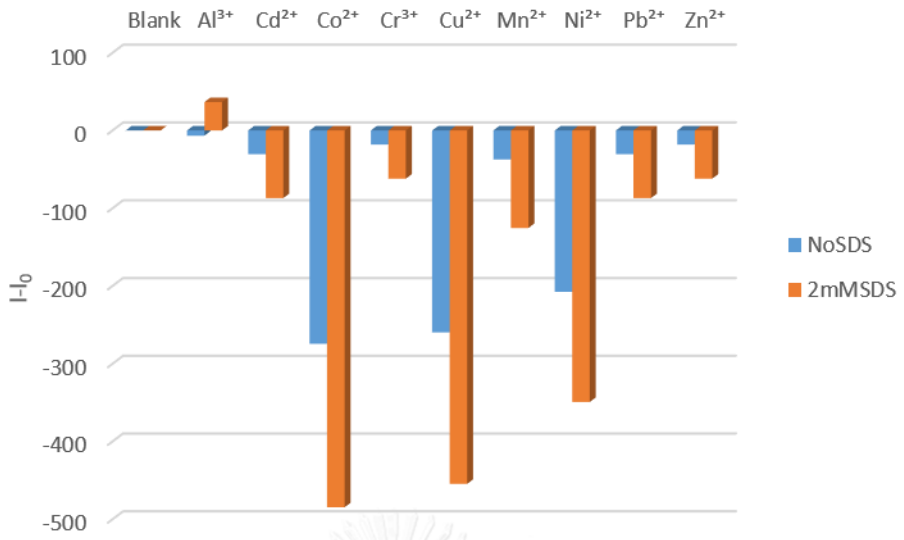

Figure 3.47 Relative fluorescence responses of **N-CQDs** toward different metal ions in the absence (blue) and presence (orange) of SDS (10 mM HEPES pH 7.4 buffer (excitation wavelength = 354 nm).

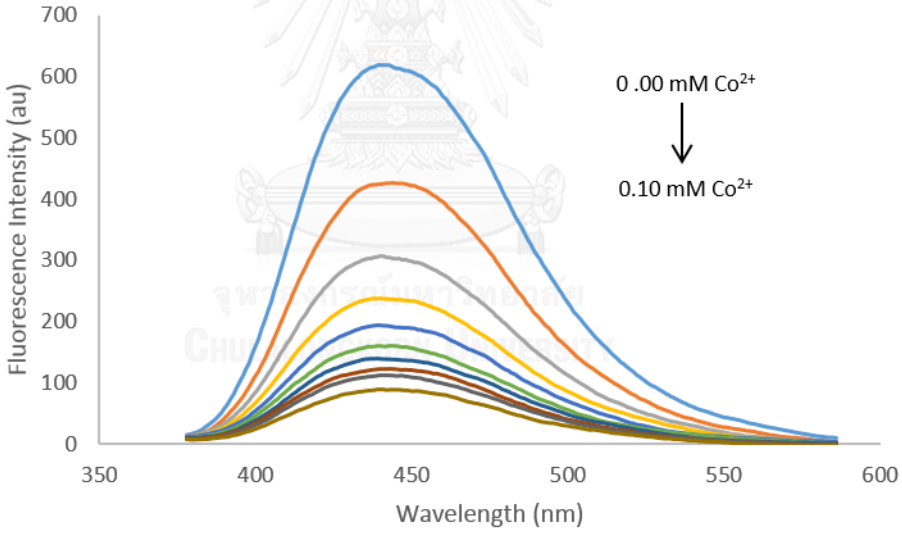

Figure 3.48 Fluorescence spectra of **N-CDs/SDS** upon the addition of Co^{2+} ion in 10 mM HEPES pH 7.4 buffer (excitation wavelength = 354 nm).

.

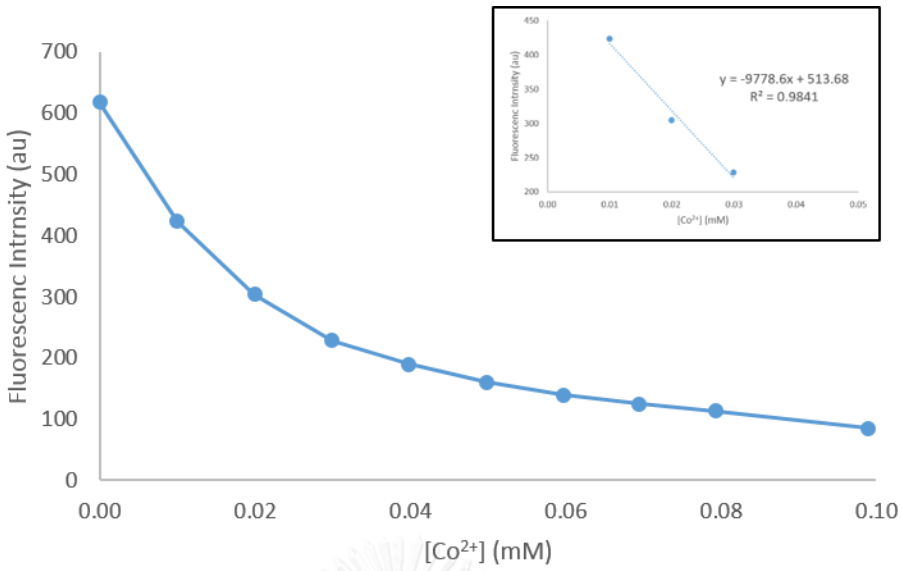

Figure 3.49 Fluorescence quenching plot between concentration of Co^{2+} ion and fluorescence intensity at 443 nm in 10 mM HEPES pH 7.4 buffer (excitation wavelength = 354 nm).

The proper amount of Co^{2+} ion for the preparation of biogenic amine probe was investigated by the fluorescence quenching of **N-CDs/SDS** upon the addition of Co^{2+} ion. According to Fig 3.48, the fluorescence spectra of N-CDs/SDS at 443 nm were quenched upon the increment of Co^{2+} ion concentration in the range of 0-0.1 mM as shown in Fig 4.49. Upon the addition of Co^{2+} ion over 0.05 mM, the **N-CDs/SDS** showed a slight fluorescence quenching. Therefore, the appropriate concentration of Co^{2+} ion for the construction of biogenic amine probe was 0.05 mM. Furthermore, the binding constant (K_{sv}) and detection limit of Co^{2+} ion over **N-CDs/SDS** were calculated by using Stern-Volmer plot method and 3σ/slope, respectively. It was found that the binding constant and limit of detection is approximately 5.47×10^4 M^{-1} and 6 μM, respectively. This suggests **N-CDs/SDS** enables to detect Co^{2+} ion in micromolar level.

*3.2.2.6 Selectivity of **N-CDs/SDS/Co^{2+}** toward various biogenic amines*

For biogenic amine sensing, the selectivity of **N-CDs/SDS/Co^{2+}** probe was examined. From the Fig 3.50, histidine showed the fluorescence recovery of **N-CDs** at 443 nm. This can be explained that histidine performs a good ligand exchange process

to remove Co^{2+} ion out of the **N-CDs/SDS/Co^{2+}** probe. In contrast, other biogenic amines cannot exhibit fluorescence changing of the probe.

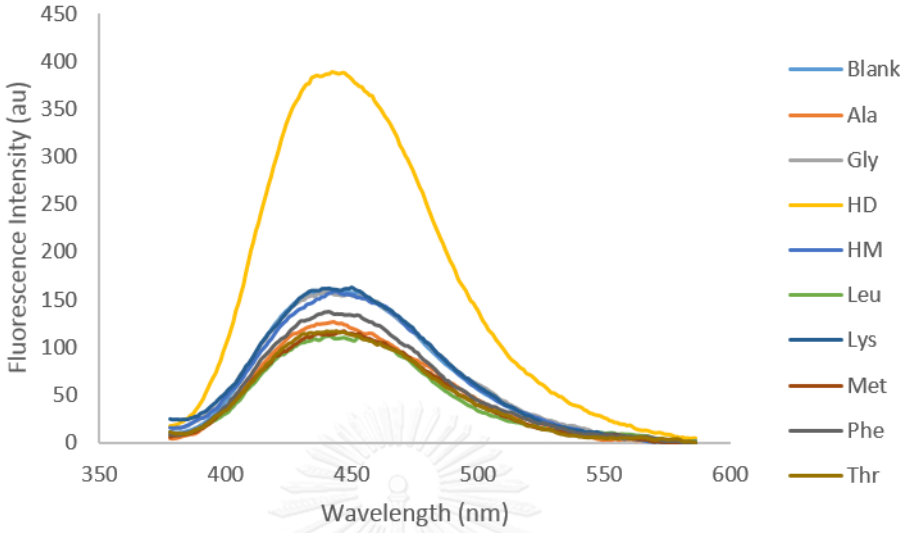

Figure 3.50 Fluorescence spectra of **N-CDs/SDS/Co^{2+}** upon the addition of different biogenic amines (2.5 mM) in 10 mM HEPES pH 7.4 buffer (excitation wavelength = 354 nm).

Based on the core structure of biogenic amine, they consist of carboxylic and amine group which is able to bind strongly with metal ion. A strong fluorescence recovery of **N-CDs/SDS/Co^{2+}** the presence of histidine can be explained that imidazole group, amino group and carboxylic group based on histidine preferentially form complex with Co^{2+} ion resulting in removal of Co^{2+} ion from the probe. Consequently, the performance of fluorescence enhancement of the probe was observed as shown in Fig 3.50 and 3.51, respectively.

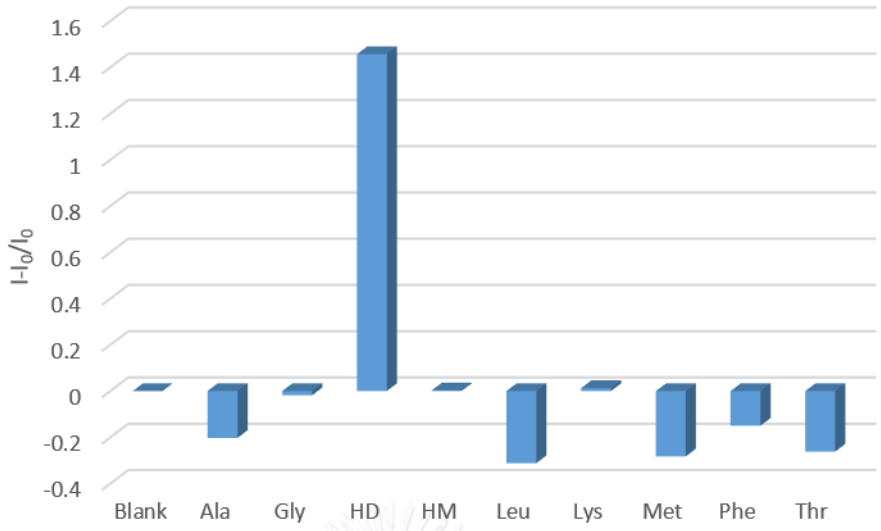

Figure 3.51 Relative fluorescence responses of **N-CDs/SDS/Co^{2+}** toward different biogenic amines (2.5 mM) in 10 mM HEPES pH 7.4 buffer (excitation wavelength = 354 nm and emission wavelength = 443 nm).

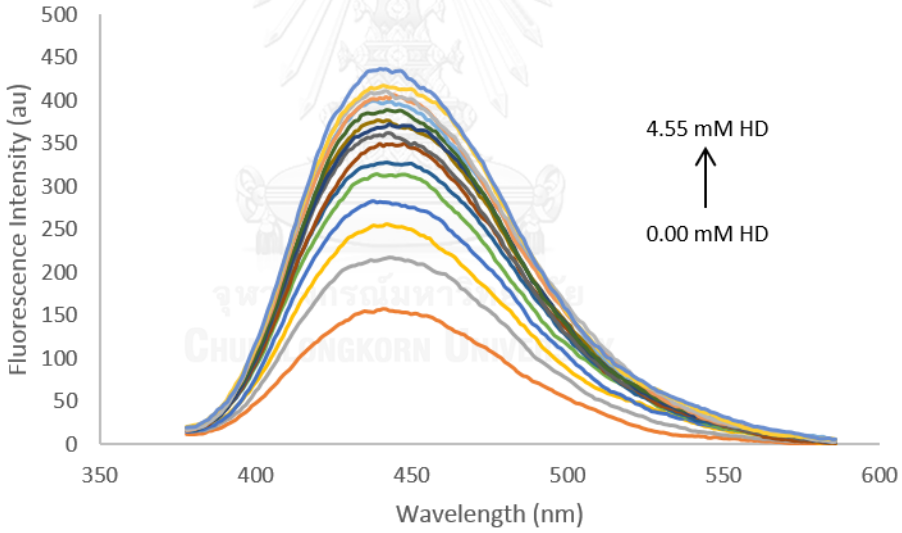

Figure 3.52 Fluorescence spectral titration of **N-CDs/SDS/Co^{2+}** upon the addition of histidine in 10 mM HEPES pH 7.4 buffer (excitation wavelength = 354 nm).

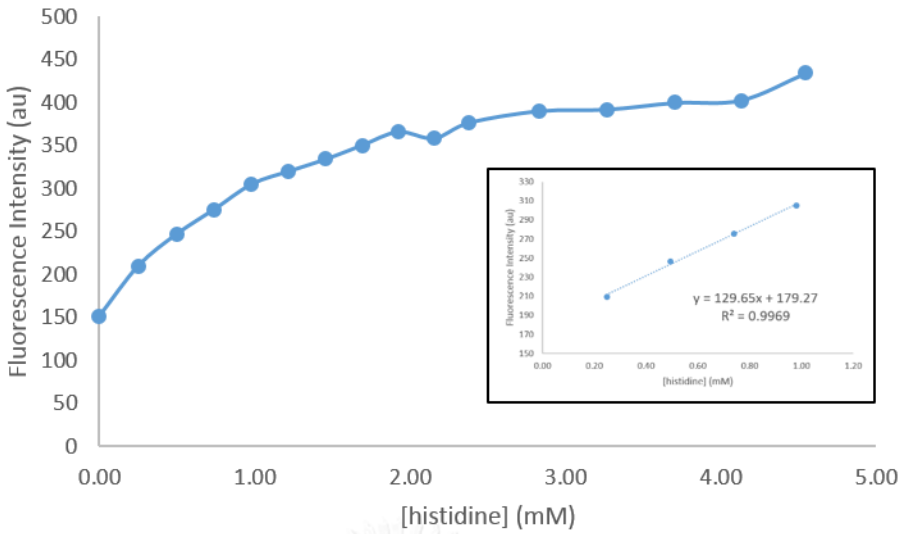

Figure 3.53 Fluorescence titration curve upon the addition of histidine in 10 mM HEPES pH 7.4 buffer (excitation wavelength = 354 nm and emission wavelength = 443 nm).

The fluorescence titration between the **N-CDs/SDS/Co^{2+}** probe and histidine was examined. The fluorescence intensity of probe was gradually increased with the increment of histidine from 0 to 0.7 mM as shown in Fig 3.53 due to ligand exchange between the probe and histidine. The plot of fluorescence intensity versus concentration of histidine showed a linear relationship with the correlation coefficient over 0.994. Furthermore, the detection limit of histidine over the probe was approximately 74 μM calculated by using 3σ/slope. This detection limit of this probe suggests that **N-CDs/SDS/Co^{2+}** probe enabled to apply for histidine determination in both normal and histidenemia patients [2].

*3.2.2.7 Proposed mechanism of **N-CDs/SDS** for histidine detection by TEM*

For better understanding of the photophysical properties of N-CDs/SDS for Co^{2+} ion and histidine detection, the TEM images of N-CDs/SDS were examined.

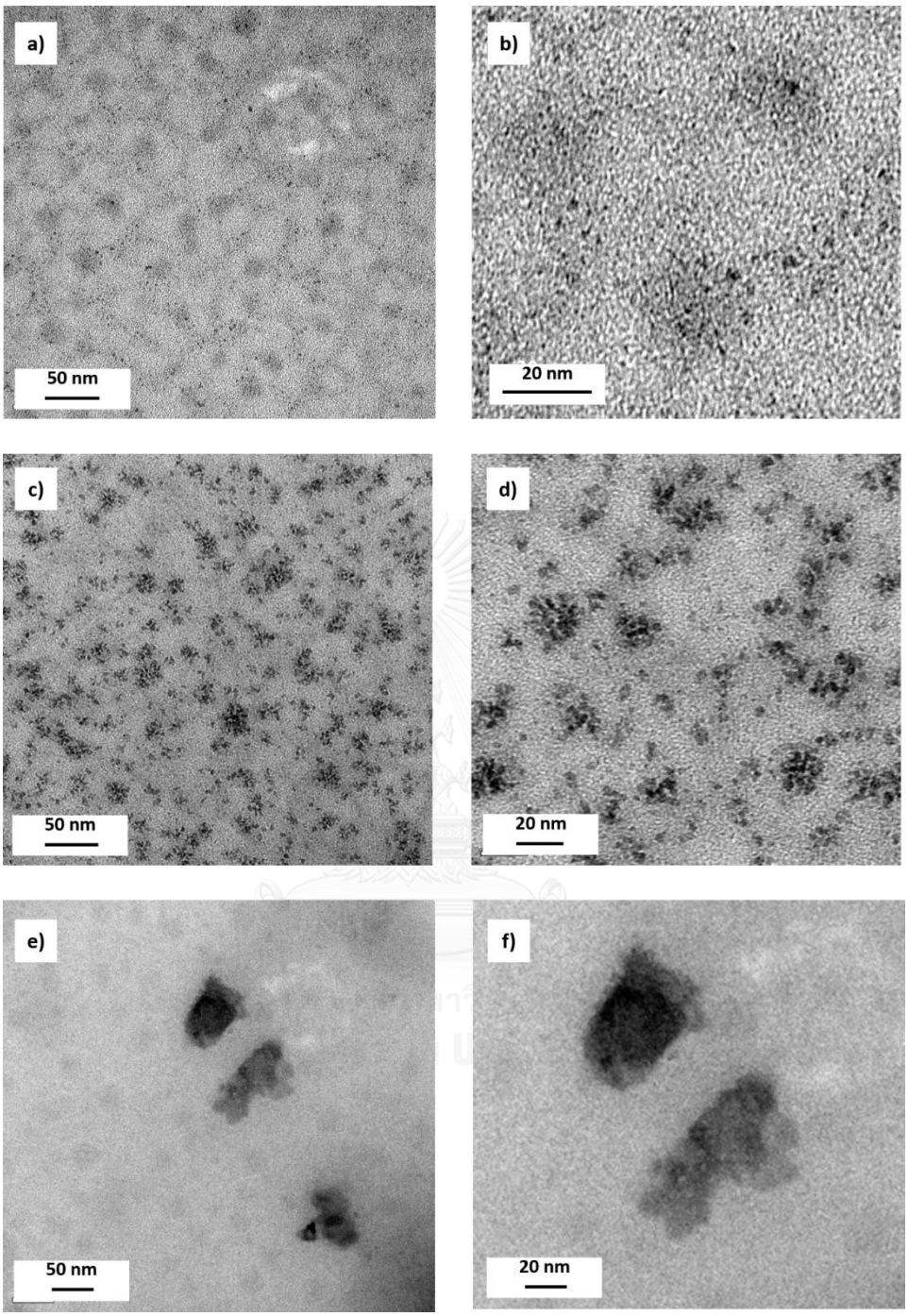

Figure 3.54 TEM images of **N-CDs** (a,b), **N-CDs/SDS** (c,d) and **N-CD/SDS/Co^{2+}** (e,f)

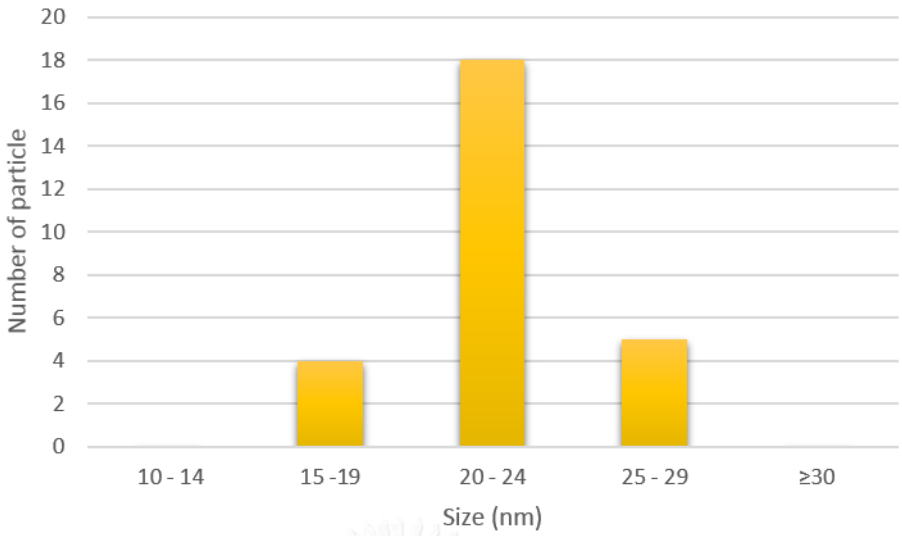

Figure 3.55 Size distribution of **N-CDs**

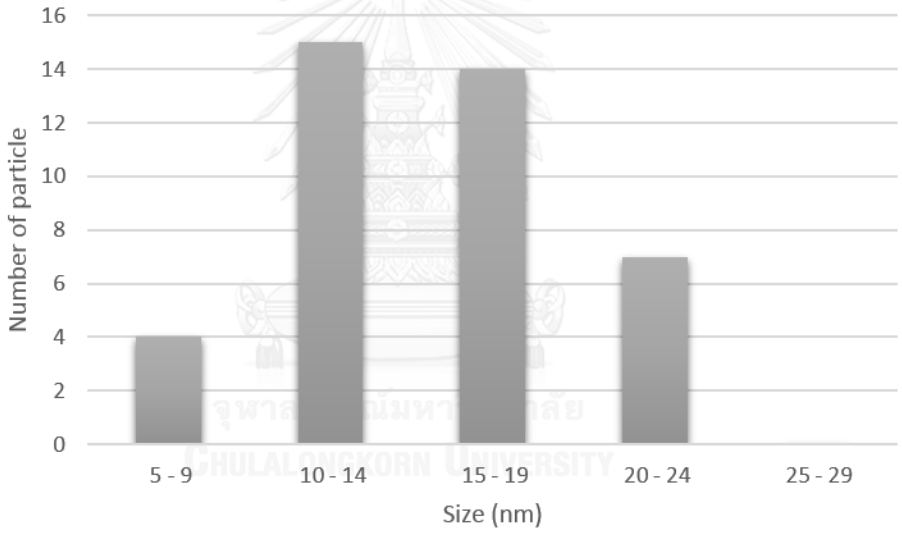

Figure 3.56 Size distribution of **N-CDs/SDS**

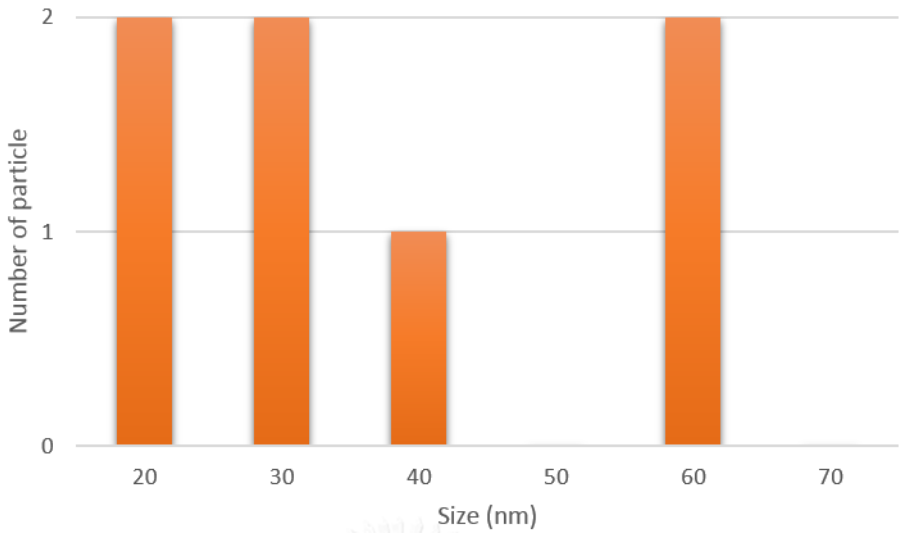

Figure 3.57 Size distribution of **N-CDs/SDS/Co^{2+}**

The fluorescence quenching mechanism of **N-CDs** was investigated by TEM measurement. According to Fig 3.54 a) and b), it can be seen that CDs distributed randomly in N-CDs. Upon the addition of SDS, these **N-CDs** were induced to the micelle as shown in Fig 3.54 c) and d). The average particle size was decreased from 22 nm to 15 nm as shown in Fig 3.56. It was expected that the formation of micelle can reduce non-radiative decay process and protect them from self-aggregation resulting in size decreasing and fluorescence enhancement. In the presence of Co^{2+} ion as shown in Fig 3.54 e) and f), amino groups of the particle can bind with Co^{2+} ion leading to aggregation of the particle, therefore, the average particle size was increased largely to 42 nm as shown in Fig 3.57. This confirms that fluorescence quenching was occurred due to the aggregation of N-CDs in the presence of Co^{2+} ion.

*3.2.2.8 Molecular logic gate of **N-CDs** for histidine detection*

The combination of logic circuit was also applied to **N-CDs/SDS** as molecular logic gate. For histidine sensing, the two chemical inputs Co^{2+} ion and histidine are designed as *In* Co and *In* HD. The presence of these inputs is assigned as "1" while the absence of these inputs is assigned as "0". Emission band at 450 nm is assigned as *Output*. The threshold value of fluorescence intensity at 450 nm is 200 a.u. as shown in Fig 3.58. The fluorescence signals are higher than the threshold values assigned as

"1" and the signals are lower than the threshold values assigned as "0", corresponding to the "on" and "off" states of the readout signals as shown in Fig 3.59, respectively.

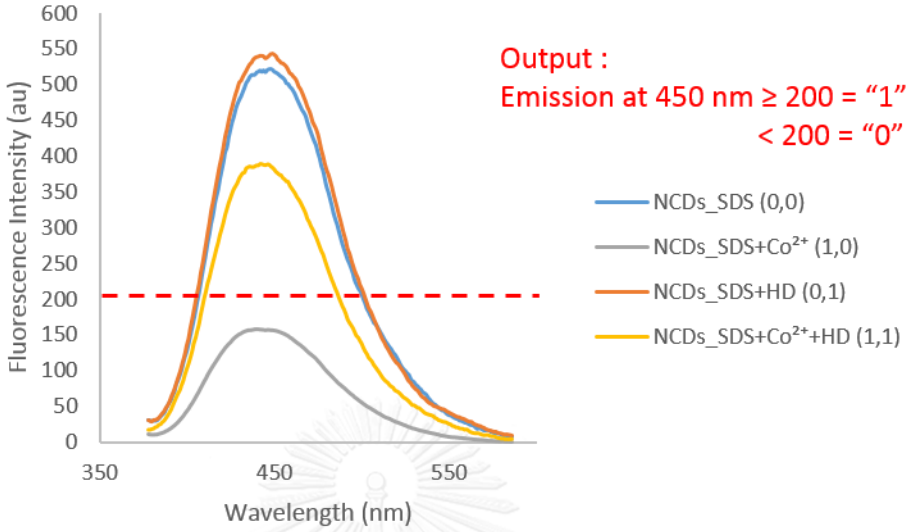

Figure 3.58 Fluorescence emission spectra of **N-CDs** at different input conditions in 10 mM HEPES pH 7.4 buffer (excitation wavelength = 354 nm).

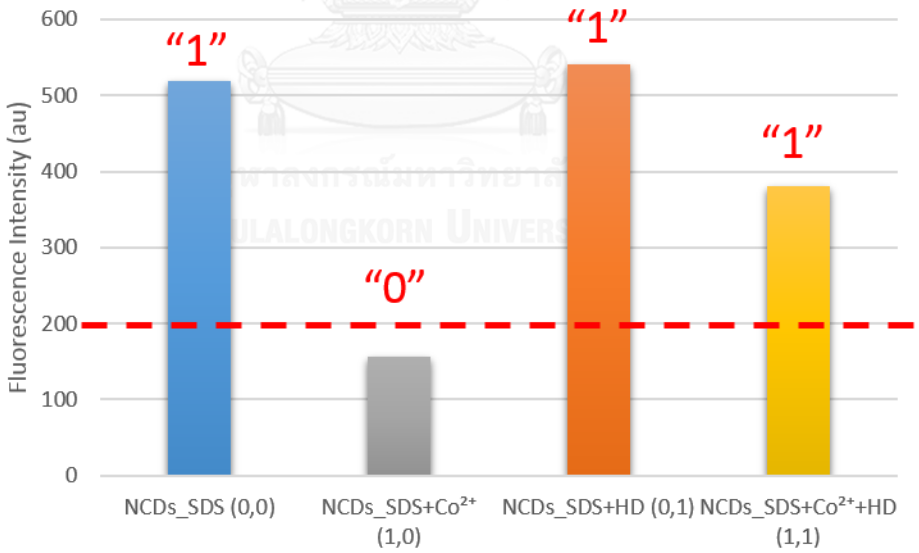

Figure 3.59 Fluorescence intensity of **N-CDs/SDS** at different input conditions for histidine detection in 10 mM HEPES pH 7.4 buffer

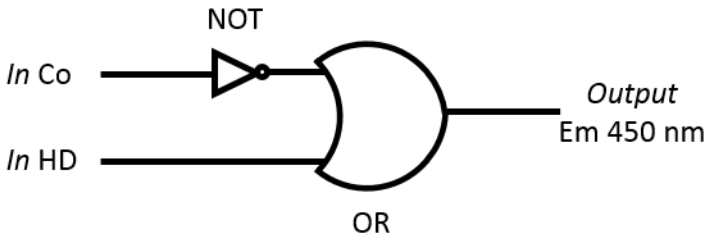

In Co	*In* Co "NOT"	*In* HD	*Output* "OR"
0	1	0	1
1	0	0	0
0	1	1	1
1	0	1	1

Figure 3.60 the combinatorial circuit of **N-CDs/SDS** with its truth table for histidine detection.

From these information, the combinatorial logic circuit with NOT and OR gate was constructed from **N-CDs_SDS** platform as shown in Fig 3.60. In the absence of all inputs (0,0), this platform exhibits strong fluorescence intensity at 450 nm with the intensity over the threshold resulting in *output* "1". In the presence of Co^{2+} with input (1,0), the fluorescence intensity was quenched to 150 a.u. which is lower than the threshold. Therefore, the *output* becomes "0". In the case of histidine with input (0,1), the fluorescence intensity of the platform remained unchanged. Therefore, the *output* becomes "1". In the presence of both chemical inputs (1,1), the fluorescence intensity is higher than the threshold as a result of *output* "1". Therefore, this platform can be used as molecular logic circuit for histidine detection.

CHAPTER IV
CONCLUSION

In this work, the fluorophore-micelle platforms for biogenic amine sensing were successfully constructed by using coumarin derivative (**CouS1**) and branch-polyethelenedimine modified carbon dots (**N-CDs**) as fluorophore and anionic surfactant namely SDS was used for micelle formation. Definitely, the presence of SDS micelle can improve sensing activity of fluorescent sensor by increase of the fluorescence intensity of fluorophore. Moreover, anionic head of SDS enables to induce metal cation to the platforms due to electrostatic force. Based on ET process, fluorescence intensity of these platforms would be quenched upon the addition of Co^{2+} ion. As a result, this approach can be applied to detect biogenic amines by ligand exchange mechanism. In the case of **CouS1/SDS/Co^{2+}**probe, histidine induced the enhancement of fluorescence intensity of the probe while fluorescence intensity quenching was observed upon the addition of histamine. For other biogenic amines, the fluorescence responses remained unchanged. It can be explained that the functional groups of histidine including amino group and carboxylic group perform a competitive formation with cobalt(II) ion bounded in **CouS1/SDS/Co^{2+}** probe resulting in fluorescence recovery of **CouS1/SDS/Co^{2+}** whereas histamine which consists of only imidazole group and amino group prefers to tightly co-bond with **CouS1/SDS/Co^{2+}**. Therefore, a high fluorescence quenching was observed. The detection limit of histidine and histamine over the probe was approximated 45 μM and 85 μM, respectively. This indicates that **CouS1/SDS/Co^{2+}** enabled to determine amount of histidine in both normal and histidenemia patient. Moreover, the luminescence of **CouS1/SDS/Co^{2+}** was brightened in the presence of histidine but the histamine induced fluorescence darkness. Therefore, this probe is the powerful tool for the discriminated detection of biogenic amines containing imidazole group from the other

by naked-eye approach and this sensor offers the differentiate detection of histidine and histamine with different behavior of optical approach. In the case of **N-CDs/SDS/Co^{2+}** probe, the morphology and functional groups of as-prepared **N-CDs** were investigated by using infrared spectroscopy (IR), X-ray photoelectron spectroscopy (XPS) and transmission electron microscope (TEM). It was found that carbon dots have been successfully modified by branch-polyethyleneimine (bPEI) due to the observation of nitrogen characteristic peaks in IR and XPS spectrum. Moreover, TEM images showed that carbon dots were distributed in the polymer randomly with average size 22 nm. The fluorescence response of **N-CDs/SDS/Co^{2+}** was investigated with various biogenic amines. It was found that only histidine exhibited fluorescence recovery of the probe. TEM images confirmed that the addition of Co^{2+} can induce aggregation of the particles leading to fluorescence quenching of the probe. The detection limit of histidine over the probe was approximately 74 μM. The different detection limits of histidine over **CouS1/SDS/Co^{2+}** and **N-CDs/SDS/Co^{2+}** possibly corresponded to the different binding constants (K_{sv}) of **CouS1/SDS** and **N-CDs/SDS** over cobalt(II) ion at $2.70x10^3$ and $5.47x10^4$, respectively. A higher binding constant of **N-CDs** was possibly caused by a large number of amino groups in **N-CDs/SDS** resulting in a tight capture with Co^{2+} ion. It is rationalization that it is difficult to remove Co^{2+} ion from **N-CDs/SDS/Co^{2+}**. However, **N-CDs/SDS/Co^{2+}** exhibits fluorescence change only the addition of histidine and it also enabled to apply to determine amount of histidine in both normal and histidenemia patient. Furthermore, molecular logic gate was constructed by the different optical changes under different stimuli of Co^{2+} ion, histidine and histamine. The molecular logic gate performed AND, NOT, OR and NAND gates.

REFERENCES

[1] Kopple, J.D. and Swendseid, M.E. Evidence that histidine is an essential amino acid in normal and chronically uremic man. Journal of Clinical Investigation 55(5) (1975): 881-891.

[2] Lam, W.K., Cleary, M.A., Wraith, J.E., and Walter, J.H. Histidinaemia: a benign metabolic disorder. Archives of Disease in Childhood 74(4) (1996): 343-346.

[3] Maintz, L. and Novak, N. Histamine and histamine intolerance. The American journal of clinical nutrition 85(5) (2007): 1185-1196.

[4] Hou, J.-T., Li, K., Yu, K.-K., Wu, M.-Y., and Yu, X.-Q. Coumarin-DPA-Cu(ii) as a chemosensing ensemble towards histidine determination in urine and serum. Organic & Biomolecular Chemistry 11(5) (2013): 717-720.

[5] You, Q.-H., Lee, A.W.-M., Chan, W.-H., Zhu, X.-M., and Leung, K.C.-F. A coumarin-based fluorescent probe for recognition of Cu2+ and fast detection of histidine in hard-to-transfect cells by a sensing ensemble approach. Chemical Communications 50(47) (2014): 6207-6210.

[6] Gu, J., et al. Carbon dot cluster as an efficient “off–on” fluorescent probe to detect Au(III) and glutathione. Biosensors and Bioelectronics 68 (2015): 27-33.

[7] Li, Z., Wang, Y., Ni, Y., and Kokot, S. A rapid and label-free dual detection of Hg (II) and cysteine with the use of fluorescence switching of graphene quantum dots. Sensors and Actuators B: Chemical 207, Part A (2015): 490-497.

[8] Qian, Z., Shan, X., Chai, L., Ma, J., Chen, J., and Feng, H. Si-Doped Carbon Quantum Dots: A Facile and General Preparation Strategy, Bioimaging Application, and Multifunctional Sensor. ACS Applied Materials & Interfaces 6(9) (2014): 6797-6805.

[9] Qu, K., Wang, J., Ren, J., and Qu, X. Carbon Dots Prepared by Hydrothermal Treatment of Dopamine as an Effective Fluorescent Sensing Platform for the Label-Free Detection of Iron(III) Ions and Dopamine. Chemistry – A European Journal 19(22) (2013): 7243-7249.

[10] Ding, L., Bai, Y., Cao, Y., Ren, G., Blanchard, G.J., and Fang, Y. Micelle-Induced Versatile Sensing Behavior of Bispyrene-Based Fluorescent Molecular Sensor for Picric Acid and PYX Explosives. Langmuir 30(26) (2014): 7645-7653.

[11] Pallavicini, P., Diaz-Fernandez, Y.A., and Pasotti, L. Micelles as nanosized containers for the self-assembly of multicomponent fluorescent sensors. Coordination Chemistry Reviews 253(17–18) (2009): 2226-2240.

[12] Zhao, Y. and Zhong, Z. Detection of Hg2+ in Aqueous Solutions with a Foldamer-Based Fluorescent Sensor Modulated by Surfactant Micelles. Organic Letters 8(21) (2006): 4715-4717.

[13] Jaffe, H.H. and Miller, A.L. The fates of electronic excitation energy. Journal of Chemical Education 43(9) (1966): 469.

[14] Albani, J.R. Fluorescence Spectroscopy Principles. in Principles and Applications of Fluorescence Spectroscopy, pp. 88-114: Blackwell Publishing Ltd, 2008.

[15] Weiss, S. Fluorescence Spectroscopy of Single Biomolecules. Science 283(5408) (1999): 1676.

[16] de Silva, A.P., Moody, T.S., and Wright, G.D. Fluorescent PET (Photoinduced Electron Transfer) sensors as potent analytical tools. Analyst 134(12) (2009): 2385-2393.

[17] Fabbrizzi, L. and Poggi, A. Sensors and switches from supramolecular chemistry. Chemical Society Reviews 24(3) (1995): 197-202.

[18] Chan, J., Dodani, S.C., and Chang, C.J. Reaction-based small-molecule fluorescent probes for chemoselective bioimaging. Nat Chem 4(12) (2012): 973-984.

[19] Fabbrizzi, L., Licchelli, M., Pallavicini, P., Perotti, A., Taglietti, A., and Sacchi, D. Fluorescent Sensors for Transition Metals Based on Electron-Transfer and Energy-Transfer Mechanisms. Chemistry – A European Journal 2(1) (1996): 75-82.

[20] Seto, D., Soh, N., Nakano, K., and Imato, T. Selective fluorescence detection of histamine based on ligand exchange mechanism and its application to biomonitoring. Analytical Biochemistry 404(2) (2010): 135-139.

[21] Zhu, S., Song, Y., Zhao, X., Shao, J., Zhang, J., and Yang, B. The photoluminescence mechanism in carbon dots (graphene quantum dots, carbon nanodots, and polymer dots): current state and future perspective. Nano Research 8(2) (2015): 355-381.

[22] Bacon, M., Bradley, S.J., and Nann, T. Graphene quantum dots. Particle & Particle Systems Characterization 31(4) (2014): 415-428.

[23] Pan, D., Zhang, J., Li, Z., and Wu, M. Hydrothermal Route for Cutting Graphene Sheets into Blue-Luminescent Graphene Quantum Dots. Advanced Materials 22(6) (2010): 734-738.

[24] Ponomarenko, L., et al. Chaotic Dirac billiard in graphene quantum dots. Science 320(5874) (2008): 356-358.

[25] Zhang, M., et al. Facile synthesis of water-soluble, highly fluorescent graphene quantum dots as a robust biological label for stem cells. Journal of materials chemistry 22(15) (2012): 7461-7467.

[26] Dong, Y., et al. Blue luminescent graphene quantum dots and graphene oxide prepared by tuning the carbonization degree of citric acid. Carbon 50(12) (2012): 4738-4743.

[27] Dong, Y., et al. Polyamine-functionalized carbon quantum dots for chemical sensing. Carbon 50(8) (2012): 2810-2815.

[28] Shen, P. and Xia, Y. Synthesis-modification integration: one-step fabrication of boronic acid functionalized carbon dots for fluorescent blood sugar sensing. Analytical chemistry 86(11) (2014): 5323-5329.

[29] Wang, X., Qu, K., Xu, B., Ren, J., and Qu, X. Microwave assisted one-step green synthesis of cell-permeable multicolor photoluminescent carbon dots without surface passivation reagents. Journal of Materials Chemistry 21(8) (2011): 2445-2450.

[30] Zhou, L., Lin, Y., Huang, Z., Ren, J., and Qu, X. Carbon nanodots as fluorescence probes for rapid, sensitive, and label-free detection of Hg 2+ and biothiols in complex matrices. Chemical communications 48(8) (2012): 1147-1149.

[31] Xu, M., Wu, S., Zeng, F., and Yu, C. Cyclodextrin Supramolecular Complex as a Water-Soluble Ratiometric Sensor for Ferric Ion Sensing. Langmuir 26(6) (2010): 4529-4534.

[32] Kotchapradist, P., et al. N-coumarin derivatives as hole-transporting emitters for high efficiency solution-processed pure green electroluminescent devices. Dyes and Pigments 112 (2015): 227-235.

[33] Cifuentes, A., Bernal, J.L., and Diez-Masa, J.C. Determination of critical micelle concentration values using capillary electrophoresis instrumentation. Analytical Chemistry 69(20) (1997): 4271-4274.

[34] Moroi, Y., Motomura, K., and Matuura, R. The critical micelle concentration of sodium dodecyl sulfate-bivalent metal dodecyl sulfate mixtures in aqueous solutions. Journal of Colloid and Interface Science 46(1) (1974): 111-117.

APPENDIX

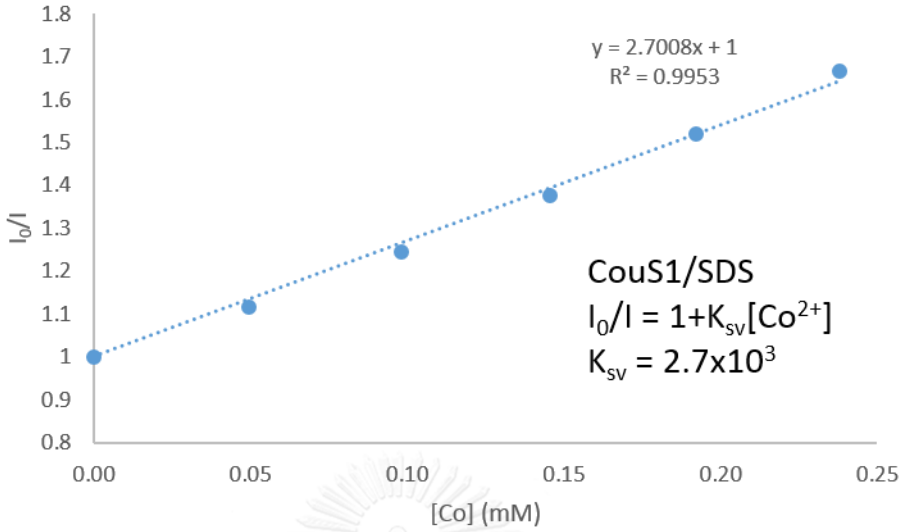

Figure A1 Stern-Volmer plot between relative fluorescence intensity of **CouS1/SDS** (518 nm) and Co^{2+} ion concentration

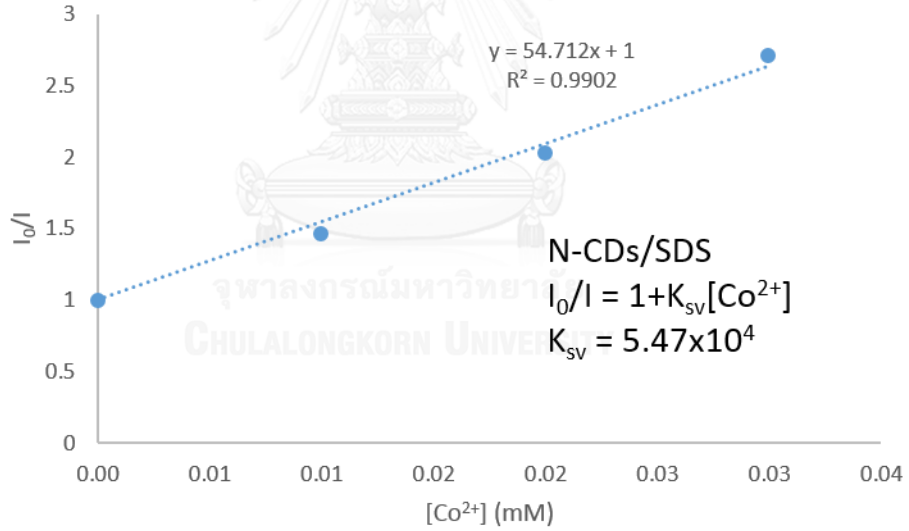

Figure A2 Stern-Volmer plot between relative fluorescence intensity of **N-CDs/SDS** (443 nm) and Co^{2+} ion concentration

VITA

Miss Manunya Tepakidareekul was born on November, 30, 1990 in Khon Kaen, Thailand. She has received the scholarship from the Development and Promotion of Science and Technology Talent Project (DPST), under the Institute for the Promotion of Teaching Science and Technology (IPST), Ministry of Education, Thailand since 2006 until present. She graduated from Khon Kaen University in Chemistry with a second class honour in 2012 and completed the program in academic year 2016.